Faculty of Engineering & Technology

Department of Civil and Environmental Engineering

Adsorptive Removal of Heavy Metals from Wastewater using Brick Waste and Copper Smelter Slag as Low Cost Adsorbents

By

GOBUSAONE MOKOKWE

Student ID Number: 19100016

A Thesis Submitted to the Faculty of Engineering & Technology in Partial Fulfilment of the Requirements for the Award of the Degree of Master of Engineering in Civil and Environmental Engineering of BIUST

Supervisor: Dr Moatlhodi Wise Letshwenyo

Department of Civil and Environmental Engineering

Faculty of Engineering & Technology, BIUST

E-mail Address: letshwenyom@biust.ac.bw

August, 2022

BOTSWANA INTERNATIONAL UNIVERSITY OF SCIENCE & TECHNOLOGY

POSTGRADUATE SCHOOL

Declaration Regarding the Work and Copyright

DECLARATION REGARDING THE WORK AND COPYRIGHT

Candidate (please write in caps or type): GOBUSAONE MOKOKWE Student ID: 19100016

Thesis Titled: Adsorptive removal of heavy metals from wastewater using brick waste and copper smelter slag as low cost adsorbents.

I, the **Candidate**, certify that the Thesis is all my own original work and that I have not obtained a degree in this University or elsewhere on the basis of any of this work.

(If the thesis is based on a group project, then the student must indicate the extent of her / his contribution, with reference to any other theses submitted or published by each collaborator in the project, and a declaration to this effect must be included in the thesis)

Signed:  Date: 11/08/2022

Primary Supervisor (please write in caps or type) DR. MOATLHODI WISE LETSHWENYO

I, the Candidate's **Primary Supervisor**, hereby confirm that I have inspected the above titled thesis and, to the best of my knowledge, it is based on the original work of the candidate.

Signed: 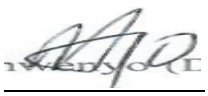 Date: 11/08/2022

CERTIFICATION

The undersigned certifies that he has read and hereby recommends for acceptance by the Faculty of Engineering and technology a thesis titled; **Adsorptive removal of heavy metals from wastewater using brick waste and copper smelter slag as low cost adsorbents,** in fulfilment of the requirements for the degree of Master of Engineering in Civil &Environmental Engineering of the BIUST.

Signature:  Date: 11/08/2021

Dr.Moatlhodi Wise Letshwenyo (Supervisor)

Faculty of Engineering and Technology

Department of Civil and Environmental Engineering

Botswana International University of Science and Technology

ACKNOWLEDGEMENT

I am deeply indebted to my sage research supervisor Dr Moatlhodi Wise Letshwenyo for his guidance, advice and input throughout this work. Without his advices this work wasn't going to be successful. The assistance of all Botswana International University of Science and Technology (BIUST) technical staff is highly appreciated, more especially Senior Technicians at Department of Earth and Environment Ms Serwalo Mercy Mokgosi and Mr Trust Manyiwa who helped me with analysis of effluent sample and characterisation of media. Department of Geological and Mining Engineering technical staff is highly acknowledged for helping with their equipment for crushing media, thanks gentlemen, without you this work was not going to be successful.

I would also like to thank Botswana Geoscience Institute (BGI) for assisting with their equipment for analysis of effluent. Without them, I would have not managed to perform well in time in my research experiments. Great thanks to Physics and Astronomy laboratory technician Mr Mothusi Madiba for assisting me with mineralogical characterisation of media and taught me how to use his equipment and explain material characterisation with detailed theories.

My most humble and sincere thanks to the wise and enthusiastic technical staff of Department of Civil and Environmental Engineering, more especially Mr Mothusi Oganne who helped me with sampling of both media and some laboratory tests. Special thanks to BCL (Ltd) mine, Bothakga Concrete Works (PTY) Ltd and Makoro Bricks for free provision of their copper smelter slag and bricks to be used in my study.

I would like to gratefully thank Botswana International University of Science and Technology for helping in financing my study and provision of teaching assistant position. Warm Thanks to Chemical Engineering technician Mr Tshepo Gaogane for the support, friendship and encouragement throughout the entire research. I appreciate all the assistance from Chemical Engineering technician and a friend Mr Tumeletso Lekgoba regarding analysis of my data and other issues such as preparation of stock solutions. Thank you very much Mr Lekgoba for your help.

Last but not least, I would like to thank God -Mighty Lord for his mercy, constant love, protection He gave me throughout this research.

DEDICATION

I dedicate this work to my family members for their love, encouragement and support. The dedication also goes to all my friends in Botswana International University of Science &Technology (BIUST). I also dedicate this work to my late maternal grandmother, Sophia Dikgole, late grandfathers, Samuel Letlole and Ntwayagae Lejage.

LIST OF RESEARCH PAPERS

The following research articles were produced from this thesis and written by Mr Gobusaone Mokokwe and Dr Moatlhodi Wise Letshwenyo as the first and core the authors respectively;

1. Mokokwe, G. and Letshwenyo, M. W. (2022) 'Utilisation of cement brick waste as low cost adsorbent for the adsorptive removal of copper, nickel and iron from Aqueous Solution: Batch and column studies', *Physics and Chemistry of the Earth*. Elsevier, 126(May), p. 103156. doi: 10.1016/j.pce.2022.103156.
2. Mokokwe, G. and Letshwenyo, M. W. (2022) 'Investigation of Clay Brick Waste for the Removal of Copper, Nickel and Iron from Aqueous Solution: batch and fixed - bedcolumnstudies',*Heliyon*.Elsevier,08(July),https://doi.org/10.1016/j.heliyon.2022.e09963

ABSTRACT

The industrial effluents contain substantial amounts of toxic heavy metal ions which pollutes surface water and groundwater. In this study, the adsorptive removal of copper, iron and nickel ions from wastewater using Makoro Granite brick waste (MGBW), Makoro Gold Satin (MGS) clay brick waste, copper smelter slag (CSS) and cement brick waste (CBW) as novel adsorbents has been investigated at batch mode. The mineralogical and chemical content of adsorbents was determined using X-ray Diffractometer (XRD) and X-ray Fluorescence (XRF) respectively. Thermogravimetric analysis (TGA) on both adsorbents prior to and after adsorption was done. Surface morphology of media and pH point of zero charge (pH_{pzc}) were respectively investigated and determined using Scanning Electron Microscopy (SEM) and pH drift method. The leaching behaviour of media was investigated at different contact times; 24, 48 and 72 hours. The batch investigations focused on the effects of contact time, pH of solution, adsorbent dosage or loading, temperature, and adsorbent size to determine the effectiveness of the media. XRD revealed amorphous and crystalline phases on both media without noticeable changes before and after adsorption. The pH_{pzc} of CBW, MGBW, MGS and CSS were found to be 6.45, 8.3, 6.25 and 7.01 respectively. SEM revealed presence of micro-pores and irregular distribution of clumps on both media. Leaching test revealed that CSS leached more of copper, iron and nickel after 48 and 72 hours exceeding consent values for environmental discharge. Only iron exceeded consent values on MGS leachate after 48 hours while the other media had leaching concentrations not exceeding permissible values. The maximum adsorption capacities of copper smelter slag were 3.3 mg g^{-1} media, 3.1, mg g^{-1} media and 3.2 mgg^{-1} media for the removal of iron, copper and nickel ions respectively after 30 minutes. In the case of MGBW, the optimal capacities were 7.6 mg g^{-1} media, 6.7 mg g^{-1} media and 6.2 mg g^{-1} media respectively, for iron, copper and nickel removal after 45 minutes. However, maximum adsorption capacities for MGS were found to be 6.7, 6.1 and 4.5 mgg^{-1} media respectively for copper, iron and nickel after 45 minutes. As for CBW maximum adsorption capacities were 8.5, 8.7 and 4.2 mgg^{-1} media for copper, iron and nickel respectively after 45 minutes. Both Pseudo First and Pseudo Second Order models described the adsorption process. Intra-particle and mass transfer diffusion were both rate controlling the reactions. Freundlich and Langmuir isotherm models were involved in adsorption process indicating that adsorption of some metals was taking place in some heterogeneous and homogenous active sites. Thermodynamic parameters for CSS, MGS, CBW and MGBW indicated that the adsorption process was non spontaneous process and was exothermic.

Reusability or regeneration studies on MGBW, MGS, CBW and CSS verified that CBW lowered its original capacity in three regeneration cycles using 0.1 M Sodium Hydroxide. Based on performance of media two media, CBW and MGBW were selected for column studies. Column results revealed that, nickel was leaching from MGBW and less removed due to large ionic radius and high electronegativity compared to other metals. However, CBW column results indicated better adsorptive removal of target metal ions. Thomas column kinetic model described the mechanism for adsorptive removal of divalent copper, iron and nickel better in the fixed bed column study and it agreed with the some batch models as the Thomas model predicts that the adsorption process follows Langmuir isotherm model and was derived based on the second order kinetics. Overall, MGBW and CBW can be applied as low cost, effective and environmentally friendly adsorbents for the adsorptive removal of copper, iron and nickel irons from wastewater. However, CSS and MGS can also be used for separation of heavy metals from wastewater provided they are modified. However further studies on MGS and CSS through fixed bed column process should be investigated before field trials. It is also however important that further studies should be done using real wastewater before field trials.

Keywords: Adsorption, brick waste, copper smelter slag, heavy metals, kinetics, thermodynamics, wastewater

Table of CONTENTS

LIST OF TABLES

LIST OF FIGURES

LIST OF ABBREVIATIONS AND ANNOTATIONS

ρ_b – bulk density

ρ_p - particle density

A - Absorbance

A - Cross-sectional area of media

AC – Activated carbon

AIV - Aggregate Impact Value

As - Arsenic

As (lll) - Arsenite

As (V) - Arsenate

ASTM - American Society for Testing Materials

$BaCl_2$ - Barium chloride

BOS - Botswana Bureau of Standards

BV - Bed Volume

C – Value of intercept giving an idea about the boundary layer thickness

^0C - degrees Celsius

Ca^{2+}- calcium ion

CBW - Cement Brick Waste

Cc-coefficient of gradation

Cd - cadmium

Ce - equilibrium metal concentration

Ci - initial metal concentration

Ci – Influent concentrations

CEC - Cation Exchange Capacity

Cet - Effluent concentrations at time, t

Cit – Influent heavy metal concentrations at time,t

Cl - chlorine

Cr - chromium

Cr (VI) - Hexavalent Chromium

CSS - copper smelter slag

Cu - copper

Cu - uniformity coefficient

$CuSO_4.5H_2O$ - Copper sulphate pentahydrate salt

Cu^{2+}- divalent copper ion

CWs – constructed wetlands

D10 - effective diameter

D30 - is the diameter of the particle size curve corresponding to 30% by weight (Finer) and 70% larger

D50 - mean particle diameter

D60 - is the diameter of the particle size curve corresponding to 60% by weight (Finer) and 40% larger

EBCT - Empty Bed Contact Time

EU - European Union

FAO - Food Agriculture Organization

Fe - Iron

Fe^{2+}- ferrous ion or divalent iron ion

Fe (II) - Ferrous iron

Fe (III) - Ferric iron

$FeSO_4.XH_2O$ - Ferrous Sulphate heptahydrate salt

FT-IR - Fourier Transmittance Infrared

g - grams

GFH – Granular Ferric Hydroxide

GFO - Granular Ferric Oxide

h - Difference in head on manometers

HDPE – High-Density –Polythene

hrs – hours

Hg - mercury

HLR - Hydraulic Loading Rate

HNO_3 - nitric acid

ICP-OES - Inductively coupled plasma-Optical Emission Spectrophotometry

IRRA - Infra-red radiation absorption

K - Coefficient of permeability

kid – Rate constant of intraparticle diffusion

KL – Langmuir adsorption constant (L/mg) related with free energy of adsorption

Kn - KiloNewton/s

K_{sat} - saturated hydraulic conductivity

L – distance between manometers

M - mass of adsorbent

MGBW - Makoro Granite Brick Waste

MGS - Makoro Gold Satin clay brick

Mg^{2+} - magnesium ion

mins – minutes

mL - milliliter

mm - millimeters

n - porosity

Na^{+} - sodium ion

NaAc - Sodium Acetate

Na_2CO_3 - sodium carbonate

Na_3PO_4 - sodium phosphate

$NaHCO_3$ - sodium hydrogen carbonate

NaOH - sodium hydroxide

$NaNo_3$ - sodium nitrate

Ni^{2+} - nickel ion

NO^{-3} - nitrate ion

Pb - Lead

Psd – Particle size distribution

PVC - Polyvinyl Chloride

pzc - point of zero charge

q - adsorption capacity

qe – equilibrium metal ion concentration on adsorbent

qi - influent heavy metal load in each column until the exhaustion of media

qm - monolayer adsorption capacity of the adsorbent

qs – mass of heavy metals adsorbed until the exhaustion of media during column experiment

Q – discharge of water

R - heavy metal removal efficiency of media

Rt – heavy metal removal efficiency of column- packed media

rpm - revolution per minute

Se (VI) - Selenate

SEM - Scanning Electron Microscopy

T – transmittance

TGA – Thermogravimetric Analysis

t- sum of time of discharge

Ti - Titanium

TiO_2 - Titanium Dioxide

USEPA - United States Environmental Protection Agency

V - volume of effluent during batch experiments

Ve - effluent volume collected from column

Vi – influent volume which has passed through the media in a column

WHO - World Health Organization

XRD - X-Ray Diffractometer

XRF - X-Ray Florescence

Zn - zinc

CHAPTER 1: INTRODUCTION

1.1. Background

The advancement of industries has taken away the salubrious of terrestrial and aquatic organisms due to an upsurge in discharge of huge volumes of toxic effluents into natural bodies (Singh *et al.*, 2008). Such huge volumes of water in countries with persistent drought and unreliable rainfall like Botswana can be of great agronomic and economic importance. In order to solve the issue of water scarcity, Botswana has begun to use treated sewage water for irrigation. This water contains diverse plant nutrients and organic matter leading to an increase in soil fertility (Börjesson and Kätterer, 2018). However, on the other hand, treated sewage water is laden with high levels of toxic heavy metals (Hussain *et al.*,2019). Heavy metals exist around us in our water, soil and air and come from natural process such volcanic activities, weathering of rocks, and natural fires (Farooq *et al.*, 2010). Moreover, the other source of heavy metals is anthropogenic process activities from industries such as textile industries, tannery industries, fertilizer production and many more. Heavy metals occur naturally in nature and may enter our bodies through the food chain. Some heavy metals are required by our bodies to function, but can be toxic in large quantities. Other heavy metals have no benefit to human body, and can actually be dangerous to the body systems (Jaishankar *et al.*, 2014).

Various researches have reported numerous conventional technologies for the removal of heavy metals from effluents. This include chemical precipitation(Ramakrishnaiah and Prathima, 2016; Int, 2019), flocculation and coagulation (Johnson *et al.*, 2008), ion exchange (Tan *et al.*, 2017), reverse osmosis (Bakalár *et al.*, 2009; Thaçi and Gashi, 2019), membrane filtration (Jasiewicz and Pietrzak, 2013; Khulbe and Matsuura, 2018) and many others. These methods have been long conducted to provide better water quality and to treat wastewater before releasing it into water bodies. However, the main challenge to use such methods is some association with high operation and maintenance cost. Chemical precipitation methods are reliable but on the other hand require large settling tanks for precipitating voluminous alkaline sludge and a subsequent treatment is required (Int , 2019). The reduction of maintenance, operation and sludge disposal costs is required by adapting to other cost effective alternatives (Chiban *et al.*, 2012). Apart from all these technologies, adsorption is considered the simplest, economically viable and effective technique useful for removing pollutants from effluents (Saydeh *et al.*, 2017). It is defined as a process whereby a substance

binds and concentrates at an interface between phases due to chemical and physical interaction (Crawford and Quinn, 2017). Adaption of novel technologies in water and waste water treatment such as utilization of novel adsorbents in heavy metal removal is gradually evolving.

The most enormous challenge faced by various researchers using adsorption technology is paucity of appropriate information about selection of low cost and high heavy metal retention adsorbent media. Various adsorbents have been investigated and evaluated through batch and column experiments. Most of investigations were done using bio adsorbents for elimination of heavy metals from industrial effluents (Waghmare *et al.,* 2014; Ali *et al.,* 2014). The widely used adsorbent is the Activated Carbon (AC) due to its high adsorption capacity, but it has a notoriety of high production prices. These biosorbents are also however associated with high regeneration costs and possesses low physical and mechanical strength, thus are likely to fail due to static forces in the bed. To date, AC is still considered the most effective adsorbent, though it has such notorieties. Rapid industrialisation and urbanisation has driven construction and mining industries to generate waste materials such as concrete waste and by products, brick waste, gravels, slags, ashes. In Botswana, brick waste and smelter slag among such materials are abundant, but not yet used for wastewater treatment. In response, such cost effective, abundant and environmentally favourable adsorbents are needed for heavy metal scavenging. An evaluation of heavy metal adsorption capacities of several media has been done through laboratory and column experiments (Shahat and Shehata 2013; Papandreou *et al.,* 2007).

1.2. Problem statement

Most of the industries generate effluents containing heavy metals which are considered to be repugnant contaminants, reported to pose detrimental environmental health threats to both terrestrial and aquatic life. Therefore, this problem can be addressed by utilization of more robust novel adsorbents mainly from mining and construction waste which is gaining more attention for the treatment of wastewater nowadays. Among other reactive media, AC has shown to have a great potential in the removal of toxic heavy metals from waste water due to its large reactive surface area and adsorption capacity. However, AC is associated with high production and operational costs just like other wastewater treatment techniques. Construction and mining industries generates millions of tonnes of waste such as brick waste, smelter slags, ashes and many others. Brick waste and copper smelter slag in Botswana appear to be abundant and have better mechanical properties. Other materials apart from slag

and brick waste might also suffer some drawbacks like hydrostatic failures in bed columns and clogging. Hence, making application of copper smelter slag and brick waste in removal of heavy metals from wastewater more profound candidates.

1.3. Aim and objectives

The overall aim of this study was to investigate the effectiveness of locally available low cost adsorbents (brick waste, copper smelter slag) in the removal of heavy metals from wastewater.

The specific objectives that have been addressed to accomplish this aim are:

1. To investigate the effects of process parameters influencing the removal of heavy metals from wastewater such as pH, adsorbent dosage, contact time, adsorbent particle size through batch studies.
2. To understand the mechanisms involved during adsorption of heavy metals using brick waste and copper smelter slag as adsorbents.
3. To investigate and understand the regeneration potential of media together with practical implications of the use of the media.
4. To investigate the environmental effects of using brick waste and copper smelter slag as adsorbents through leaching test.
5. To understand practical implications of the best performing media through column studies.

1.4 .RESEARCH QUESTIONS

This research intends to address the following research questions;

1. Which adsorbent particle size will best perform in heavy metal removal?
2. Which media will perform the best in heavy metal removal?
3. At which solution pH levels and dosage will the media best adsorb heavy metals?
4. Will the energy be required to migrate heavy metal ions from the solution to the surface of media?
5. Which kinetic models will the adsorption process best fit?
6. Will the adsorption process take place in heterogeneous or homogeneous active sites?
7. Will the media used as an adsorbent be environmental friendly?

1.5 .OUTLINE OF STUDY (THESIS PLAN)

The chapters of this thesis are presented as shown below;

Chapter 1, ***Background*** This chapter gives the background information about wastewater treatment technologies used for heavy metal removal, problems associated with the techniques, the best technology being adsorption. The motivation of this work is also outlined in this chapter.

Chapter 2, ***Literature review on wastewater treatment technologies;*** This chapter focuses on the main characteristics considered during the selection of adsorbent media. The chapter also investigates the physical and chemical process parameters influencing performance of media on adsorption of heavy metals from wastewater.

Chapter 3, ***Research methodology on adsorption of heavy metals from wastewater using brick waste and smelter slag,*** looks at detailed procedures followed in both characterisation of media, batch experimental studies and column studies.

Chapter 4, ***Results and discussions,*** In this chapter, key findings of the study were found to address research questions with a concern on the use of brick waste and smelter slag as adsorbents.

Chapter 5, ***Conclusions,*** is a chapter which concludes the findings of this research work.

References

Ali, S. M., Khalid, A. R. and Majid, R. M. (2014) 'The removal of Zinc , Chromium and Nickel from industrial waste water using Corn cobs ', *Iraqi Journal of Science*, No.1, 55(1), pp. 123–131.

Al-Saydeh, S. A., El-Naas, M. H. and Zaidi, S. J. (2017) 'Copper removal from industrial wastewater: A comprehensive review', *Journal of Industrial and Engineering Chemistry*. The Korean Society of Industrial and Engineering Chemistry, 56(July), pp. 35–44. doi: 10.1016/j.jiec.2017.07.026.

Börjesson, G. and Kätterer, T. (2018) 'Soil fertility effects of repeated application of sewage sludge in two 30-year-old field experiments', *Nutrient Cycling in Agroecosystems*, 112(3), pp. 369–385. doi: 10.1007/s10705-018-9952-4.

Crawford, C. B. and Quinn, B. (2017) 'The interactions of microplastics and chemical pollutants', *Microplastic Pollutants*, pp. 131–157. doi: 10.1016/b978-0-12-809406-8.00006-2.

Hussain, A., Priyadarshi, M. and Dubey, S. (2019) 'Experimental study on accumulation of heavy metals in vegetables irrigated with treated wastewater', *Applied Water Science*. Springer International Publishing, 9(5), pp. 1–11. doi: 10.1007/s13201-019-0999-4.

Int, C. (2019) 'Chemical precipitation method for chromium removal and its recovery from tannery wastewater in Ethiopia', (May). doi: 10.31221/osf.io/m7h5k.

Jaishankar, M., Tseten, T ,Anbalagan,N ,Mathew,B.B.and Beeregowda,K.N (2014) 'Toxicity, mechanism and health effects of some heavy metals', *Interdisciplinary Toxicology*, 7(2), pp. 60–72. doi: 10.2478/intox-2014-0009.

Jasiewicz, K. and Pietrzak, R. (2013) 'Metals ions removal by polymer membranes of different porosity', *The Scientific World Journal*, 2013. doi: 10.1155/2013/957202.

Johnson,P.D.,Girinathannair,P,Ohlinger,K.N,Ritchie,S,Teuber,L.andKirby,J.(2008)'Enhance d Removal of Heavy Metals in Primary Treatment Using Coagulation and Flocculation', *Water Environment Research*, 80(5), pp. 472–479. doi: 10.2175/106143007x221490.

Khulbe, K. C. and Matsuura, T. (2018) 'Removal of heavy metals and pollutants by membrane adsorption techniques', *Applied Water Science*. Springer Berlin Heidelberg, 8(1), pp. 1–30. doi: 10.1007/s13201-018-0661-6.

Ramakrishnaiah, C. R. and Prathima, B. (2016) 'Hexavalent Chromium Removal by Chemical Precipitation Method : A Comparative Study', *International Journal of Environment Research and Development*, 1(January 2011), pp. 41–49.

Thaçi, B. S. and Gashi, S. T. (2019) 'Reverse osmosis removal of heavy metals from wastewater effluents using biowaste materials pretreatment', *Polish Journal of Environmental Studies*, 28(1), pp. 337–341. doi: 10.15244/pjoes/81268.

El-Shahat, M. and Shehata, A. M. A. (2013) 'Adsorption of lead, cadmium and zinc ions from industrial wastewater by using raw clay and broken clay-brick waste', *Asian Journal of Chemistry*, 25(8), pp. 4284–4288.

Farooq, U. Kozinski, J.A , Khan,M.A .and Athar,M.(2010) 'Biosorption of heavy metal ions using wheat based biosorbents – A review of the recent literature', *Bioresource Technology*. Elsevier Ltd, 101(14), pp. 5043–5053. Doi: 10.1016/j.biortech.2010.02.030.

Int, C. (2019) 'Chemical precipitation method for chromium removal and its recovery from tannery wastewater in Ethiopia', *Chemistry International*, 3(4), pp. 291-305.Doi: 10.31221/osf.io/m7h5k.

Khulbe, K. C. and Matsuura, T. (2018) 'Removal of heavy metals and pollutants by membrane adsorption techniques', *Applied Water Science*. Springer Berlin Heidelberg, 8(1), pp. 1–30. Doi: 10.1007/s13201-018-0661-6.

Mohamed Chiban (2012) 'Application of low-cost adsorbents for arsenic removal: A review', *Journal of Environmental Chemistry and Ecotoxicology*, 4(5), pp. 91–102. Doi: 10.5897/jece11.013.

Papandreou, A., Stournaras, C. J. and Panias, D. (2007) 'Copper and cadmium adsorption on pellets made from fired coal fly ash', *Journal of Hazardous Materials*, 148(3), pp. 538–547. Doi: 10.1016/j.jhazmat.2007.03.020.

Ramakrishnaiah, C. R. and Prathima, B. (2016) 'Hexavalent Chromium Removal by Chemical Precipitation Method : A Comparative Study', *International Journal of Environment Research and Development*, 1(January 2011), pp. 41–49.

Singh, R. K.,Kumara,S, Kumara,S . and Kumar,A.(2008) 'Development of parthenium based activated carbon and its utilization for adsorptive removal of p-cresol from aqueous solution', *Journal of Hazardous Materials*, 155(3), pp. 523–535. Doi: 10.1016/j.jhazmat.2007.11.117.

Tan, J. J.,Yu,H,Zhi-qi,W.and Xi,C. (2017) 'Ion Exchange Resin on Treatment of Copper and Nickel Wastewater', *IOP Conference Series: Earth and Environmental Science*, 94(1). Doi: 10.1088/1755-1315/94/1/012122.

Thaçi, B. S. and Gashi, S. T. (2019) 'Reverse osmosis removal of heavy metals from wastewater effluents using biowaste materials pretreatment', *Polish Journal of Environmental Studies*, 28(1), pp. 337–341. Doi: 10.15244/pjoes/81268.

Waghmare, V. H. and Chaudhari, U. E. (2014) ‘Removal of hexavalent chromium from aqueous solution by adsorption on commiphora myrrha bark’, *Rasayan Journal of Chemistry*, 7(1), pp. 16–19.

CHAPTER 2: LITERATURE REVIEW

2.0 REVIEWS ON WASTEWATER TREATMENT TECHNOLOGIES FOR HEAVY METAL REMOVAL FROM WASTEWATER

2.1 Introduction

Water is an important natural resource needed by man and the environment for healthy living (Rao *et al.*, 2017). Most of the developing countries including Botswana experience a solemn challenge of scarcity of water due to unreliable rainfall which results in persistent droughts. Globally, researchers are putting much effort into their investigations to discover possible ways to assure undisturbed access of good quality water. The use of treated industrial effluents for irrigation has been discovered as a solution to scarcity of water because it contains plant nutrients which may favours plant growth. However, such effluents are laden with substantial amounts of toxic heavy metals such as iron (Fe), nickel (Ni) and copper (Cu) which must be lowered prior to discharge to aquatic environments (Tytła, 2019). The sources of heavy metals are anthropogenic and natural activities such as industrial wastes, rock weathering, natural fires, volcanic eruptions (**Table 2.1**) (Farooq *et al.*, 2010). Such metals are reported to be neurotoxic, mutagenic, carcinogenic to human at higher concentrations (Farooq *et al.*, 2010).

It has been reported that some vegetable crops can uptake heavy metals from irrigation water and soils ending up into humans through food chain (Letshwenyo and Mokokwe, 2020). To alleviate a problem of ingesting food with accumulated heavy metals, national bodies such as Food Agriculture Organisation (FAO) and other organisations have set stringent laws for maximum contamination levels of heavy metals in irrigation water (**Table 2.3 and Table 2.4**). Moreover, locally, Botswana Standards (BOS) have also set threshold limit of toxic metal ions including Fe, Ni and Cu not to exceed concentration of 1.0 mgL^{-1} in aquatic environments and drinking water (**Table 2.2**).

Wastewater treatment techniques such as membrane adsorption (Khulbe and Matsuura, 2018) , chemical precipitation (Brbooti et al., 2011, Ramakrishnaiah and Prathima, 2016), reverse osmosis (Bakalár et al.,2009; Thaçi and Gashi, 2019), ion exchange resin (Tan *et al.*, 2017) and adsorption have been examined by numerous researchers for potential in heavy metal removal. Among such techniques, adsorption have been preferred as an effective technology with numerous advantages being secondary waste reduction, high metal extraction efficiency, low cost and many more (Zhang and Wang, 2015). To date, due to economic considerations,

industrial waste materials are preferred alternative adsorbents as they solve environmental problem like solid waste pollution.

To date, local brick manufacturing companies in Botswana generated large quantities of brick waste which pollute environment. The abundance and ready availability of such materials provide a low cost alternative to study its potential as an adsorbent. In the past, numerous materials have been investigated as adsorbents for heavy metal ion removal from wastewater. These include nanocomposite of montmorillonite for nickel (II) removal (Zhang and Wang, 2015), coal fly ash for divalent copper and nickel adsorptive removal (Lekgoba et al., 2020), tailings, adsorptive removal of nickel and copper waste rock, coal ash clinker and copper smelter slag (Letina and Letshwenyo, 2018) and many more. Cement brick waste can be considered as an ideal media for adsorption of heavy metals because of its structural and chemical properties such as high bulk density, various reactive minerals from cement, sand, crushed rock which favours the adsorption of heavy metals. Moreover, a nanolamellar structure of silicate minerals in clay or cementous materials have been reported to adsorb metals in broken surfaces due to its low swelling and dispersion of water (Barati *et al.*, 2013). Recently, strong affinity, high retention expensively modified media took attention of many researchers. However, substantial investigations on numerous practical issues such as structural strength, porosity, environmental friendliness of adsorbents were not much conducted. The review focuses on the use of brick waste and copper slag as novel adsorbents media for the removal of heavy metals from aqueous solutions. This review investigates the main characteristics considered during the selection of adsorbent media. The review also investigates the physiochemical process parameters influencing the performance of media on adsorption of heavy metals. The review also intends to identify some knowledge gaps from past studies on heavy metal removal by adsorption.

Table 2.1 Human toxicological effects and sources of some heavy metals (Farooq *et al.*, 2010)

Toxic Heavy metals	Anthropogenic/Natural Sources	Health effects	References
Lead (Pb)	Batteries, pigment, Electroplating industries	Damage of brain, anemia, lack of appetite, anorexia	(Niu, Xu and Wang, 1993; Gaballah and Kilbertus, 1998)
Mercury (Hg)	Mercury wear areas, volcanic eruptions, Forest fires from nature causes, battery production, burning fossil fuels, mining and metallurgy.	Renal and neurological damage, spoilage to the lung function, corrosive to eyes, skin and muscles, dermatitis, liver damage.	(Boening, 2000; Manohar *et al.*, 2002)
Chromium (VI) (Cr VI)	Leather tanning, textiles, metallurgy, wood preservation, paints and pigments.	Mutagenic, carcinogenic, teratogenic, epigastric pain, nausea, vomiting, severe diarrhea, lung tumors.	Singh *et al.*, 2008.
Arsenic (As)	Enamels, mining, energy production from fossil fuels, sediment rock weathering.	Gastrointestinal symptoms, damage to cardiovascular and nervous system, melanosis in bones, hemolysis, polyneuropathy, encephalopathy, liver tumor.	(Dudka and Markert, 1992)
Nickel (Ni)	Non-ferrous materials, mineral processing, formulation of paints, electroplating, coated porcelain, thermoelectric.	Chronic bronchitis, reduced lung function, lung cancer.	(Akhtar *et al.*, 2004; Öztürk, 2007)
Copper (Cu)	Electronics coating, galvanizing, paints production, printing, wood preservation.	Develops acute toxicity, neurotoxicity, sleep, and diarrhea.	(Yu *et al.*, 2000); Chuah *et al.*, 2005; Papandreou *et al*, 2007)
Cadmium (Cd)	Electroplating, enamel, pigments production, plastics, mining, refinery.	Carcinogenic, kidney damage, boney injury, hypertension, loss of appetite.	(Chen and Hao, 1998; Godt *etal* ., 2006)

Table 2.2 Maximum threshold of heavy metal concentrations in portable water formed by various regulatory bodies.

Permissible limit of toxic heavy metals for drinking water according to different bodies (mg/L)				
Heavy metal	**WHO**	**USEPA**	**EU standards**	**BOS**
Nickel	0.020	0.100	0.020	0.020
Lead	0.010	0.015	0.010	0.010
Zinc	3.000	5.000	-	0.01
Chromium	0.050	0.100	0.050	0.050
Arsenic	0.010	0.010	0.010	0.010
Copper	2.000	1.300	2.000	1.000
Cadmium	0.003	0.005	0.005	0.003

Table 2.3 Maximum Contaminated Level (MCL) in mg/L of heavy metals in waste water developed by various bodies (Babel and Kurniawan, 2003) .

Heavy metal ion concentrations (mgL^{-1})	**United States Environmental Protection Agency (USEPA)**
Arsenic	0.05
Cadmium	0.01
Chromium	0.05
Copper	0.25
Nickel	0.20
Zinc	0.80
Lead	0.006
Mercury	0.00003

Table 2.4 Recommended maximum concentration level for heavy metals in irrigation water established by Food Agriculture Organisation, Portugal and Canada (Vareda *et al.*,2019).

Heavy metal ion (µ g/L)	Food Agriculture Organisation	Portugal	Canada
Arsenic	100	100	100
Cadmium	10	10	5
Copper	200	200	-
Nickel	200	500	200
Zinc	2000	2000	1000 pH < 6.5
Lead	5000	5000	200
Mercury	-	-	-

2.2 Conventional methods for heavy metal removal

There have been some investigations on the reduction of heavy metal ions from water systems, in order to meet specified permissible levels put by regulatory bodies, and to minimise the environmental health effects of heavy metals. The commonly used conventional water treatment methods for the removal of heavy metals from effluents comprise of some of the following techniques (Blázquez *et al.*, 2009; Singha and Das, 2011):

- Chemical precipitation
- Flocculation and coagulation
- Ion exchange and Nano filtration
- Reverse osmosis
- Micro, Ultra Membrane filtration
- Flotation
- Biological
- Adsorption
- Electrodialysis (EDS)
- Reductive precipitation/ reduction crystallization

2.2.1 Heavy metal removal by chemical precipitation

Chemical precipitation is considered as one commonly applied effective methods for heavy metal removal (Ku and Jung, 2001). It operates by producing chemical precipitates of metals in the form of carbonates, phosphates, hydroxides and sulphides. Heavy metal or metal removal mechanism of chemical precipitation is based on generation of insoluble salts as precipitates. The mechanism is achieved by reaction of heavy metals in solution form with some precipitating agents. According to (Fu and Wang, 2011), during chemical precipitation there is production of fines which are enlarged with flocculants and removed through filtration as sludge. Large production of sludge and proper storage of chemical precipitating agents makes the method unfavourable due to high maintenance costs. Usually, chemical precipitation using hydroxide treatment technology is common due to its simplicity and low cost of lime used. It has been reported by Gunatilake, 2015 that distinct heavy metal hydroxide solubility is minimised in pH 8 up to 11. Some investigations were done by (Brbooti et al., 2011, Ramakrishnaiah and Prathima, 2016) on heavy metal removal by chemical precipitation.

2.2.2 Flocculation and Coagulation method

According to (López-Maldonado *et al.,* 2014), zeta potential measurement is a mechanism which this technology depends on to understand electrostatic effect between contaminant and flocculation-coagulation agents. Reduction of net surface charge of colloids in order to generate stability of electrostatic repulsive forces is done by coagulation method. According to (Tripathy and De, 2006), flocculation method is conducted after coagulation by continually enlarging colloidal particles to be easily separated individually by filtration or straining. (Amuda *et al.,* 2006) studied heavy metal removal from industrial effluents by coagulation-flocculation method by polymer addition in coagulation process applying Jar test protocol. The individual performance of ferric chloride and organic polymer and a combination of ferric chloride-polymer was examined. Findings showed that heavy metal removal was possible. However, flocculation and coagulation method have disadvantages which comprise of sludge generation and use of high cost chemicals (Guo et al., 2014).

2.2.3 Metal removal by Ion Exchange

This is a conventional water treatment technique which operates by ion exchange reversible mechanism. Here the pollutant ions are removed by ionic exchanging between ions solid and solution phase. According to (Jorgensen, 2002), ion exchange is commonly utilised in water softening; situations whereby calcium and magnesium ions exchange with ions of sodium in

liquid-solid phase. Moreover, (Jorgensen, 2002), reported that ion exchange is usually used to remove distinct pollutants such as nitrates, barium, arsenic, radium. The effectiveness of Ion exchange resin in heavy metal removal was studied by some researchers like (Tan *et al.*, 2017). Ion exchange treatment is accomplished by passage of polluted solution via resin beds which mostly manufactured by polymerization of organic composites. The main drawbacks of this technique are high regeneration costs of exhausted resins, specified or selective pollutant removal and low pollutant removal efficiency.

2.2.4 Micro, Ultra Membrane Filtration

Membrane filtration is a water treatment collective term which comes in different forms or types. Such types include membrane adsorption, microfiltration, ultrafiltration, and Nano-filtration. Usually microfiltration and ultrafiltration are applied in the suspended solids (SS) and turbidity or colour removal. According to (Trivunac and Stevanovic, 2006), micro and ultrafiltration are effective in heavy metal removal more especially divalent cadmium and zinc metal ions in solution pH of 9.0 utilising Diethylaminoethyl cellulose. The technology is deemed unsuitable for water and wastewater treatment due to high infrastructure and maintenance costs. In addition, according to (Joshi, 2017), such filtration techniques have some concerns over production of large sludge during treatment process thus limiting the method. According to (Englehardte *et al.*, 2013), ultrafiltration has daily capital cost of \$10,000 for 1.510 m^3 per day.

2.2.5 Biological Methods

Heavy metal removal from effluents through biological water treatment technology involves utilisation of microorganisms in treatment process. It has been reported by (Gunatilake, 2015), that microorganisms are responsible for solid settlement in effluents during effluent treatment. The application of microorganisms usually takes places in process such as activation of sludge, anaerobic digestion, trickling filtration. Bio-sorption and bio polymerisation are also other bio-techniques usually applied in water treatment. The merits of biological treatment method include cost effectiveness, high efficiency and eco-environmental friend. The drawbacks of the technique include high labour intensity; for instance, sufficient supply of volatile fatty acids is needed, thus making the method laborious more especially in fermentation processes. Constructed wetlands (CWs) are one of the eco techniques which can be applied in treatment of wastewater. Constructed wetlands are increasingly applied in the remediation of heavy metals and metalloids (Yu *et al.*, 2022). In this method, plants are utilised for bioaccumulation of water contaminants like heavy metals,

metalloids. CWs are considered cheap, resilient, environmental friendly water treatment technology (Kataki et al., 2021; Yu *et al.*, 2022) . In this technology, heavy metals and metalloids removal depends on a number of factors; plant species, substrate type and microbial activity (Yu *et al.*, 2022). However, the method is considered disadvantageous due to its instability and unpredictable heavy metal removal efficiencies (Yu *et al.*, 2022). The use of CWs for heavy metal removal from wastewater was investigated by some researchers (Gill *et al.*, 2017).

2.2.6 Floatation

Here surfactants are applied in surfaces of non-active materials to active their surfaces. During the activation of non-surface active materials a product formed as a float is removed by gas bubbling via a solution to generate foam. Documentation of studies on heavy metal and other contaminant removal using foam method has been done by (Ferguson et al., 1974; Robertson et al., 1976). The advantages of employing such a technique comprise of small production of concentrated sludge and simple operation. However, the method is deemed unfavourable due to concerns over minimal efficiency of floatation up surged by grain size and strength of ions in solution.

2.2.7 Reverse osmosis and Nano filtration

According to (Kim *et al.*, 2009), reverse osmosis is a treatment method which involves pressurisation of effluent molecules via semi-permeable cellulosic or polyamide membranes to scavenge pollutants in the effluent. Though, reverse osmosis is an effective heavy metal removal method, it is associated with high membrane regeneration costs as membranes are often damaged by chlorine in water (Kim *et al.*,2009). Some studies were conducted by (Bakalár et al.,2009; Thaçi and Gashi, 2019) to find the effectiveness of reverse osmosis on heavy metal removal.

The water treatment technique, Nano filtration operates by restoring and excluding ion charges present in the effluent. This technique depends on some influential factors for it to divide organic materials which are uncharged. Such influential factors include; filtration membrane size and pore or void distribution in a membrane. Investigations on the effectiveness of the techniques was done by (Khulbe and Matsuura, 2018) and found that metal ions were reduced in the solution. However, application this method is limited because it is associated with high expenses (Amin *et al.*, 2006). According to (Côté *et al.*, 2005), the nano filtration systems requires large amount of money; U$321/ ($m^3$·day) for only pre-treatment and infrastructure.

2.2.8 Electrodialysis (EDS)

Numerous industrial processes require huge volumes of water to operate (Razzak *et al.*, 2022). Therefore reduction, recovery, recycling of materials and other effluent products can be done for great economic beneficiation. Electrodialysis is defined as a water treatment technology whereby charged metal ions are separated from the solution using ion exchange membranes (Razzak *et al.*, 2022). The advantages of this method include its simplicity, high efficiency, elevated selectivity (Razzak *et al.*, 2022). However, this water treatment technology is associated with high operation costs mainly high energy consumption as well as fouling of membranes (Razzak *et al.*, 2022). Some studies were conducted on the application of electro-dialysis method on heavy metal removal from water (Sivakumar *et al.*, 2014). More studies on the application of EDS on heavy metal removal can be reviewed on (Razzak *et al.*, 2022).

2.2.9 Reductive precipitation/ reduction crystallization

According to (Mashifana et al., 2019), reduction crystallisation is defined as a process in which metal ions are reduced to their element state. Reduction is defined as a reaction process in which oxidation number of species is reduced by gaining of electrons (Mashifana et al., 2019). The method is almost similar to chemical precipitation besides that the recovery of soluble metal cations is done by chemical reduction (Phetla et al., 2012). Here, chemically reduced aqueous ions of metals are plated without the requirement of electrical current for deposition followed by electrodes plating process (Phetla et al., 2012). This water treatment technology involves the use of reducing agents for the recovery of metals. Numerous reducing agents can be utilised in the recovery of metals; for example gaseous reducing agents like sulphur dioxide, carbon monoxide, hydrogen and liquid reagents like sodium hypophosphite, hydrazine and borohydride. Among such reducing agents, hydrazine is considered strong reducing agent and can be applied in the recovery of heavy metals and precious metals (Mashifana et al., 2019). The costs of such reducing agents make the water treatment technology unfavourable. Researchers have done some studies on reduction of metal ions from solutions. For instance, a study on precipitation of nickel from salt solution by hydrogen reduction method was done. In this study, it was found that powder used can be modified using Ethylene Maleic Anhydride polymers (EMA) to improve its physical characteristics (Mashifana et al., 2019).

2.3 Heavy metal removal by adsorption

According to (Zhang and Wang, 2015), amid such conventional water treatment technologies, adsorption have been considered effective technology with some merits being secondary waste reduction, high metal removal efficiency, low maintenance and operation cost. Nowadays, for economic considerations, waste materials from industries are considered optional adsorbents. The most commonly used water treatment method, chemical precipitation was deemed unfavourable due to concerns over utilization of high cost chemicals requiring special handling and also leads to environmental pollution by sludge produced during treatment process. As a resolution to such an issue, different scientific researchers have found it fit that adsorptive removal of heavy metals utilizing high retention, environmental friendly effective and low cost media as adsorbents is required. **Table 2.5** exhibits findings on performance of media from previous studies on adsorptive removal of heavy metals from wastewater.

Table 2.5 Results of distinct media used for adsorption of heavy metals from previous studies

Heavy metal ions	Adsorbent	Ideal solution pH	Initial ionic concentration(mgL^{-1})	Removal efficiency (%)	Maximum capacity(mgg^{-1})	Applied batch isotherms models	Equilibrium contact time(hrs or mins)	Mode of adsorption	References
Ni (II)	Coal fly ash	7.0 -8.0	500	65.1	5.0	Freundlich	2hrs	Batch and Column	Lekgoba et al.,2020
Cu (II)		5.0-6.5		97.1	11.65	Modified Langmuir			
Pb (II)				82	44.83	Langmuir			
Cd (II)	Synthesised silicate tailings	6	20-1000	71	35.36	Freundlich	20hrs	Batch and Column	Ouyang et al.,2019
Cu (II)		7		98	32.26				
Cu (II)	Coal ash clinker	2.6	3.98	98	-	Langmuir	24 hrs	Batch and Column	Letina and Letshwenyo,2018
Ni (II)			32.00	46	-	Freundlich			
Cu (II)	Red soil	-	10-50	97.3	-	Langmuir	480 mins	Batch	Mishra et al.,2017
Ni (II)	Black soil	-	10	99.9	-	Freundlich Temkin	300mins		
Cu (II)	Activated Tunisian date stone	5.0	10-100	-	31.25	Dubinin-Radushkalich(D-R) Langmuir	2hrs	Batch	Bouhamed et al.,2012
Cu	Activated carbon of date stones	5.5	10-100	-	18.68	Langmuir	2hs	Bath	Bouhamed et al.,2016
Ni					16.12	Freundlich			
Zn					12.19				

2.3.1The competition for heavy metal removal with other common ions

Competition of heavy metals to be removed on active sites is mostly depending on the ionic radius and electronegativity of ions to be removed. It has been reported by (Osińska, 2017) that less adsorptive removal capacity of metals might be ascribed to large ionic radius and low electronegativity ,thus slow diffusion of metals into pores of media. The competition of coexisting ions with hexavalent chromium ion such as Sodium (Na^{+}), Calcium (Ca^{2+}), Magnesium (Mg^{2+}), Copper (Cu^{2+}) and Nickel (Ni^{2+}) were examined by (Hu et al., 2005). Cation exchange between sodium and calcium or magnesium is likely to occur during sorption. The competition of Nitrates (NO^{-3}) as well as Chlorides (Cl^{-}) during such a study was ignored as such ions are regarded poor ligands during sorption.

2.3.2 Factors influencing the selection of adsorbent

There are some factors influencing the selection of best media to be used for adsorption in field scales. These include retention capacity or contaminant removal efficiency, particle size, porosity, mineralogy, environmental friendliness, elemental composition and many others. Mineralogical and elemental content of adsorbent amid all other factors have been extensively utilised as a momentous factor to determine the potential of media in contaminant adsorptive removal. The presence of oxide and silicate minerals on media have been well known to be effective minerals which are ideal in adsorption processes (Tang and Lo, 2013). This has been evidenced by some investigators who used relative adsorbent; calcined brick powder foe adsorptive separation of Nickel and Hexavalent Chromium in wastewater (Hemalatha and Rao, 2014). In such study the optimal adsorptive removal efficiency of 81% and 75% at ideal pH of 2 and 4 was attained with respect to Hexavalent chromium and Nickel. Such good adsorptive characteristics were ascribed by the presence of oxides such as quartz. However, presence of the oxide, Lime (CaO) in the adsorbent has been reported to elevate the pH of solutions through dissolution of calcium ions from lime (Letshwenyo and Sima, 2020). According to (Ahmad *et al.*, 2012), calcite presence in the adsorbent may yield high heavy metal adsorptive characteristics. Prior to adsorption in field scale, the best or ideal size of the adsorbent has to be selected from batch and column adsorption findings. According to (Kara *et al.*, 2007), media of lager size is attributed to low adsorption capacities while smaller sized media is ascribed to higher sorption capacities due to presence of large surface area thus more available active sites for sorption.

2.3.3 Some Adsorbent characteristics used for selection of best adsorbent

There are some other factors which are used during selection best media for adsorption in field operations. Such factors include column regeneration potential, permeability, media leachability and natural pH of media (**Table 2.6**).

Table 2.6 Other examples of media features during adsorption

Some features of media	Remarks	Author
Thermogravimetric analysis(TGA)	Weight loss of media at 100-200 ^{o}C may be ascribed to moisture removal. Determines whether media undergone precipitation during sorption.	(Janbuala and Wasanapiarnpong, 2015)
pH Point of zero charge	Identifies the best pH conditions for adsorption	(Khan and Sarwar, 2007)
Leaching	Hazardous or leaching media limits its application.	Jing et al.,(2005)
Reusability or regeneration	Minimize disposal cost of media and allow recovery of some metals.	(Thallapalli and Prasad, 2015)
Media porosity	Porous adsorbent increases saturation time and generates high adsorption.	(Kumar *et al.*, 2019)

2.3.3.1Leaching behaviour of adsorbent

Leachability behaviour of adsorbent is an indicator of environmental friendliness of material used as an adsorbent. Various regulatory organisations such as WHO, USEPA, EU and others have posited and approved the maximum threshold of different heavy metals in aquatic environments. Numerous researchers in this area of adsorption have paid less attention to this issue of leaching behaviour of media, which can consequently lead to some similar health threats reviewed by (Farooq et al., 2010). The chosen media for heavy metal adsorption must be non- hazardous to the environment and should also possess high retention capacity. Some investigators or researchers have conducted studies on leaching behaviour of adsorbents as shown in (**Table 2.7**). The leaching tests were conducted both in batch and column mode as per studies reported by (Jing *et al.*, 2005) , (Yue *et al.*, 2010).

Table 2.7 Media leachability and toxicity results from previous studies

Adsorbent	Leachates	Mode of leaching	Remarks	References
GFO, Tio_2, GFH	As	Batch test utilizing WET &Toxicity Characteristic Leaching Procedure	(1)Leachate ionic concentration of Arsenic from GFH was higher than limits hence non-environment friend. (2) GFO as well as TiO_2 were environmental friend as Arsenic ionic concentration were less than permissible limit.	Jing *et al.*, 2005
Coal fly ash	As, Cr, Cu, Fe, Ni, Zn, Mn, Pb	Batch	All leachate concentrations were less than regulatory threshold, thus making media non-hazardous.	Lekgoba et al.,2020
Sewage sludge bricks	Cu, F^-, Pb, Zn, Se, Br^-, SO^{2-}_4, As, Ba, Cd, Co, Cr, Ni, Sb, Sn, Cl^-, Mo	Netherlands Leaching Tank	Bricks were non-leaching thus excellent adsorbents.	Cusidó and Cremades, 2012
Coal Ash clinker	Ni, Fe, Cu, Silica	Dynamic leaching test using Constant Head permeameter	Target leachates were lower than regulatory limit making coal ash clinker environmental friend.	Letina and Letshwenyo,2018
Red mud grains	Pb, Cd, Ag, Ba, As, Ni, ,Zn, Hg, Cr	Column leaching test	Leachate concentrations were less than permissible threshold.	Yue *et al.*, 2010

2.3.3.2 Adsorbent regeneration or Reusability

Reusability or regeneration potential of media has a goal, being the restoration of the adsorptive capacities of the used media. Regeneration of adsorbent is a great step as it outlines the numbers of cycles for media to be used before disposal. Though regeneration of adsorbent is important, according to (Lata *et al.*, 2015), less attention has been made recovery and recycling of such materials. Regeneration of adsorbents solves the problem of environmental pollution and may allow extraction or recovery of some metals. Media to be used for sorption of heavy metals should have high desorption efficiencies utilising low cost eluents or regeneration agents, to reduce disposal and replacement costs. **Table 2.8** illustrates different regeneration findings from previous studies outlining eluents utilised, desorption efficiencies of media and recovery of metals from exhausted media.

Table 2.8 Regeneration or reusability findings from other reports

Media	Contaminant	Regeneration Eluent	Desorption Efficiency (%)	Metal ion recovery	Comment	Reference
Maghemite	Cr	0.01M NaOH, 0.01M $NaHCO_3$ 0.01M Na_2CO_3 0.01M Na_3PO_4	19.70 87.70 73.50 69.60 82.90	No metal recovery	NaOH, Na_2CO_3 & Na_3PO_4 were used as eluents. NaOH was most effective. Disposal of metal free adsorbents was not considered.	(Hu et al., 2005)
Iron-oxide-coated-sand	Pb (II) Cd (II) Cu (II)	Water recovery Acid recovery Base recovery	-	101 % 86 % 84 %	The recovery of most metals was efficient. The recovery was inefficient neither with acid nor with base.	(Benjamin *et al.*, 1996)
Manganese dioxide-coated sand	As (III) As (V)	0.2 N NaOH and Water	-	94.6–98.3 % For 10 cycles	More investigations are required for regeneration of the adsorbent for safe disposal.	Bajpai and Chaudhuri (1999)
Red mud	As (V) As (III) Se (VI) Se (IV)	NaOH	78–85 % 26–49 % 90–92 % 43–58 %	No metal recovery	Safe disposal of adsorbent is matter of concern. Recovery of metals must be considered as an alternative.	(Zhou and Haynes, 2012)
Titanium dioxide nanoparticles	Pb (II) Cu (II) Zn (II)	0.01 M NaNO3 metal-free solution	49 % 85 % 88 % at pH 4 in 15 minutes	97 % initial metal concentration and 95 % TiO2 recovered	Recovery and regeneration alternatives or options were mentioned in further studies	(Hu and Shipley, 2012)

2.4 Knowledge Gaps identified from the review

- There are a few reports where bricks waste as an adsorbent was used for heavy metal removal from effluents (Shahat and Shehata, 2013). Although the effect of various parameters such as contact time, pH of solutions, media dosage and metal concentration on adsorption has been studied, there is paucity of information on media compressive strength, media permeability, leachability, regeneration or desorption of media. In response, an evaluation of brick waste adsorbents particularly their leachability and toxicity is required for proper understanding of potential use of brick waste as an adsorbent in field works. Despite such factors, there are no studies available only on the influence of competitive ions coexisting with heavy metals on adsorption of both brick waste and copper smelter slag.

- Copper smelter slag has been also used as an adsorbent of Nickel and Copper ions from mine wastewater in few studies (Letina and Letshwenyo, 2018). Though factors such as leachability of media, effect of pH of solution were studied, the influence of permeability on adsorption capacity of the copper smelter slag was not studied. Consequently, its permeability as well as its influence on adsorption capacity has to be determined.

- Moreover, there are few reports available on the effect of (brick waste and copper smelter slag) on heavy metal adsorption suggesting that adsorption takes place at lower pH while at high pH precipitation occur (Bennour, 2012). Consequently, a study on the influence of natural pH of such materials on adsorption is required.

- There are also little documentation of previous studies describing the thermodynamic nature of adsorption process of heavy metals using brick waste and copper smelter slag.

Therefore in response, this research seeks to close some of the gaps identified from this literature by investigating the potential of brick waste and copper smelter slag in adsorption of heavy metals from aqueous solutions.

References

Ahmad, K., Bhatti , I.J , Muneer,M, Iqbaland,M and Iqbal,Z.(2012) 'Removal of heavy metals (Zn , Cr , Pb , Cd , Cu and Fe) in aqueous media by calcium carbonate as an adsorbent', *International Journal of Chemical and Biochemical Sciences*, 2, pp. 48–53.

Akhtar, N., Iqbal, J. and Iqbal, M. (2004) 'Removal and recovery of nickel(II) from aqueous solution by loofa sponge-immobilized biomass of Chlorella sorokiniana: Characterization studies', *Journal of Hazardous Materials*, 108(1–2), pp. 85–94. doi: 10.1016/j.jhazmat.2004.01.002.

Amin, N., Kaneco,S, Kitagawa,T, Begum,A, Katsumata,H, Suzuki, T . and Ohta,K. (2006) 'Removal of arsenic in aqueous solutions by adsorption onto waste rice husk', *Industrial and Engineering Chemistry Research*, 45(24), pp. 8105–8110. doi: 10.1021/ie060344j.

Amuda, O.S., Amoo, I.A, Ipinmoroti, K.O . and Ajayi, O.O.(2006) 'Coagulation / flocculation process in the removal of trace metals present in industrial wastewater', *Journal of Applied Sciences and Environmental Management*, 10(3), pp. 1–4. doi: 10.4314/jasem.v10i3.17339.

Babel, S. and Kurniawan, T. A. (2003) 'Low-cost adsorbents for heavy metals uptake from contaminated water: A review', *Journal of Hazardous Materials*, 97(1–3), pp. 219–243. doi: 10.1016/S0304-3894(02)00263-7.

Bakalár, T., Búgel, M. and Gajdošová, L. (2009) 'Heavy metal removal using reverse osmosis', *Acta Montanistica Slovaca*, 14(3), pp. 250–253.

Barati, A. *et al.* (2013) 'Removal and recovery of copper and nickel ions from aqueous solution by poly(methacrylamide-co-acrylic acid)/montmorillonite nanocomposites', *Environmental Science and Pollution Research*, 20(9), pp. 6242–6255. doi: 10.1007/s11356-013-1672-3.

Benjamin, M. M., Sletten,R.S, Bailey,R.P. and Bennett,T. (1996) 'Sorption and filtration of metals using iron-oxide-coated sand', *Water Research*, 30(11), pp. 2609–2620. doi: 10.1016/S0043-1354(96)00161-3.

Blázquez, G., Hernáinz, F. Calero, M, Martín-Lara, M.A .and Tenorio,G. (2009) 'The effect of pH on the biosorption of Cr (III) and Cr (VI) with olive stone', *Chemical Engineering Journal*, 148(2–3), pp. 473–479. doi: 10.1016/j.cej.2008.09.026.

Boening, D. W. (2000) 'Ecological effects, transport, and fate of mercury: A general review', *Chemosphere*, 40(12), pp. 1335–1351. doi: 10.1016/S0045-6535(99)00283-0.

Brbooti, M. M., Abid, B. a and Al-shuwaiki, N. M. (2011) 'Removal of Heavy Metals Using Chemicals Precipitation', *Enginering and Technology Journal*, 29(August 2017).

Chandra Joshi, N. (2017) 'Heavy metals, conventional methods for heavy metal removal, biosorption and the development of low cost adsorbent', *European Journal of Pharmaceutical and Medical Research*, 4((2)), pp. 388–393.

Chen, J. M. and Hao, O. J. (1998) 'Microbial chromium (VI) reduction', *Critical Reviews in Environmental Science and Technology*, 28(3), pp. 219–251. doi: 10.1080/10643389891254214.

Chuah, T. G., Jumasiah, A, Azni, I, Katayon, S. and Thomas Choong, S.Y. (2005) 'Rice husk as a potentially low-cost biosorbent for heavy metal and dye removal: An overview', *Desalination*, 175(3), pp. 305–316. doi: 10.1016/j.desal.2004.10.014.

Côté, P., Siverns, S. and Monti, S. (2005) 'Comparison of membrane-based solutions for water reclamation and desalination', *Desalination*, 182(1–3), pp. 251–257. doi: 10.1016/j.desal.2005.04.015.

Cusidó, J. A. and Cremades, L. V. (2012) 'Environmental effects of using clay bricks produced with sewage sludge: Leachability and toxicity studies', *Waste Management*, 32(6), pp. 1202–1208. doi: 10.1016/j.wasman.2011.12.024.

Dudka, S. and Markert, B. (1992) 'Baseline concentrations of As, Ba, Be, Li, Nb, Sr and V in surface soils of Poland', *Science of the Total Environment, The*, 122(3), pp. 279–290. doi: 10.1016/0048-9697(92)90046-U.

El-shahat, M. F. and Shehata, A. M. A. (2013) 'Adsorption of lead, cadmium and zinc ions from industrial wastewater by using raw clay and broken clay-brick waste', *Asian Journal of Chemistry*, 25(8), pp. 4284–4288.

Englehardt, J. D., Wu, T. and Tchobanoglous, G. (2013) 'Urban net-zero water treatment and mineralization: Experiments, modeling and design', *Water Research*. Elsevier Ltd, 47(13), pp. 4680–4691. doi: 10.1016/j.watres.2013.05.026.

Farooq, U. Kozinski, J.A , Khan,M.A .and Athar,M.(2010) 'Biosorption of heavy metal ions using wheat based biosorbents - A review of the recent literature', *Bioresource Technology*. Elsevier Ltd, 101(14), pp. 5043–5053. doi: 10.1016/j.biortech.2010.02.030.

Fu, F. and Wang, Q. (2011) 'Removal of heavy metal ions from wastewaters: A review', *Journal of Environmental Management*. Elsevier Ltd, 92(3), pp. 407–418. doi: 10.1016/j.jenvman.2010.11.011.

Gaballah, I. and Kilbertus, G. (1998) 'Recovery of heavy metal ions through decontamination

of synthetic solutions and industrial effluents using modified barks', *Journal of Geochemical Exploration*, 62(1–3), pp. 241–286. doi: 10.1016/S0375-6742(97)00068-X.

Gill, L. W. *et al.* (2017) 'Long term heavy metal removal by a constructed wetland treating rainfall runoff from a motorway', *Science of the Total Environment*. Elsevier B.V., 601–602, pp. 32–44. doi: 10.1016/j.scitotenv.2017.05.182.

Godt, J., Scheidig, F, Grosse-Siestrup,C, Esche,V, Brandenburg,P, Reich,A. and Groneberg,D.A.(2006) 'The toxicity of cadmium and resulting hazards for human health', *Journal of Occupational Medicine and Toxicology*, 1(1), pp. 1–6. doi: 10.1186/1745-6673-1-22.

Gunatilake, S. K. (2015) 'Methods of Removing Heavy Metals from Industrial Wastewater', 1(1), pp. 12–18.

Guo, T., Englehardt, J. and Wu, T. (2014) 'Review of cost versus scale: Water and wastewater treatment and reuse processes', *Water Science and Technology*, 69(2), pp. 223–234. doi: 10.2166/wst.2013.734.

Hemalatha, P. V and Rao, V. V. P. (2014) 'Adsorption Batch Studies on Calcined Brick Powder in Removing Chromium and Nickel Ions', *International Journal of Advanced Research in Chemical Science (IJARCS)*, 1(6), pp. 14–21. Available at: www.arcjournals.org.

Hsu, H. W., Bondy, S. C. and Kitazawa, M. (2018) 'Environmental and dietary exposure to copper and its cellular mechanisms linking to Alzheimer's disease', *Toxicological Sciences*, 163(2), pp. 338–345. doi: 10.1093/toxsci/kfy025.

Hu, J., Chen, G. and Lo, I. M. C. (2005) 'Removal and recovery of Cr(VI) from wastewater by maghemite nanoparticles', *Water Research*, 39(18), pp. 4528–4536. doi: 10.1016/j.watres.2005.05.051.

Hu, J. and Shipley, H. J. (2012) 'Evaluation of desorption of Pb (II), Cu (II) and Zn (II) from titanium dioxide nanoparticles', *Science of the Total Environment*. Elsevier B.V., 431, pp. 209–220. doi: 10.1016/j.scitotenv.2012.05.039.

Janbuala, S. and Wasanapiarnpong, T. (2015) 'Effect of rice husk and rice husk ash on properties of lightweight clay bricks', *Key Engineering Materials*, 659(July 2017), pp. 74–79. doi: 10.4028/www.swcientific.net/KEM.659.74.

Jing, C., Liu,S,Patel,M. and Meng,X. (2005) 'Arsenic leachability in water treatment adsorbents', *Environmental Science and Technology*, 39(14), pp. 5481–5487. doi: 10.1021/es050290p.

Jorgensen, T. C. (2002) 'Removal of ammonia from wastewater by ion exchange in the

presence of organic compounds. M.Sc. Thesis, Department of Chemical and Process Engineering, University of Canterbury ,Christchurch, New Zealand', *Graduate Theses and Dissertations*.

Kara, S., Aydinera, C, Demirbasb, E, Kobyaa, M .and Dizge, N. (2007) 'Modeling the effects of adsorbent dose and particle size on the adsorption of reactive textile dyes by fly ash', *Desalination*, 212(1–3), pp. 282–293. doi: 10.1016/j.desal.2006.09.022.

Khan, M. N. and Sarwar, A. (2007) 'Determination of points of zero charge of natural and treated adsorbents', *Surface Review and Letters*, 14(3), pp. 461–469. doi: 10.1142/S0218625X07009517.

Khulbe, K. C. and Matsuura, T. (2018) 'Removal of heavy metals and pollutants by membrane adsorption techniques', *Applied Water Science*. Springer Berlin Heidelberg, 8(1), pp. 1–30. doi: 10.1007/s13201-018-0661-6.

Kim, M. *et al.* (2009) 'appendix a . supporting information Arsenic removal from Vietnamese groundwater using the arsenic-binding DNA aptamer', pp. 1–13.

Ku, Y. and Jung, I. L. (2001) 'Photocatalytic reduction of Cr(VI) in aqueous solutions by UV irradiation with the presence of titanium dioxide', *Water Research*, 35(1), pp. 135–142. doi: 10.1016/S0043-1354(00)00098-1.

Kumar, P.S., Korving,L, Keesman,K.J , Loosdrecht,M.C.M .and Witkamp,G. (2019) 'Effect of pore size distribution and particle size of porous metal oxides on phosphate adsorption capacity and kinetics', *Chemical Engineering Journal*. Elsevier, 358(July 2018), pp. 160–169. doi: 10.1016/j.cej.2018.09.202.

Lata, S., Singh, P. K. and Samadder, S. R. (2015) 'Regeneration of adsorbents and recovery of heavy metals: a review', *International Journal of Environmental Science and Technology*, 12(4), pp. 1461–1478. doi: 10.1007/s13762-014-0714-9.

Lekgoba, T., Ntuli, F. and Falayi, T. (2020) 'Application of coal fly ash for treatment of wastewater containing a binary mixture of copper and nickel', *Journal of Water Process Engineering*. Elsevier Ltd, (July), p. 101822. doi: 10.1016/j.jwpe.2020.101822.

Letina, D. and Letshwenyo, W. M. (2018) 'Investigating waste rock, tailings, slag and coal ash clinker as adsorbents for heavy metals: Batch and column studies', *Physics and Chemistry of the Earth*. Elsevier, 105(March), pp. 184–190. doi: 10.1016/j.pce.2018.02.013.

Letshwenyo, M. W. and Mokokwe, G. (2020) 'Accumulation of heavy metals and bacteriological indicators in spinach irrigated with further treated secondary wastewater',

Heliyon. Elsevier Ltd, 6(10), p. e05241. doi: 10.1016/j.heliyon.2020.e05241.

Letshwenyo, M. W. and Sima, T. V. (2020) 'Phosphorus removal from secondary wastewater effluent using copper smelter slag', *Heliyon*. Elsevier Ltd, 6(6), p. e04134. doi: 10.1016/j.heliyon.2020.e04134.

López-Maldonado, E. A., Oropeza-Guzmana, M.T, Jurado-Baizavala, J.L.and Ochoa-Terán, A. (2014) 'Coagulation-flocculation mechanisms in wastewater treatment plants through zeta potential measurements', *Journal of Hazardous Materials*. Elsevier B.V., 279, pp. 1–10. doi: 10.1016/j.jhazmat.2014.06.025.

Manohar, D. M., Krishnan, K. A. and Anirudhan, T. S. (2002) 'Removal of mercury (II) from aqueous solutions and chlor-alkali industry wastewater using', *Water research*, 36, pp. 1609–1619.

Mashifana, T. P., Matshavha, R. and Magwa, N. (2019) 'Reduction crystallization of nickel with hydrazine in the presence of an additive ethylene maleic anhydride', *Procedia Manufacturing*. Elsevier B.V., 35, pp. 649–656. doi: 10.1016/j.promfg.2019.07.009.

Niu, H., Xu, X. S. and Wang, J. H. (1993) 'Communication to the Editor Removal of Lead from Aqueous Solutions by Penicillium Biomass', *Biotechnology and Bioengineering*, 42, pp. 785–787.

Osińska, M. (2017) 'Removal of lead(II), copper(II), cobalt(II) and nickel(II) ions from aqueous solutions using carbon gels', *Journal of Sol-Gel Science and Technology*, 81(3), pp. 678–692. doi: 10.1007/s10971-016-4256-0.

Öztürk, A. (2007) 'Removal of nickel from aqueous solution by the bacterium Bacillus thuringiensis', *Journal of Hazardous Materials*, 147(1–2), pp. 518–523. doi: 10.1016/j.jhazmat.2007.01.047.

Papandreou, A., Stournaras, C. J. and Panias, D. (2007) 'Copper and cadmium adsorption on pellets made from fired coal fly ash', *Journal of Hazardous Materials*, 148(3), pp. 538–547. doi: 10.1016/j.jhazmat.2007.03.020.

Phetla, T. P., Ntuli, F. and Muzenda, E. (2012) 'Reduction crystallization of Ni, Cu, Fe and Co from a mixed metal effluent', *Journal of Industrial and Engineering Chemistry*. The Korean Society of Industrial and Engineering Chemistry, 18(3), pp. 1171–1177. doi: 10.1016/j.jiec.2012.01.008.

Ramakrishnaiah, C. R. and Prathima, B. (2016) 'Hexavalent Chromium Removal by

Chemical Precipitation Method : A Comparative Study', *International Journal of Environment Research and Development*, 1(January 2011), pp. 41–49.

Rao, V. D., Rao,M.V.S. and Murali Krishna, M.P.S. (2017) 'Removal of Chromium (VI) from aqueous solutions using chemically activated Syzygium cumini leaves carbon Powder as an adsorbent', 10(8), pp. 20–27. doi: 10.9790/5736-1008012027.

Razzak, S. A. *et al.* (2022) 'A comprehensive review on conventional and biological-driven heavy metals removal from industrial wastewater', *Environmental Advances*. Elsevier Ltd, 7(October 2021), p. 100168. doi: 10.1016/j.envadv.2022.100168.

Singh, R. K.,Kumara,S, Kumara,S . and Kumar,A.(2008) 'Development of parthenium based activated carbon and its utilization for adsorptive removal of p-cresol from aqueous solution', *Journal of Hazardous Materials*, 155(3), pp. 523–535. doi: 10.1016/j.jhazmat.2007.11.117.

Singha, B. and Das, S. K. (2011) 'Biosorption of Cr(VI) ions from aqueous solutions: Kinetics, equilibrium, thermodynamics and desorption studies', *Colloids and Surfaces B: Biointerfaces*. Elsevier B.V., 84(1), pp. 221–232. doi: 10.1016/j.colsurfb.2011.01.004.

Sivakumar, D. *et al.* (2014) 'Application of electro-dialysis on removal of heavy metals', *Pollution Research*, 33(3), pp. 627–631.

Tan, J. J. *et al.* (2017) 'Ion Exchange Resin on Treatment of Copper and Nickel Wastewater', *IOP Conference Series: Earth and Environmental Science*, 94(1). doi: 10.1088/1755-1315/94/1/012122.

Tang, S. C. N. and Lo, I. M. C. (2013) 'Magnetic nanoparticles: Essential factors for sustainable environmental applications', *Water Research*. Elsevier Ltd, 47(8), pp. 2613–2632. doi: 10.1016/j.watres.2013.02.039.

Thaçi, B. S. and Gashi, S. T. (2019) 'Reverse osmosis removal of heavy metals from wastewater effluents using biowaste materials pretreatment', *Polish Journal of Environmental Studies*, 28(1), pp. 337–341. doi: 10.15244/pjoes/81268.

Thallapalli, B. and Prasad, S. (2015) 'Removal of Chromium From Wastewater Using Low Cost Removal of Chromium From Wastewater Using Low', *World Journal of Pharmacy and Pharmaceutical Sciences*, 4(10).

Tripathy, T. and De, B. R. (2006) 'JPS10art9', 10, pp. 93–127.

Trivunac, K. and Stevanovic, S. (2006) 'Removal of heavy metal ions from water by complexation-assisted ultrafiltration', *Chemosphere*, 64(3), pp. 486–491. doi:

10.1016/j.chemosphere.2005.11.073.

Tytła, M. (2019) 'Assessment of Heavy Metal Pollution and Potential Ecological Risk in Sewage Sludge from Municipal Wastewater Treatment Plant Located in the Most Industrialized Region in Poland—Case Study', *International Journal of Environmental Research and Public Health*, 16(13), p. 2430. doi: 10.3390/ijerph16132430.

Vareda, J. P., Valente, A. J. M. and Durães, L. (2019) 'Assessment of heavy metal pollution from anthropogenic activities and remediation strategies: A review', *Journal of Environmental Management*. Elsevier, 246(December 2018), pp. 101–118. doi: 10.1016/j.jenvman.2019.05.126.

Yu, B., Zhang,Y, Alka Shukla,Shukla,S.S. and Dorris,K.L. (2000) 'The removal of heavy metal from aqueous solutions by sawdust adsorption - Removal of copper', *Journal of Hazardous Materials*, 80(1–3), pp. 33–42. doi: 10.1016/S0304-3894(00)00278-8.

Yu, G. *et al.* (2022) 'Enhanced removal of heavy metals and metalloids by constructed wetlands: A review of approaches and mechanisms', *Science of the Total Environment*. Elsevier B.V., 821, p. 153516. doi: 10.1016/j.scitotenv.2022.153516.

Yue, Q., Zhao,Y, Li,Q, Li,W, Gao,B, Han,S, Qi,Y .and Yu,H.(2010) 'Research on the characteristics of red mud granular adsorbents (RMGA) for phosphate removal', *Journal of Hazardous Materials*, 176(1–3), pp. 741–748. doi: 10.1016/j.jhazmat.2009.11.098.

Zhang, X. and Wang, X. (2015) 'Adsorption and desorption of Nickel(II) ions from aqueous solution by a lignocellulose/montmorillonite nanocomposite', *PLoS ONE*, 10(2), pp. 1–21. doi: 10.1371/journal.pone.0117077.

Zhou, Y. F. and Haynes, R. J. (2012) 'A comparison of water treatment sludge and red mud as adsorbents of As and Se in aqueous solution and their capacity for desorption and regeneration', *Water, Air, and Soil Pollution*, 223(9), pp. 5563–5573. doi: 10.1007/s11270-012-1296-0.

CHAPTER 3: MATERIALS AND METHODS

3.1. Sampling and Preparation of media

Samples of different clay brick waste were randomly collected from waste heaps of a brick manufacturing companies named Makoro (PTY) Ltd and Bothakga Concrete Products (PTY) Ltd. The samples were mixed to give a representative of the brick waste produced at Makoro (PTY) Ltd. Copper smelter slag samples were collected at BCL (Ltd) mine using the same protocol for clay brick waste. Cement brick waste was sourced from a local brick manufacturing company. Each media was washed with deionised water (DI) to remove soluble organic materials and other impurities. Media was air dried after washing with DI water. The dried media was ground into smaller particles using a jaw crusher to be used for batch and column experimental studies.

3.2 Characterisation of adsorbents

3.2.1 Determination of mineral composition of adsorbents

Each media particles were ground with a pulveriser. Initially, the pulverising cups and charge balls were cleaned with DI water and Ethanol to avoid media contamination with other impurities. 200g of particles of each media were placed into pulverising cups with 8 charge balls. A pulveriser was then run for 30minutes. All ground samples were placed in sample bags and sealed to avoid contamination with external the environment. Powdered samples of both brick waste and smelter slag were taken to physics laboratory for determination of mineral composition using X-Ray powder diffraction (Brucker, D8 Advance). X-Ray powder diffraction machine was calibrated prior determination of mineralogical composition. XRD patterns with peaks of each media were produced from X-Ray powder diffraction (Brucker, D8 Advance). XRD pattern peaks were matched different standards and detected crystalline phases present. Mineral content of various minerals such as silicates, oxides was determined using Match! 3software.

3.2.2 Determination of elemental composition of adsorbents

Preparation of media for elemental composition test: Each media particles were pulverised with a pulveriser. The pulverising cups and charge balls were cleaned with an alcohol (Ethanol) to avoid contamination of the sample with impurities from other media previously used. The particles of each media (200 g) were placed into pulverising cups with 8 charge balls and run for 30 minutes. The whole pulverised samples were placed in samples bags and sealed to avoid contamination by external environment. Pulverised samples of each media were taken to the laboratory for determination of elemental concentrations using X-Ray-

Fluorescence Analyser (Delta Professional). XRF Analyser (Delta Professional) was calibrated using steel coins prior determination of elemental composition. A report showing different elemental concentrations in ppm was produced from XRF.

3.2.3 Determination of pH of media

The pH of both brick and copper smelter slag waste were determined in accordance with ASTM D4972 -95A standard operating procedures, as per the protocol of SOPS for soil pH determination adopted from (US EPA, 2002).

The pH meter (Multi-Parameter PCS Testr^{TM} 35) was initially standardized or calibrated using buffer solutions, 4.00, 7.00 and 10.00 every three hours prior to pH measurement. Raw media was air dried at room temperatures (27^{o}C). Media sample was sieved through a NO.10 sieve (2.00 mm mesh) to remove coarser fractions.10grams of air-dried and sieved media sample was weighted and mixed with 10 mL deionised water. The mixture was thoroughly shaken and allowed to stand for about 1 hour. Samples were analysed immediately after 1hr. The measurements were accomplished by rinsing the probes of pH meter with double distilled water. The probes were therefore blot dried and the electrode was placed in a partially settled media sample suspensions. Readings displayed on a meter were recorded once the meter readings stabilised.

3.2.2 Techniques Used For Physical Characterisation of Media

3.2.2.1 Grain size distribution of media

The particle size of media was determined through mechanical sieving in accordance with American Society for Testing Materials (ASTM C136) standard procedure. The coefficient of uniformity *(Cu)* of the media was also determined after grounding the brick waste. In case of copper smelter slag, particle size distribution and coefficient of uniformity were determined directly as media was already in granular form. To measure how uniformly distributed the media particles are, uniformity coefficients *(Cu)* of media were computed using the following equation:

$$\mathrm{Cu} = \frac{\mathrm{D60}}{\mathrm{D10}} \qquad (1)$$

where Cu denote uniformity coefficient, D10 is the diameter of the particle size distribution curve corresponding to 10% by weight Finer and 90% are larger whereas D60 is the diameter corresponding to 60% finer in particle size distribution curve and 40% are larger particles.

Gradation coefficient (Cc) of media was determined using the equation below:

$$Cc = \frac{(D30)^2}{D60 \times D10} \quad (2)$$

where Cc is grade coefficient,D30 is the diameter of the particle size curve corresponding to 30% by weight (Finer) and 70% larger and D10 as well as D60 are the same as mentioned above.

3.2.2.2 Determination of particle density (ρ_p) bulk density (ρ_b), porosity (n) of the media

Bulk density (ρ_b) of the adsorbents was determined by transferring 50 g of the media into a 100 mL measuring cylinder. The media was allowed to settle in a measuring cylinder. The settling of the media was accomplished by taping the cylinder three times. The volume of the media was read and recorded carefully. The bulk density was calculated as per (Dan-Asabe *et al.*, 2013) using the following equation:

$$\rho b = \frac{\text{mass of media(g)}}{\text{volume of media(mL)}} \quad (3)$$

Particle density (ρ_p) is the ratio of the total mass of solids to the volume of solids. The determination of particle density was achieved by adding 60 mL of water to a 100 mL measuring cylinder and the volume of water was recorded assuming its density to be 1.0 g cm $^{-3}$. A 50g of the media was then transferred into the measuring cylinder containing water. The mixture was then carefully stirred in order to remove air trapped between water and media particles. The volume of the media and water was then recorded. The difference between the two volumes was recorded as the volume of the particles of media. The mathematical equation employed in determination of particle density is as follows:

$$\rho_p = \frac{\text{mass of media(g)}}{\text{particle's volume(mL)}} \quad (4)$$

Porosity is the portion of media occupied by the pores. It is calculated using the values of bulk and particle density using the following equation;

$$n=(1-\frac{\rho b}{\rho p})\times 100 \quad (5)$$

where; n is the porosity (%), ρ_b is the bulk density and (g cm $^{-3}$), ρ_p is the particle density (g cm $^{-3}$) of the media.

The data of porosity of media was supported by determination of the surface morphology of media using Scanning Electron Microscopy (JEOL7100SEM). SEM images were observed before and after heavy metal loadings to study the differences in micro-pores of media before and after adsorption.

3.2.2.3 Determination of permeability and hydraulic conductivity of media

Permeability test measures the rate of the flow of water through the pores of media. This test was accomplished by forcing the water at constant pressure into media specimen of known dimensions. The rate of flow was therefore determined. To determine the hydraulic conductivity of the media, constant head method was used since it is suitable for granular materials. The procedure for the test was achieved by allowing the water to move through the media (both brick waste and copper smelter slag) under steady state conditions. The volume of water flowing through the media was measured over period of time. The coefficient of permeability (K) for the method was determined using the following equation as per (Letina and Letshwenyo, 2018):

$$K = \frac{QL}{Ath} \quad (6)$$

where, K denotes coefficient of permeability, Q denote discharge of water, L denote distance between manometers, A is cross-sectional area of media, t is sum of time of discharge and h is difference in head on manometers.

3.2.3 Techniques used for chemical characterisation of media

3.2.3.1 Leachability test of media

The leaching behaviour of CSS, MGS, CBW and MGBW was studied through agitating adsorbents for 24, 48 and 72 hours using DI water of pH 6.81. After those contact times the mixtures were separated by filtering and leachates were subjected to ICP-OES to measure concentrations of metal ions. The filtrate was analysed for concentration of heavy metals (Cd, Cu, Cr, Hg, Zn, Ni, P b, As) using Inductively Coupled Plasma Optical Emission Spectrometer (iCAP 7000SERIES). The target elements were identified by the X-Ray Fluorescence Analyser (Delta Professional). Batch experimental tests were conducted in duplicates and mean values and standard deviations were calculated. ICP-OES (iCAP 7000SERIES) was calibrated prior each analysis. The concentration values of borderline metals were compared with Environmental Agency (USEPA) threshold values. The comparison was done to determine the vulnerability of the media to be toxic.

3.2.3.2 Determination of pH point of zero charge (pH_{pzc}) of adsorbents using pH drift method

Point of zero charge is defined as pH at which the surface of media is globally neutral. An aqueous solution (0.01 M NaCl) was initially prepared and adjusted to a pH value between 2 and 10. The adjustment of pH achieved using 0.5 M HCL and or 0.5 M NaOH. An adsorbent of mass 0.2 g was added to 50 mL of pH adjusted NaCl solution in a capped vial and was

agitated for 24 hr. The solution was filtered with 0.45 µm Cellulose Nitrate Filter membrane its final pH was measured and plotted against the initial pH. The pH p z c was taken as the pH at which the line of graph crosses the initial pH equivalent to final pH. This method is called pH drift method and was reported as per Hajira et al., (2018).

3.2.3.3 Thermogravimetric analysis (TGA): Thermogravimetric analysis (TGA) was used to evaluate the thermal stability of the adsorbent using TGA/DSC3+, manufactured by Mettler Toledo, 2018. The atmospheric gas used during TGA analysis was the Nitrogen gas at 20 mL.

Table 3.1 Summary of media characterisation and their purpose

Parameters	Analytical method used	Purpose of test	References
Media mineralogy	X- ray Diffraction (XRD)	To identify and quantify mineral content of media.	(Sima *et al.*, 2018)
Media elemental composition	X-ray Fluorescence (XRF)	To find the composition of elements on media.	(Sima *et al.*, 2018)
Porosity of media	Porosity	To find how porous the media is.	(Dan-Asabe *et al.*, 2013)
Bulk density	Bulk density	To determine whether media will float or sink in wastewater.	(Dan-Asabe *et al.*, 2013)
Permeability	Constant head method	To determine the permeability of media.	(Letina and Letshwenyo, 2018)
Functional groups	Fourier Transform Infra-Red	To determine functional groups present in the adsorbent.	(Lekgoba et al., 2020)
Particle size distribution	ASTM (C136)	To find the distribution of particle sizes. Coefficient of uniformity *(Cu)* and gradation *(Cc)* as well as effective grain size of media *(D10)* were also determined in this analysis.	(Sima *et al.*, 2018)
Media leachability	Batch leaching test	This test was performed to determine the leachability and toxicity potential of media. This test was used to find the environmental effects of using media as adsorbents.	(Lekgoba et al., 2020)
pH point of zero charge (pH_{pzc})	pH drift method	To determine pH at which global surface charge of media is equals to zero.	Hajira et al., (2018)
Surface morphology	Scanning Electron Microscopy (SEM)	To investigate the morphological surface of media.	(Sima *et al.*, 2018)
Thermogravimetric Analysis	Thermogravimetric analyser (TGA)	To investigate thermal stability of media.	(Janbuala and Wasanapiarnpong, 2015)

3.3 Preparation of synthetic water samples for batch and column studies

Synthetic water imitating the basic chemistry of industrial wastewater was prepared using hydrated salts containing heavy metals. Synthetic water allows us to investigate the sorption performance of media under different conditions.

3.3.1Preparation of multi-solute stock solution

Multi-cation stock solution was prepared by mixing the stock solutions mentioned above. Alternatively, 3.906 g of $CuSO_4.5H_2O$, 4.975 g of $FeSO_4.XH_2O$ and 4.484 g of $NiSO_4.6H_2O$ were dissolved in a 1000 mL double distilled water to make 1000 mgL^{-1} Cu^{2+}, Ni^{2+} and Fe^{2+}. Different concentrations were produced by simple dilution. The preservation or conservation of stock solutions was accomplished as (Haile and Fuerhacker, 2018).

3.4 Batch adsorption experimental studies

3.4.1 Determination of the effect of Adsorbent Particle Size on heavy metal removal

For each adsorbent, an aliquot of 100 mL of synthetic water at room temperature was poured into three different 100 mL volumetric flasks. Then, 2.0 g of different sizes of adsorbent from 6.7 mm to 0.075 mm was added in different beakers for 1hour and the mixture was gently stirred. After one hour all the solutions were filtered with 0.45 μm cellulose membrane filter and subjected to the Inductively Coupled Plasma Optical Emission Spectrometer (iCAP7000SERIES) to measure the absorbance of different heavy metals in accordance with the standard method. The cellulose membrane filters were soaked in dilute (1% v/v) HNO_3 for an hour and rinsed thoroughly with DI water before use as (Jain, 2001). Percentage heavy metal removal was calculated for each solution. The experiment was done in duplicates and average data was used to select the best grain size for adsorption. The following equation was used to calculate the metal removal efficiency (R).

$$R = \frac{C_i - C_e}{C_i} X100 \quad (7)$$

The adsorbed concentration, C_r was calculated using equation below:

$$C_r = C_i - C_e \quad (8)$$

where, C_i and C_e denotes initial and equilibrium metal concentrations, respectively. The metal uptake capacity *(q)* was calculated using the following mass balance equation explained by (Kumar and Kirthika, 2009).

$$q = \frac{(C_i - C_e)\,V}{M} \quad (9)$$

where, q (mgg^{-1}) is the adsorption capacity of the adsorbents at any time, M (g) is the adsorbent dosage, and V (L) is the volume of the solution.

3.4.2. Determination of the effect of adsorbent dosage on adsorption

At room temperature (about 20^{o}C**),** aliquot of 50mL of synthetic waste water was mixed with finely powdered adsorbents of various dosages ranging from 0.5g-5.0g. Agitation of solution in a shaker for an hour was done. After that, the solution was filtered and filtrates were subjected to an ICP-OES to determine the absorbance. The removal efficiency (R) of heavy metals was calculated for each solution as per mathematical methods shown in previous tests.

3.4.3. Determination of the effect of contact time on adsorption

The adsorption process was conducted by allowing 2.0 g of each adsorbent to be mixed with 100 mL of synthetic water to stand for various times with gentle stirring, for instance, 30 minutes, 60 minutes, 90 minutes, 120 minutes and 180 minutes. The supernatant was filtered with 0.45µm Whatman filter paper for each after contact time and removal efficiency was calculated after measuring of heavy metal ion concentrations with Inductively Coupled Plasma Optical Emission Spectrometry (ICP OES).

3.4.4 Determination of the effect of pH on adsorption

The same media to solution ratio as above was used at different pH values ranging from 2 to 10. The eluents of buffer solutions which were used to control pH of the solution to be acidic and alkaline were 0.1 M Nitric acid and 0.1 M Sodium hydroxide respectively. The experiments were conducted at room temperatures, with optimum agitation speed and optimum contact time selected from the aforementioned experiments. The heavy metal removal efficiencies of media were computed at different pH levels.

3.4.5 Determination of the effect of temperature on adsorption

To study the effect of temperature on adsorption, experiments were conducted in a series of 100 mL Erlenmeyer flasks where 100 mL synthetic water was transferred into flasks with desired amount of adsorbents. The flasks were then placed in a Thermo-shaker where the solution was agitated at varying temperatures 20, 30 and 40 ^{o}C as per protocol of (Jain, 2001). The flasks were covered with Paraflim sheets to avoid introduction of foreign particles as per (Jain, 2001)

3.4.6 Regeneration or reusability studies

The primary objective of this study was to restore the adsorption capacity of exhausted brick waste and smelter slag. To find the most potential eluent for desorption of heavy metals, 0.1M Sodium hydroxide (Na OH) was used in desorption test. An alkali solution was used since it is not likely to destroy adsorption active sites like acidic solutions (Ahmad et al., 2012). Media regeneration test was carried out by placing 2.0 g of each media into 250 mL

flask which contains 100 mL Na OH. The mixture the eluent and media was agitated for 24 hours in an orbital shaker at optimum agitation speed. The mixture was then filtered through 0.45 µm filter paper after 24 hours. The residue were rinsed with Deionized water, dried and weighted before use in the next cycle. 150 mL of 0.1M NaOH was added to each media and agitated again for 24 hours. Residues were then separated from solution using filter paper and the concentration of heavy metal ions were measured using (ICP-OES). The procedure above was repeated for 3 cycles. Analytical instrument (ICP-OES) was calibrated prior to each analysis.

Desorption efficiency of each test was computed using a mathematical equation shown below.

$$\text{Desorption} = \frac{C_i - C_e}{C_i} X100 \quad (10)$$

where C_i and C_e denote initial and final heavy metal ion concentrations respectively.

3.5 Adsorption isotherm studies

Heavy metal ions were transferred from the solution to the solid adsorbent until equilibrium attained with adsorbate on the solid adsorbent. The amount adsorbed per unit mass of adsorbents and concentration of heavy metals in solution at a given temperature was represented by adsorption isotherms.

For each media, 100 mL of wastewater was placed into 250 mL conical flasks containing different dosages of media from 0.1 to15 g. The mixtures were agitated in an orbital shaker at 12 rpm for 24 hours at room temperature. After agitation the mixtures were filtered through a 0.45µm filter paper and filtrates pH and concentration of heavy metals was measured using a portable multi-parameter Testr™ 35 series meter (Thermo Fisher Scientific, UK) and ICP-OES (iCAP 7000 series) respectively.

Experimental data was fitted onto equation representing isotherm models to determine mechanism depicting adsorption. The following isotherm models were used to determine adsorption mechanism;

3.5.1 Langmuir adsorption isotherm

The model was based on three assumptions.

1. Adsorption is of monolayer thickness.
2. The surface of adsorbent is uniform and all active sites are equal.
3. Ability of a molecule to adsorb at a given site is independent of the occupation.

After equilibrium was attained, the amount of heavy metal adsorbed per unit mass of adsorbent and the concentration of adsorbate in effluent solution were represented as:

$$q_e = \frac{q_m K_L C_e}{1+K_L C_e} \quad (11)$$

The linear form of Langmuir equation was represented as:

$$\frac{C_e}{q_e} = \frac{C_e}{q_m} + \frac{1}{K_L q_m} \quad (12)$$

Where q_e is equilibrium metal ion concentration on adsorbent (mgg^{-1}), C_e is the equilibrium metal ion concentrations in the solution (mgL^{-1}), q_m is the monolayer adsorption capacity of the adsorbent (mgg^{-1}), K_L is Langmuir adsorption constant (Lmg^{-1}) related with free energy of adsorption.

3.5.2 Freundlich adsorption isotherm

Freundlich adsorption isotherm was used to express the variation of adsorption with concentration of heavy metals in bulk solution at constant temperature. The isotherm was expressed as follows:

$$q_e = K_f C_e^{1/n} \quad (13)$$

Where q_e is the mass of heavy metal per unit mass of adsorbent.

Linearized form of equation is given below:

$$\log q_e = \log k_f + \frac{1}{n} \log C_e \quad (14)$$

Where K_f is a constant value which is a measure of adsorbent capacity where as $\log qe$ and logCe were plotted and produced a straight line with a slope of $\frac{1}{n}$ and intercept being K_f. The values of K_f and n were calculated from the slope of the graph. When K_f values increases, it's an indication of better uptake of heavy metal ions and low values of $\frac{1}{n}$ indicate that the affinity of metal is better. The y-intercept of line from Freundlich plot is approximately an indicator of adsorption capacity. Moreover, the slope is an indicator of the intensity of adsorption.

3.5.2.1Determination of suitable adsorption isotherm

To identify the suitable isotherm model for adsorption of heavy metals from wastewater onto brick waste and smelter slag, the R^2 analysis was carried out.

3.6 Adsorption kinetic Studies

The kinetics experiments were done in three sets of 500 mL solutions. The adsorbents were then added into the solution at dosage of 2.0 g. The mixed solution was stirred continuously,

and the solution pH values were maintained at 7.0 ± 0.1 by adding 0.1 M HCl or 0.1M NaOH solutions. The samples were collected at appropriate time intervals, filtered through a 0.45µm filter paper, and the concentration of heavy metal ions in the solution were analysed with ICP-OES. In order to investigate the mechanism of adsorption, Lagergrens Pseudo-first-order and Pseudo second order and intraparticle diffusion models were fitted into the experimental data.

Linear form of Lagergren pseudo-first-order rate equation takes the following form,

$$\log(q_e - q) = \log q_e - \frac{K_1}{2.303} t \quad (15)$$

Where qe (mgg^{-1}) and q (mgg^{-1}) were the quantity of heavy metals adsorbed at equilibrium time (mgg^{-1}) and time, t in minutes respectively. Linear graph showing plots of $\log(q_e - q)$ versus t was produced by applying the above equation. The experimental data were again tested by the pseudo-second-order kinetic model which was represented in the following form:

$$\frac{t}{q} = \frac{1}{k2qe^2} + \frac{1}{qe} t \quad (16)$$

where k2 (g/ (mg min)) denotes the rate constant of second–order equation, q (mg/g) is the amount of adsorption at time, t (min) and q_e (mgg^{-1}) was the quantity of heavy metals adsorbed at equilibrium. Values of t/q_t were plotted against t. The R^2 values were obtained from the graphs.

Equation corresponding to intraparticle diffusion model was expressed as shown below;

$$q = K_{id}\, t^{0.5} + C \quad (17)$$

where q (mgg^{-1}) is the amount of heavy metals adsorbed at time t (minutes), K_{id} ($mg/(gmin^{0.5})$) is the rate constant of intraparticle diffusion, C is the value of intercept giving an idea about the boundary layer thickness, i.e. the larger the intercept, the greater the boundary effect. If intraparticle diffusion is the sole rate determining step, plots of q versus $t^{0.5}$ must be linear and passing through the origin.

3.6.1 Fitness of adsorption kinetic models

Root Mean Square Error (RMSE) analysis was applied to identify the best fitting batch kinetic model for adsorption of target heavy metals. The mathematical expression of RMSE is as the equation below:

$$RMSE = \sum \left(\frac{q_{e,exp} - q_{e,model}}{q_{e,model}} \right)^2 \quad (18)$$

3.7 Thermodynamic studies

To describe the thermodynamic behaviour of the adsorption of heavy metal ions using copper smelter slag and brick waste, thermodynamic parameters such as change in Gibbs Free energy (ΔG^o), entropy (ΔS^o) and enthalpy (ΔH^o) were calculated using the linearized equations (Equation 19 - 21) in accordance with (Duan and Fedler, 2021).

$$LnK_d = \frac{\Delta S^0}{R} - \frac{\Delta H^0}{RT} \quad (19)$$

$$\Delta G^0 = -RTLn\ K_d \quad (20)$$

$$K_d = \frac{C_i - C_e}{C_e} x \frac{V}{M} \quad (21)$$

Where, T (K) denotes the absolute temperature, K_d (Lg^{-1}) represents distribution coefficient and R ($J.molK^{-1}$) symbolises universal gas constant.

Enthalpy and Entropy were estimated from the slope and intercept of plot of lnK_d versus 1/T. Positive value of enthalpy indicates the endothermic nature of adsorption. Gibbs free energy indicates the degree of spontaneity of the adsorption process. Positive value of entropy suggests increase in randomness at the solid or solution interface during sorption.

3.8 Laboratory Fixed Bed Column Studies

3.8.1 Laboratory Fixed Bed Column design

Column breakthrough experiments were conducted in Polyvinyl Chloride (PVC) column of 215 mm internal diameter with equivalent height of 1000 mm. The column had a total volume of approximately 0.0363 m^3. The column was placed on top of a steel plate, sealed or joined together with a rubber using Polyvinyl Acetate (PVA) glue. The outlet effluent pipe was installed at the bottom of the column. A 70 Litre holding tank was also placed on a steel stand with a submersible pump (WH1200, distributed by East Dune Trading (Pty) Ltd T/A Warehouse). The pump had a maximum discharge capacity of 1200 Lhr^{-1}. A discharge capacity of 1200 Lhr^{-1} is quite high for such small column as more of hydrostatic failures may occur at the bed of the packed media due to high hydraulic loading rate. To overcome such a challenge, a rotameter (TECH FLUID) with a control valve was connected towards the end of the influent pipe. The valve was made of High-Density –Polythene (HDPE). The valve of such a material was selected because it has excellent characteristics such as being tough, light, flexible and resistant to corrosion thus making it suitable to withstand harsh conditions such as high hydrostatic forces and also capable of preventing corrosive property of

wastewater. The control of flow-rate was managed by such as technique. An illustration of the column is as per the schematic diagram below (**Fig 3.2**). The aim of this column study was to investigate the long term capacity of the best adsorbents as filter media to remove target heavy metal ions and to predict the its life span. This was accomplished by packing clean media (<4.75 mm, 10.19 kg) up to 290 mm depth yielding a bed volume of approximately 0.01053 m^2. The media was then levelled and slightly compacted to evenly distribute the porosity of filter media. Media was then flushed with DI water for 24 hours to remove air bubbles entrapped into media prior to operation. A 70 L synthetic water of 200 mgL^{-1} of target metal ions was prepared as in batch experimental studies, fed into the column by pumping a solution at a flow rate of 20 ml min^{-1}, which is equivalent to 28.8 $Lday^{-1}$. The effluent was sampled for every 90 minutes time interval. The experimental setup was monitored daily while continuously sampling. The samples were filtered with a 0.45 µm Cellulose Nitrate Filter paper (Sartorius, stedim biotech, Filter Type AC, Sc) using vacuum pump. The filter was made in Germany. Filtered samples were preserved with 65% HNO_3 (1% of volume of solution) and kept at 4 ^oC while awaiting analysis as per (Haile and Fuerhacker, 2018). Samples were analysed using ICP-OES. The breakthrough time was taken at the wastewater discharge limits by Botswana Standards (BOS). The adsorption capacity of the adsorbent at breakthrough point, q_B (mgg^{-1}) was calculated as per the equation used by (Biswas and Mishra, 2015):

$$q_B = Q_v \left(C_o - \frac{C_B}{2}\right)\frac{t_B}{M} \quad (22)$$

where C_o is the concentration of influent (mgL^{-1}), M is the mass of the adsorbent packed in the column (g), Qv is the influent flow rate ($mLmin^{-1}$), C_B is target metal ionic concentration at breakthrough point (mgL^{-1}) while breakthrough time is t_B (mins).

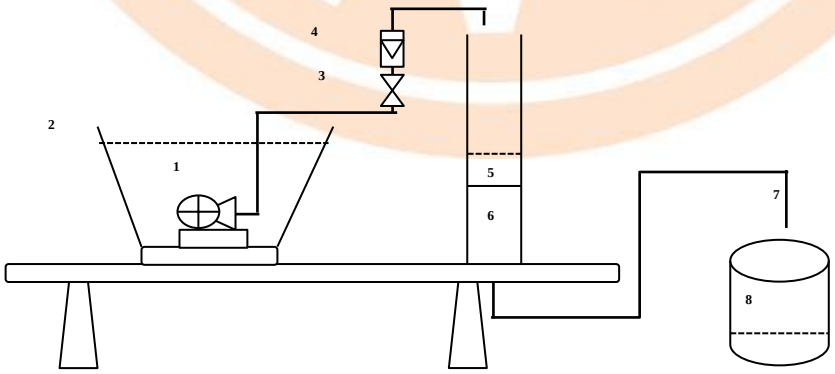

1- Submersible pump, 2- Influent tank, 3- Valve, 4- Water rotameter

5- Water level, 6- Bed (Adsorbent), 7- Sampling point, 8- Storage tank

Fig 3.2 Schematic diagram for column experimental studies

3.8.2 Fixed Bed Column Kinetics

3.8.2.1Thomas and Yoon-Nelson model

Thomas model was used during column studies to predict performance of column and breakthrough curves. The model was based on assumption that axial dispersion is negligible. Thomas model has a limit of basing on pseudo second order kinetics and thus not restricting chemisorption and surface mass transfer is controlling it. The Yoon-Nelson model was also applied in this study. The models were expressed utilising the following mathematical formulas shown (**Table 3.2**). In case of the fitness of suitable column kinetic model, the coefficient of determination (R^2) was applied to identify the best fitting column kinetic model for adsorption of target heavy metals.

Table 3.2 Linearized formulas of column kinetic models

Column kinetic model	Linear equation
Thomas model	$\ln\left(\frac{C_0}{C_e} - 1\right) = \frac{K_{TH}\, q_o M}{Ø} - \frac{K_{TH} C_o V}{Ø}$
Yoon-Nelson model	$t = Ƭ\ \frac{1}{K_{YN}} \ln \frac{C_e}{C_o - C_e}$

3.8.2.2 Statistical analysis

Adsorption experiments were conducted in triplicates and averages were computed for statistical data analysis using Microsoft Excel XLSTAT software.

References

Ahmad, R., Kumar, R. and Haseeb, S. (2012) 'Adsorption of Cu 2+ from aqueous solution onto iron oxide coated eggshell powder: Evaluation of equilibrium, isotherms, kinetics, and regeneration capacity', *Arabian Journal of Chemistry*. King Saud University, 5(3), pp. 353–359. doi: 10.1016/j.arabjc.2010.09.003.

ASTM C136 "Standard Test Method for Sieve Analysis of Fine and Coarse Aggregates." (www.astm.org)

Biswas, S. and Mishra, U. (2015) 'Continuous Fixed-Bed Column Study and Adsorption Modeling: Removal of Lead Ion from Aqueous Solution by Charcoal Originated from Chemical Carbonization of Rubber Wood Sawdust', *Journal of Chemistry*, 2015. doi: 10.1155/2015/907379.

Dan-Asabe, B., Yaro, S. A, Yawas, D. S, Aku .and S. Y. (2013) 'Water Displacement and Bulk DensityRelation Methods of Finding Density of Powdered Materials', *International Journal of Innovative Research in Science, Engineering and Technology*, 2(9), p. 6.

Duan, R. and Fedler, C. B. (2021) 'Adsorptive removal of Pb2+ and Cu2+ from stormwater by using water treatment residuals', *Urban Water Journal*. Taylor & Francis, 18(4), pp. 237–247. doi: 10.1080/1573062X.2021.1877742.

Haile, T. M. and Fuerhacker, M. (2018) 'Simultaneous adsorption of heavy metals from roadway stormwater runoff using different filter media in column studies', *Water (Switzerland)*, 10(9), pp. 1–18. doi: 10.3390/w10091160.

Hajira, T., Atika, S. and Muhammad, S. (2018) 'Synthesis of kaolin loaded Ag and Ni nanocomposites and their applicability for the removal of malachite green oxalate dye', *Iranian Journal of Chemistry and Chemical Engineering*, 37(3), pp. 11–22.

Jain, C. K. (2001) 'Adsorption of zinc onto bed sediments of the River Ganga': adsorption model sand kinetics, Hydrological Sciences Journal, 46:3, 419434,doi:10. 1080/02626660109492836

Janbuala, S. and Wasanapiarnpong, T. (2015) 'Effect of rice husk and rice husk ash on properties of lightweight clay bricks', *Key Engineering Materials*, 659(July 2017), pp. 74–79. doi: 10.4028/www.scientific.net/KEM.659.74.

Kumar, P. S. and Kirthika, K. (2009) ‘Equilibrium and kinetic study of adsorption of nickel from aqueous solution onto bael tree leaf powder’, *Journal of Engineering Science and Technology*, 4(4), pp. 351–363.

Lekgoba, T., Ntuli, F. and Falayi, T. (2020) ‘Application of coal fly ash for treatment of wastewater containing a binary mixture of copper and nickel’, *Journal of Water Process Engineering*. Elsevier Ltd, (July), p. 101822. doi: 10.1016/j.jwpe.2020.101822.

Letina, D. and Letshwenyo, W. M. (2018) ‘Investigating waste rock, tailings, slag and coal ash clinker as adsorbents for heavy metals: Batch and column studies’, *Physics and Chemistry of the Earth*. Elsevier, 105(March), pp. 184–190. doi: 10.1016/j.pce.2018.02.013.

Sima, T. V., Letshwenyo, M. W. and Lebogang, L. (2018) ‘Efficiency of waste clinker ash and iron oxide tailings for phosphorus removal from tertiary wastewater: Batch studies’, *Environmental Technology and Innovation*. Elsevier B.V., 11, pp. 49–63. doi: 10.1016/j.eti.2018.04.008.

US EPA (2002) ‘standard operating procedures soil pH determination’, pp. 1–6.

CHAPTER4: RESULTS AND DISCUSIONS

4.1 Media characterisation

4.1.1Particle Size Distribution of adsorbents

The grain size distribution of CSS, MGBW, MGS and CBW are represented in **Fig 4.1**. The effective sizes d_{10} of MGBW, MGS and CBW are 0.382, 0.425 and 0.486 mm respectively as shown in **Table 1.0**. Comparatively, the effective size of CSS is 0.300 mm. According to European guidelines, the recommended range of the effective size of slow sand filters is 0.15-0.35mm and coefficient of uniformity (*Cu*) is 1.5-3.0. Other studies have reported effective size of sand to be 0.3-0.45mm (Healy et al.,2007). In this case, the effective size of all media was all within the range except of CBW (**Table 1.0**.). The higher readings of *Cu* values of media implies that range of size of particles is larger and might consequently affect filtration performance at higher hydraulic loading rates as fines of media may fill space between large particles and reduce hydraulic conductivity of media and lead to excessive clogging (Healy et al.,2007). The problem of clogging is normally prevented by using media of size 5-12 mm (Letshwenyo and Sima, 2020).

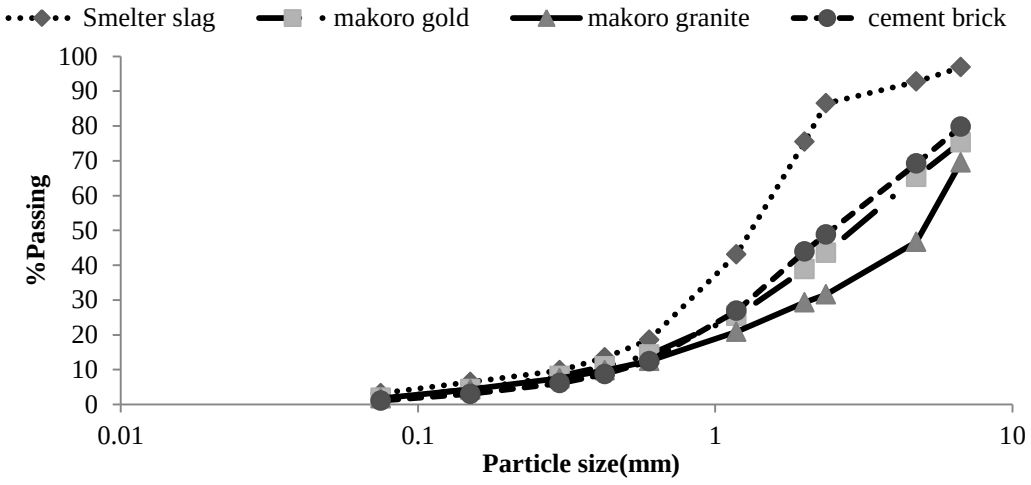

Fig 4.1 Particle size distribution curve of adsorbents

Table 4.1 Summary of sieve analysis of media

Media	D10	D30	D50	D60	Cu	Cc
CSS	0.3	0.870	1.355	1.608	5.36	1.57
MGBW	0.382	1.460	3.063	4.160	10.89	1.34
MGS	0.425	2.106	5.031	5.889	13.86	1.77
CBW	0.486	1.330	2.497	3.672	7.56	0.99

4.1.2 Bulk, particle densities, porosities, morphology and hydraulic conductivities of adsorbents

The physical characteristics of copper smelter slag and brick waste adsorbents are shown in **Table 4.2**. The media bulk density results revealed that smelter slag had the highest value compared to brick waste adsorbents. Smelter slag had a bulk density of 1.9 gcm^{-3}, followed by MGS with 1.5 gcm^{-3}, 1.4 gcm^{-3} MGBW and 1.2 gcm^{-3} CBW. Both adsorbents had particle and bulk densities greater than of wastewater suggesting that media can be able to withstand hydrostatic forces encountered in the fixed bed column during filtration. Smelter slag had highest bulk density than other media. On the other hand, MGBW and MGS had the highest particle densities, 19 gcm^{-3} for both of them. Other authors have reported that media with high density is useful to ensure high media structural strength which reduce losses of weight during handling (Guo and Lua, 2003; Letshwenyo and Sima, 2020). Media with low porosity suggests short time saturation thus media is likely have low heavy metal retention capacity. In this study, media had porosity ranging from 42.3 to 50% (**Table 4.2**). The presence of micro pores in both media was shown by SEM images in **Fig 4.2(a-h)** before and after heavy metal ion adsorption. Media with more pores suggests high rate of contaminant diffusion (Sima *et al.*, 2018). However,highly porous adsorbent does not assure that it possess high contaminant affinity (Drizo *et al.*, 1999; Sima *et al.*, 2018). Pores were found to be more visible in CBW and MGBW than on CSS and MGS. Moreover, rough surfaces with irregular distribution of clumps were found on SEM images after and prior to adsorption of heavy metals. In addition, Letshwenyo and Sima, 2020 reported that adsorbents with low hydraulic conductivities might clog in fixed filter bed and minimise contact time during short circuiting. In this case, smelter slag is likely to be prone to less clogging followed by MGBW, MGS and CBW because it has high hydraulic conductivity compared to other media.

Table 4.2 Physical properties of adsorbents

Parameters	CSS	MGBW	MGS	CBW
Bulk density(gcm^{-3})	1.9 ±0.07	1.4 ±0.07	1.5 ±0.07	1.2 ±0.07
Particle density(gcm^{-3})	13 ± 0.04	19 ±0.07	19 ±0.04	2.2 ±0.04
Porosity (%)	50 ± 5	46.2 ±5	42.3 ±5	45.5 ±5
Hydraulic conductivity (ms^{-1})	8.04 $X10^{-4}$	7.99 $X10^{-4}$	7.65 $X10^{-4}$	7.87 $X10^{-4}$

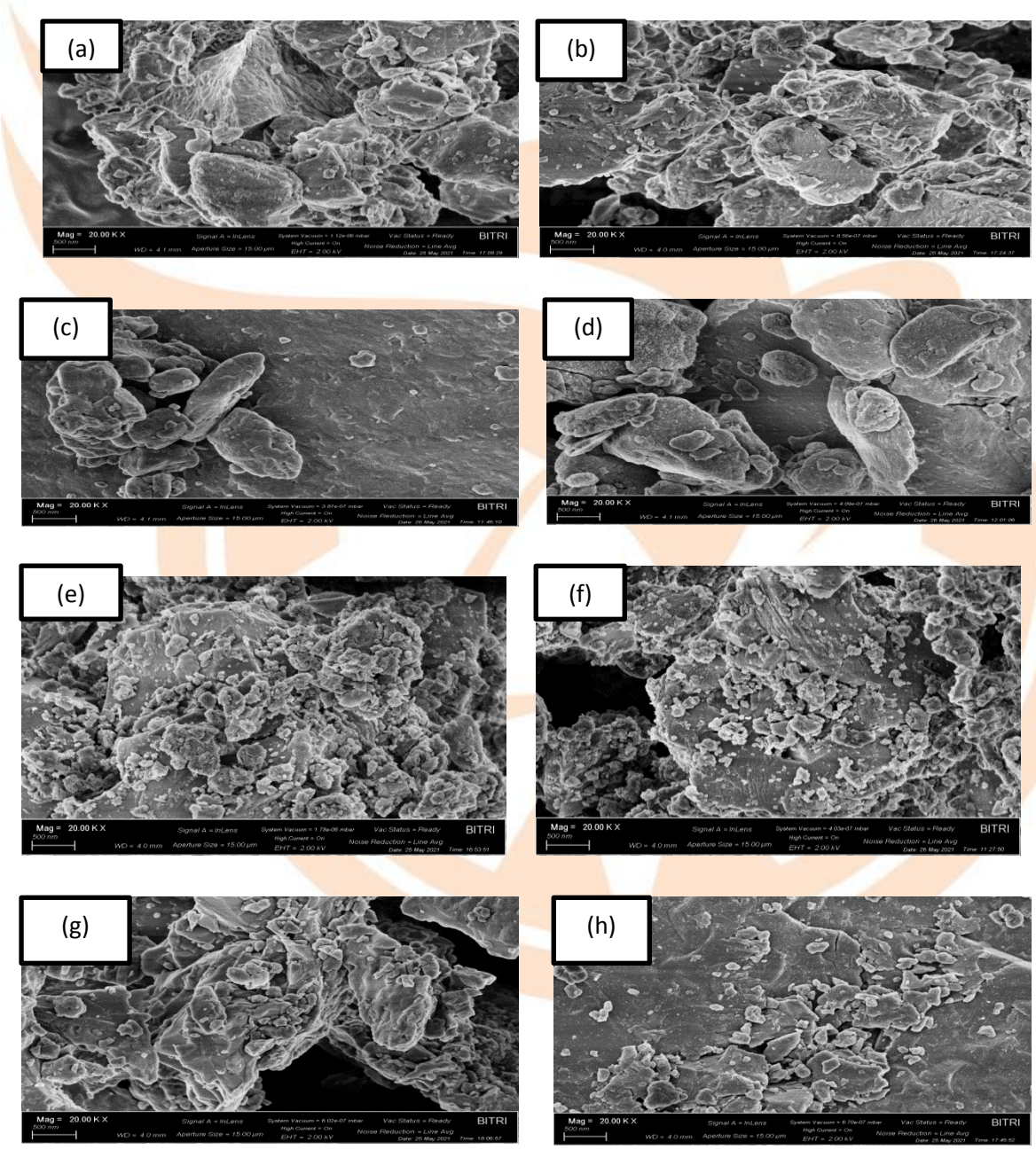

Fig 4.2 SEM morphology of (a)Fresh MGBW (b) Loaded MGBW (c) Fresh CSS (d) Loaded CSS (e) Fresh CBW (f) Loaded CBW (g)Fresh MGS (h)Loaded MGS at 2.00kV with magnification of 20.00KX.

4.1.3 Mineralogical and Elemental composition of adsorbents

The concentrations of the different elements present in the four adsorbents are shown in **Table 4.3** and the oxides in **Table 4.4.** As chemical reactivity of adsorbent surface plays an important role in adsorption, chemical properties of the both adsorbents were also investigated. Several reports indicate that iron (Fe^{3+}), calcium (Ca^{2+}), aluminium (Al^{3+}) ions present in the media can react with other common ions coexisting in wastewater, thus competing for active sites (Arias et al., 2003). In consideration of elemental concentrations, X-ray Fluorescence (XRF) results revealed that CSS contains 33.730 mgL^{-1}Fe, 1.777 mgL^{-1}Ca, and 6.110 mgL^{-1} of Si while MGBW contains 1.7811 mgL^{-1} Fe (**Table 4.3**). Oxides of iron and silicon are commonly known to play a great influential role in adsorptive removal of metal ions from solutions (Tang and Lo, 2013). XRD results revealed that the dominant mineral present in CSS is Hematite (Fe_2O_3) and Silica (SiO_2) with percentage composition of 45.44 and 14.89% respectively. However, MGBW constituted 13.61% Fe_2O_3 and 51.28% SiO_2 respectively. Such mineralogical results of adsorbents are comparable and likely to be congruous to studies reported by El-Shahat and Shehata, (2013), Letina and Letshwenyo, (2018), Sanad et al., (2021) who used clay brick waste, copper smelter slag and clay respectively. Moreover, oxides of transition metals and nano-materials possess chemically active surfaces with large surface areas which can be used to remove a wide range of the ions from effluents Sarma et al.,(2019). The presence of oxides of transition metal like Manganese (II) oxide (MnO) in both adsorbents (**Table 4.4**) might help in adsorption of metals. CSS and MGBW contain low amount of Lime (CaO) being 2.35 % and 2.11 % respectively. Such adsorbents consist of low content of CaO compared to 47.08 % and 42.74 % reported by Han et al., (2016) and Bowden et al., (2009) respectively. Dissolution of Ca ions from CaO of media is well known to raise pH of solutions; therefore less CaO content in all media would reduce costs of solution pH adjustment in effluent treatment systems using such media.

Table 4.3 Elemental concentrations of fresh and loaded adsorbents

Elements(mgg^{-1})	Fresh CSS	Loaded CSS	Fresh MGBW	Loaded MGBW	Fresh MGS	Loaded MGS	Fresh CBW	Loaded CBW
Al	0.00531	0.00601	0.00266	0.00253	0.00326	0.00396	0.00112	0.00078
Si	0.00611	0.00577	0.00874	0.00753	0.00842	0.00941	0.01371	0.01093
K	0.0004907	0.0004271	0.0007238	0.0004359	0.0003141	0.0002758	0.0013407	0.0011392
Cu	0.0017777	0.0018156	0.0022825	0.0014803	0.0009168	0.0007083	0.0047312	0.0035971
Ti	ND	ND	0.0002300	0.0001900	0.0003000	0.0003000	ND	ND
Cr	0.0000755	0.0000310	0.0000310	ND	ND	0.0000292	0.0000292	0.0000431
Mn	0.0001270	0.0000985	0.0000275	0.0000538	0.0000379	0.0000522	0.0000489	0.0000593
Fe	0.03373	0.03117	0.0017811	0.0013429	0.0023629	0.0020549	0.3974	0.0003437
Co	ND	ND	ND	ND	ND	ND	ND	ND
Ni	0.0000267	0.0000254	ND	ND	ND	ND	ND	ND
Cu	0.0003076	0.0002799	ND	0.0000199	ND	0.0000122	ND	0.0000121
Zn	0.0000392	0.0000374	0.0000108	0.0000073	0.0000123	0.0092	ND	ND
Pb	0.0000038	0.0000031	0.0000041	0.0000032	0.0000134	0.0000111	0.0000014	0.0000007
As	ND	ND	0.0000013	ND	ND	ND	ND	ND

ND = Elements not detected by analytical instrument.

4.1.4 X-ray diffraction (XRD) patterns of media

Adsorption mechanism was also investigated using XRD to identify phases of minerals present in media. According to (Kapur and Mondal, 2014) amorphous and crystalline phases in XRD pattern are represented by broaden and sharp peaks respectively. In case of CBW, the XRD pattern clearly indicated the presence of crystalline mineralogical phases of Quartz (SiO_2), lime (CaO), Hematite (Fe_2O_3) and Alumina (Al_2O_3) constituting 53.58, 7.18, 6.03 and 16.51 % respectively (**Fig 4.6**). In case of CSS, the dominant crystalline phases found were of Fayalite ($(Mg, Fe)_2 SiO_4$) and less of Chromite ($FeCr_2O_4$) amounting to 12.88 % and 0.91 % respectively (**Fig 4.3**). The remaining amount was of amorphous phases. Sharp peaks shown in both MGBW and MGS were of Mullite and Quartz (**Fig 4.4 and Fig 4.5**). In this study it can be concluded that CSS is predominantly amorphous material while MGS, CBW, MGBW were crystalline materials. No notable differences were depicted in diffraction patterns before and after adsorption suggesting that the adsorption of copper, nickel and iron did not impose any changes in the pattern. The XRD patterns are comparable to those reported by Ouyang *et al.*, 2019 , Xue *et al.*, 2021 and Sanad *et al.*, 2021.

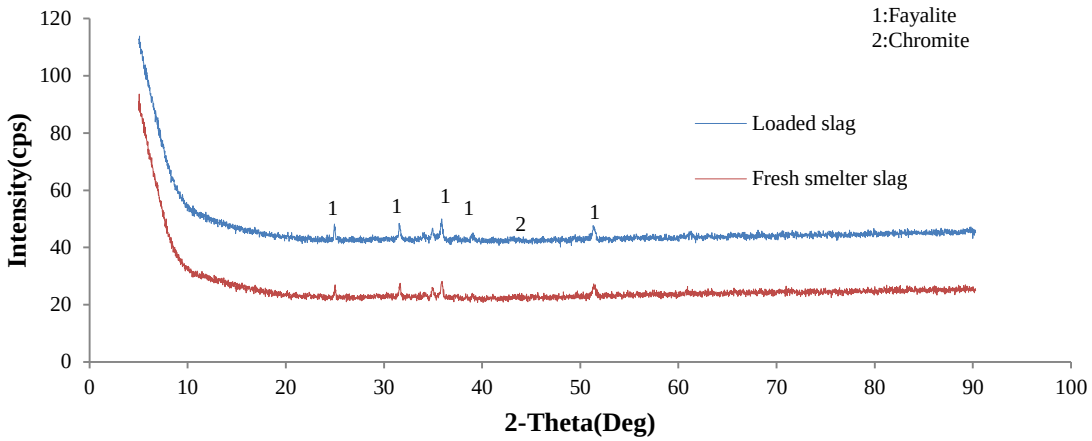

Fig 4.3 XRD patterns of Fresh and loaded CSS

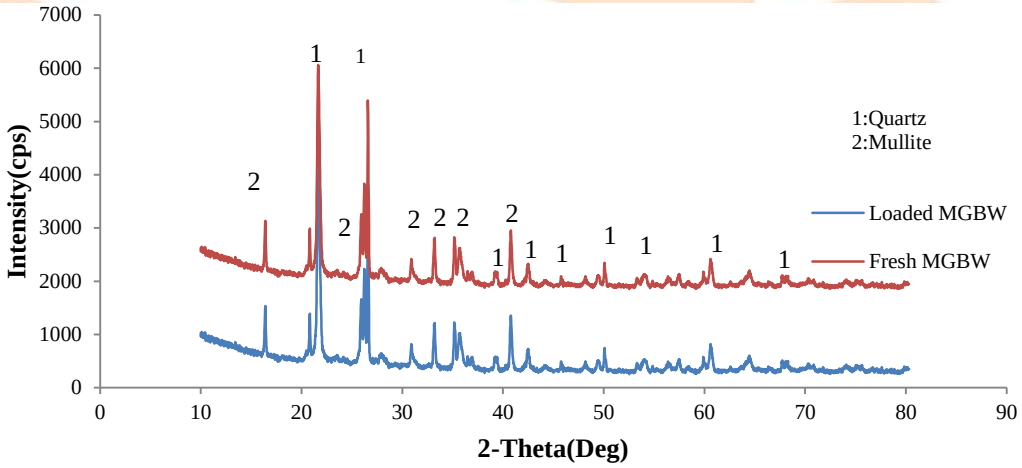

Fig 4.4 XRD patterns of Fresh and loaded MGBW

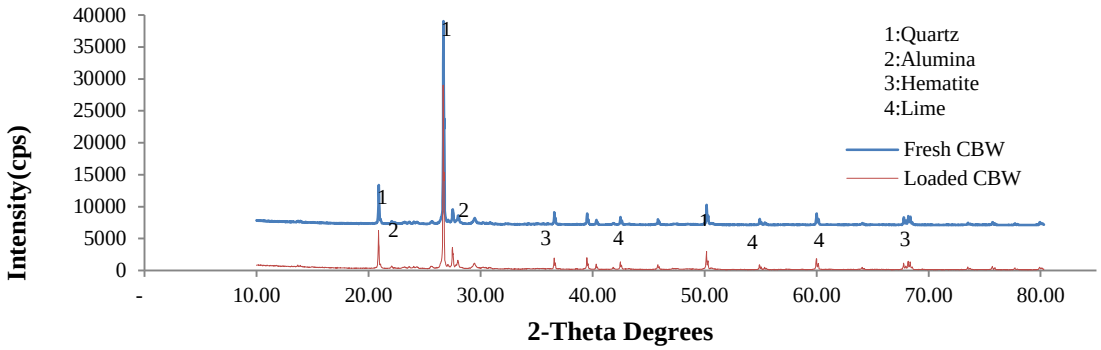

Fig 4.5 XRD patterns of Fresh and loaded CBW

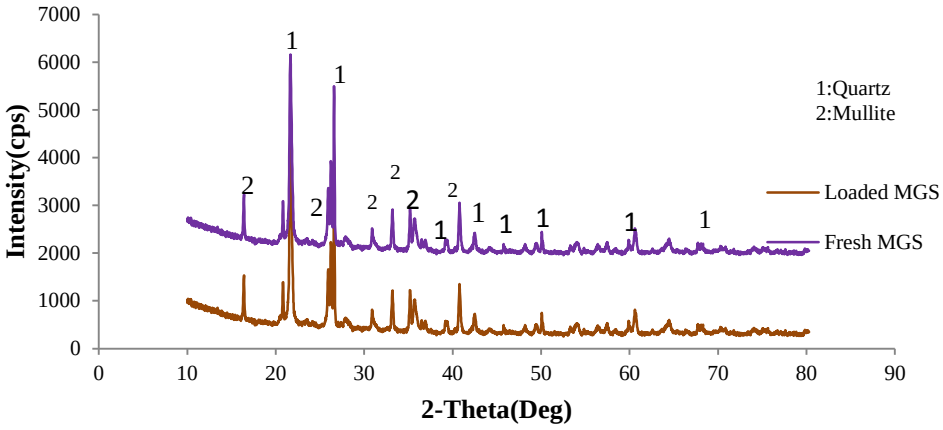

Fig 4.6 XRD patterns of Fresh and loaded MGS

Table 4.4 Compositions of some major minerals in adsorbents

Minerals (%)	Fresh CSS	Fresh MGBW	Fresh CBW	Fresh MGS
Al_2O_3	3.28±0.05	14.31±0.185	16.51±0.115	11.21±0.113
SiO_2	14.89±0.04	13.61±0.073	53.58±0.05	13.70±0.069
Fe_2O_3	45.44±0.35	51.28±0.782	6.03 ±0.235	51.29±0.777
CaO	2.35±0.01	2.11±0.04	7.18±0.331	2.13±0.02
MnO	1.38±0.01	2.50±0.05	-	2.41±0.05
SO_3	0.043±0.002	0.12±0.03	-	0.11±0.05
MgO	1.78±0.056	0.10±0.01	-	0.12±0.03
$(Mg, Fe)_2SiO_4$	12.88±0.003	-	-	-
$FeCr_2O_4$	0.89±0.002	-	-	-

4.1.5 Thermogravimetric analysis (TGA) of adsorbents

TGA profiles shown in **Fig 4.7(a-d)** depict mass loss pattern of media before and after adsorption of heavy metals. An observation can be made that there was no chemical precipitation involved during adsorption process as similar total mass loss was observed to be 6.97 % for CBW (**Fig 4.7(a)**). This suggests that only sorption of Cu^{2+}, Ni^{2+}, and Fe^{2+} was involved and no hydroxides were formed. As for fresh and loaded CSS, total mass gain of 3.8659 and 4.3061 % were respectively observed. Moreover, a mass loss <1 % was observed up to temperatures of 567.184 and 554.555 ^oC respectively for fresh and loaded CSS (**Fig 4.7(b)**), then CSS started to gain weight which may probably be due to precipitation. In case of fresh and loaded MGBW, total mass loss of 2.151 and 2.255 % were observed (**Fig 4.7(c)**). As for fresh and used MGS, observations can be made that there were mass losses of 1.257

and 1.204 % respectively (**Fig 4.7(d)**). About 0.96, 0.370, 0.507 and 0.449% mass losses of CBW, CSS, MGBW and MGS at temperatures less than or equal to 100 ^{o}C may be due to evaporation of the adsorbed water vapour (humidity) in sample (Favero *et al.*, 2016). As for the temperatures from 100 to 200 ^{o}C, weight losses of 0.68, 0.1997, 0.394% were found respectively for fresh CBW, CSS, MGBW, MGS and may be due to chemical coordination of moisture removal (Janbuala and Wasanapiarnpong, 2015). A breakdown of chemical bonds in CBW, MGBW, and MGS at temperatures above 200 ^{o}C resulted in mass losses of approximately 5.33, 1.353, and 0.587 % respectively. TGA pattern is comparable to pattern of clay and clay bricks used by Favero et al., 2016, Janbuala and Wasanapiarnpong, 2015).

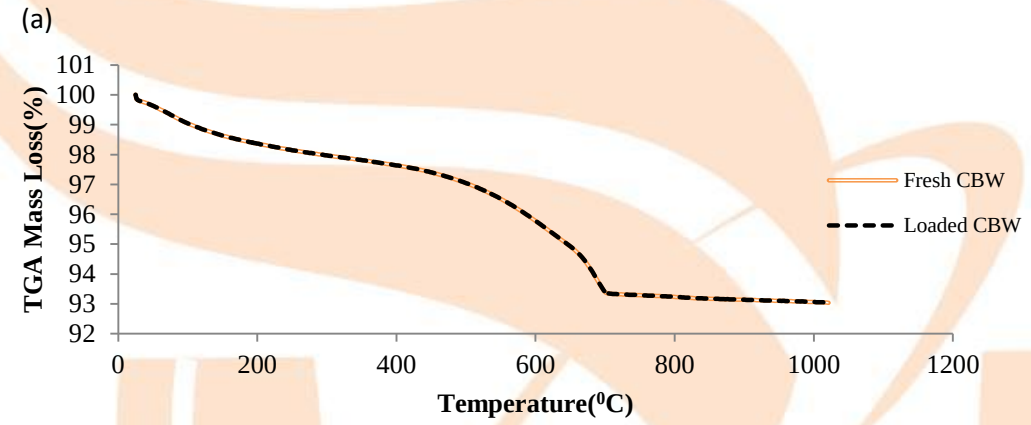

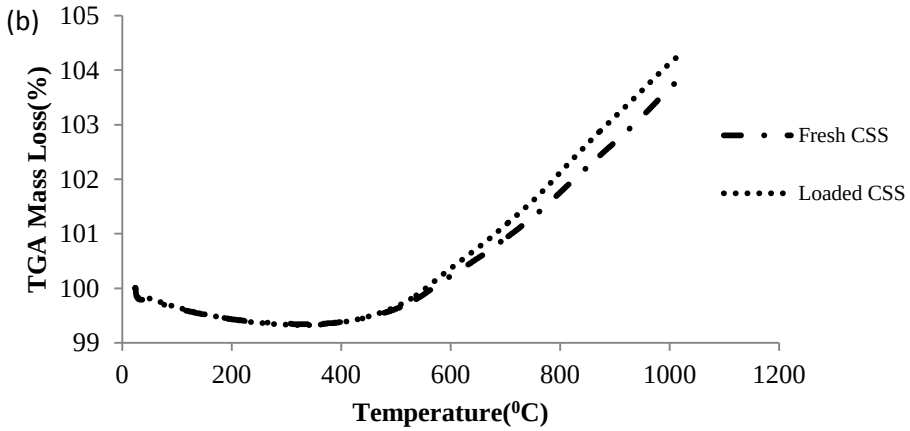

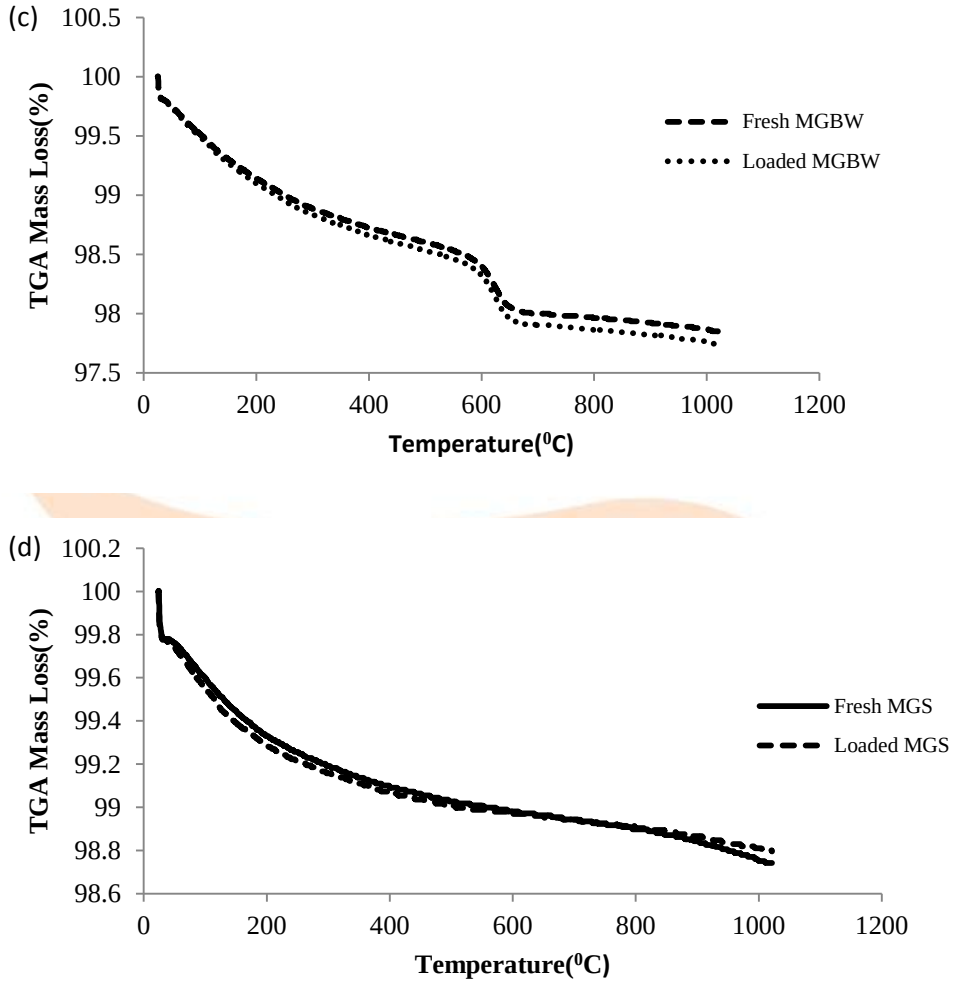

Fig 4.7 Thermogravimetric profile of virgin and loaded CBW (a), CSS (b), MGBW (c) and MGS (d)

4.1.6 The influence of pH point of zero charge (pH $_{pzc}$) of media

The pH_{pzc} of MGBW, CSS, CBW and MGS were determined to be 8.3, 7.01, 8.8 and 6.25 respectively (**Fig 4.8 and Table 4.5**). The global surface charge of adsorbents is zero at this point (Khan and Sarwar, 2007). The surface of adsorbents is positively charged when pH of solution is less than pH_{pzc} thus favouring sorption of anions present in wastewater. However, at pH > pH_{pzc} the surface of adsorbents is negatively charged and favouring the adsorption of cations, copper, iron and nickel in this case. This suggests that as pH increases, cations removal from solution was more favoured due to negatively charged media surfaces. Contrarily, the pH_{pzc} for copper smelter slag used by Letshwenyo and Sima, (2020) was slightly less than of CSS and MGBW used in this study. The reason behind this might be due to changes in mineralogy caused by long exposure to some environmental conditions such as precipitation and solar radiation.

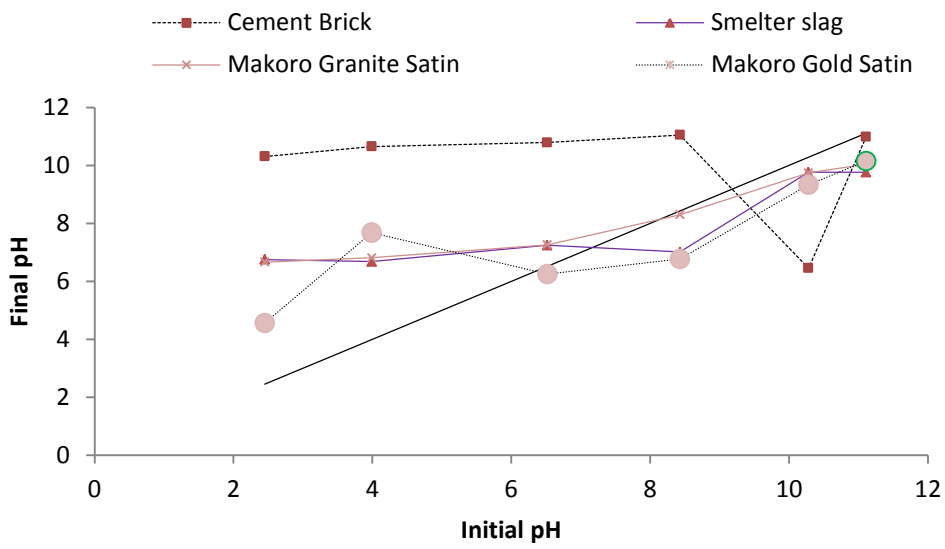

Fig 4.8 pH $_{pzc}$ of the adsorbents.

Table 4.5 Summary of pH $_{pzc}$ of adsorbents

Adsorbents	pH $_{pzc}$
CBW	8.8
MGBW	8.3
MGS	6.25
CSS	7.01

4.1.7 Leaching behaviour of adsorbents

The leaching behaviour of CSS, MGS, CBW and MGBW was studied through agitating adsorbents for 24, 48 and 72 hours using DI water of pH 6.81. After those contact times the mixtures were separated by filtering and leachates were subjected to ICP-OES to measure concentrations of metal ions. The results indicate that metal ion concentrations in leachate of MGBW were all less than 1.0 mgL^{-1} (**Table 4.6**). As for CSS, some metal ion concentrations were also less than1.0 mgL^{-1} except Fe and Ni with concentrations of 28.1 and 1.276 mg L^{-1} respectively after 48 and 72 hours (**Table 4.6**). Concentrations of 2.340 mg L^{-1} Cu and 3.314 mg L^{-1} Fe was also observed after 72 hours for CSS. In case of CBW, it can be noted that all concentrations of metals were less than 1.0 mgL^{-1} set by Botswana Standards (BOS) for discharge in the environments. However, MGS produced Fe and Ni concentrations exceeding regulatory levels after 24 hours while less concentration were observed after 24 and 72 hours. Consequently, environmental application of MGBW and CBW is quite promising than CSS and MGS as they do not leach heavy metals thus non-hazardous.

Table 4.6 Leaching results of adsorbents.

Adsorbent	Heavy metal ion (mgL^{-1})	Leaching time (hours)		
		24	48	72
CSS	Cu	0.122±0.041	0.23±0.016	2.34±0.025
	Fe	0.192±0.001	28.1±0.001	3.314±0.003
	Ni	0.061±0.003	0.358±0.001	1.276±0.001
MGBW	Cu	0.178±0.025	0.0454±0.005	0.016±0.001
	Fe	0.018±0.001	0.00484±0.001	0.074±0.002
	Ni	0.003±0.001	0.00167±0.0001	0.246±0.005
CBW	Cu	0.056±0.002	0.0777±0.0061	0.17878±0.031
	Fe	0.0645±0.001	0.0278±0.001	0.0102±0.002
	Ni	0.0034±0.0013	0.00498±0.001	0.0087±0.001
MGS	Cu	0.345±0.032	0.32445±0.045	0.034±0.004
	Fe	0.0107±0.002	3.039±0.006	0.0595±0.003
	Ni	0.0108±0.005	1.838±0.054	0.148±0.041

4.2 Batch adsorption experiments

4.2.1 The effect of adsorbent dosage on removal of heavy metals

Adsorbent dosage influences the adsorption capacity and the removal efficiency of metal ions from solutions. The effect of adsorbent dosage ranging from 0.5 g to 6.0 g was investigated for the removal of Cu^{2+},Fe^{2+} and Ni^{2+} (**Fig 4.9, 4.10, 4.11 and 4.12**). It was observed that the maximum adsorption capacity of Cu^{2+}, Fe^{2+} and Ni^{2+} was achieved at dose of 2.0 g for CSS, MGS and MGBW. In case of CBW, maximum sorption of all target heavy metal ions was achieved at mass dose of 5.0g (**Fig 4.11**). The final concentrations of heavy metal ions in the solution at optimal dose were found to be 27.130, 68.837, 56 and 2.345 mgL^{-1} for Cu^{2+}, 26.188, 63.256, 26 and 3.126 mgL^{-1} for Fe^{2+}, 27.570, 70.657, 44 and 3.108 mgL^{-1} for Ni^{2+} respectively for CSS, MGS, MGBW and CBW (**Table 4.7**). This means that only water treated using CBW can be conveyed to the public or private sewer as heavy metal concentrations are lower. In order of magnitude, the removal efficiency by CSS decreased in the order Fe^{2+} , Ni^{2+} and Cu^{2+} with the removal of Fe^{2+} 1.01 times greater than Ni^{2+} and that for Ni^{2+} 1.02 times greater than Cu^{2+} removal. This showed similar magnitude of adsorption at that optimum dose. Any increase in adsorbent dose thereafter did not reveal any increased

efficiency but instead decreases in removal for all the metal ions. This is due to overlapping of the adsorption sites because of overcrowding of adsorbent particles beyond the optimum dose and shielding of the adsorption sites (Garg et al., 2003). The same order was observed when MGBW was the adsorbent (**Fig 4.10**) with Fe^{2+} removal being 1.12 more than Ni^{2+}, whose removal was 1.08 times more than Cu^{2+} removal. The initial increase in percentage removal when adsorbent dose was increased from 0.5, 1.0 and 2.0 g was due to the increased availability of many exchangeable adsorption sites or increased in surface area of the adsorbents as also observed by Gebretsadik et al., (2020) . The results are comparable to the findings reported by (Bouhamed et al., 2016; Ouyang et al., 2019).

Table 4.7 Comparative results of initial concentration of metals with final concentrations at optimal media dosage.

Adsorbents	Solution Initial concentration of Cu, Fe and Ni (mgL^{-1})	Solution Final concentration (mgL^{-1})			BOS Public sewer discharge standards (mgL^{-1}, max)		
		Cu	Fe	Ni	Cu	Fe	Ni
CSS	200	27.130	26.188	27.570			
MGBW	200	56	26	44	5.0	20	20
CBW	200	2.345	3.126	3.108			
MGS	200	68.837	63.256	70.657			

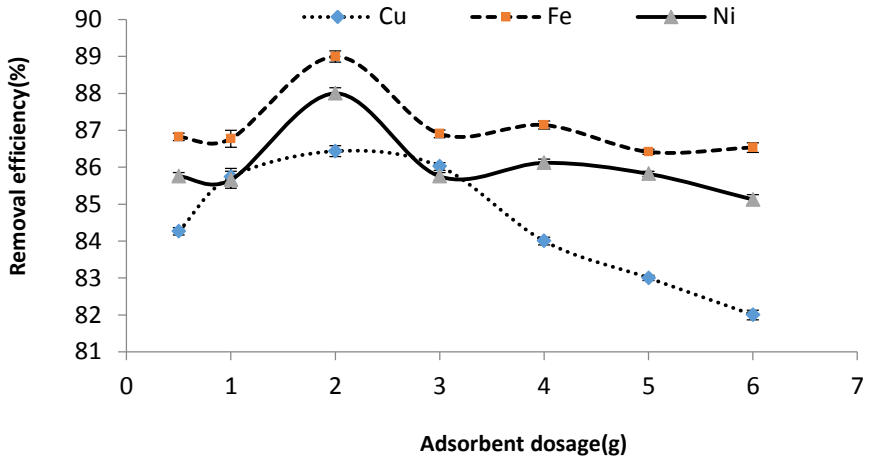

Fig 4.9 The effect of adsorbent dosage on heavy metal ion removal using CSS

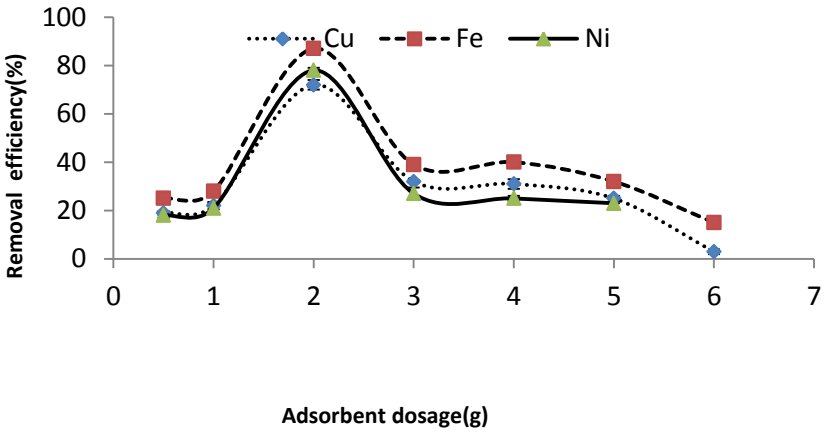

Fig 4.10 Effect of media dosage on heavy metal removal using MGBW

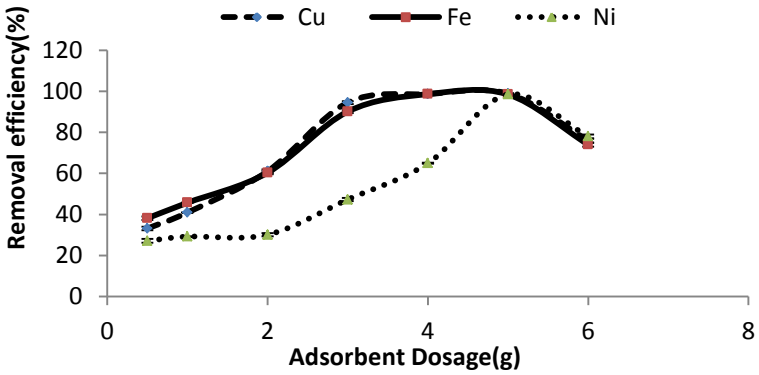

Fig 4.11 Effect of adsorbent dosage on removal of heavy metals using CBW

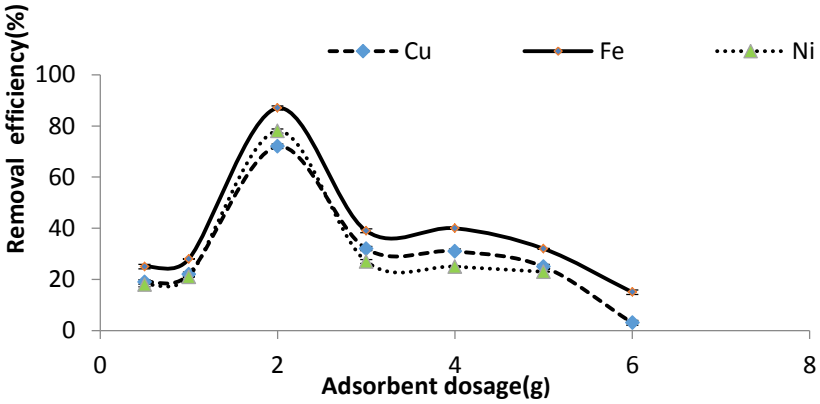

Fig 4.12 Effect of adsorbent dosage on adsorption of heavy metal ions using MGS

4.2.2 The effect of solution pH on heavy metal removal

The effects of pH on heavy metals removal by CSS, MGBW, CBW and MGS is shown in **Figures 4.13, 4.14, 4.15 and 4.16** respectively. The pH of solution is an important parameter for the removal of metal ions as it has an impact on adsorbate solubility, degree of ionisation of adsorbates during adsorption (Sharma and Bhattacharyya, 2005). The pH also affects the surface charge of the adsorbents which in turn influences which ions of adsorbate (anions or cations) are to be adsorbed or exchanged. The adsorption of heavy metals (Cu^{2+}, Fe^{2+} and Ni^{2+}) was studied over the pH ranging from 2 to 12 using CSS and MGBW. The initial concentration of the solution was 200 mgL^{-1} and 120 rpm agitation speed. It was observed that the optimum pH for the adsorption of Cu^{2+}, Fe^{2+} and Ni^{2+} onto CSS was 6.0 with removal percentages of 31, 33 and 32% respectively (**Fig 4.13**). This was not in agreement with earlier observation where pH_{pzc} of CSS was 7.01 suggesting that adsorption of the heavy metals will be favourable at pH greater than 7.01. However, it was observed that lower adsorption capacities were at lower pH and since the media surfaces were positively charged, there were repulsion forces between positively charged media surfaces and the positively charged cations. The adsorption capacities of CSS remained constant after pH_{pzc} was reached for the removal of Fe^{2+} and Ni^{2+} except for Cu^{2+} removal which decreased.

However, the optimum pH was 8.0 for the adsorption of Fe^{2+} onto MGBW with 76% removal, pH 10 and pH 6 for Cu^{2+} and Ni^{2+} removal respectively with 70 and 64% removal efficiencies **(Fig 4.14).** The optimum pH was similar to pH_{pzc} which was 8.33 and any increase in pH after optimum value shows a decrease in percent removal for all the three metal ions. As for CBW, optimal pH of 4 was reached during sorption of Cu^{2+} and Fe^{2+} both maximum removals of 87%, while pH 4 was observed as maximum pH during adsorption of Ni^{2+} with removal of 56% (**Fig 4.15**). In case of MGS, an optimum pH of 6 was also attained with removal efficiencies of 76, 67 and 62 % for Fe^{2+}, Cu^{2+} and Ni^{2+} respectively (**Fig 4.16**). The results are comparable to the findings by Bagali et al., (2017) who observed decrease in lead (II) removal from aqueous solution using Banana Pseudo-stem. For both cases, there might have been high proton concentrations which then minimised adsorption of heavy metal ions as reported by Lai et al., (2010) but metal precipitation favoured at pH values above pH_{pzc}. The same was reported by Farhan and Khadom, (2015) who concluded that at low pH protons compete with metal ions for the available active adsorption sites responsible for the uptake of metal ions hence decreasing the metal ions adsorption. The observed decrease in adsorption efficiency with increasing pH could be due to the formation of insoluble metal

hydroxides at high pH values as reported by Nithya *et al.*, (2018) on the adsorption of Ni^{2+} on green extract capped super paramagnetic iron oxide nanoparticles. The same was reported by Bakhtiari and Azizian, (2015) that at pH values greater than 6, copper ion precipitates as copper hydroxide Cu $(OH)_2$. The removal of Fe ions from the solution at high pH values could be due to their hydrolysis and precipitation reactions of the hydrolysed products such as ferric hydroxides (Nosrati et al. 2009), and this could have been the case in this study. Although not investigated in this study, the report by Nosrati et al., (2009) suggested that the ionic concentration of Fe decreases with increasing pH, which could be due to hydrolysis and precipitation, hence the decrease in Fe removal observed in this study.

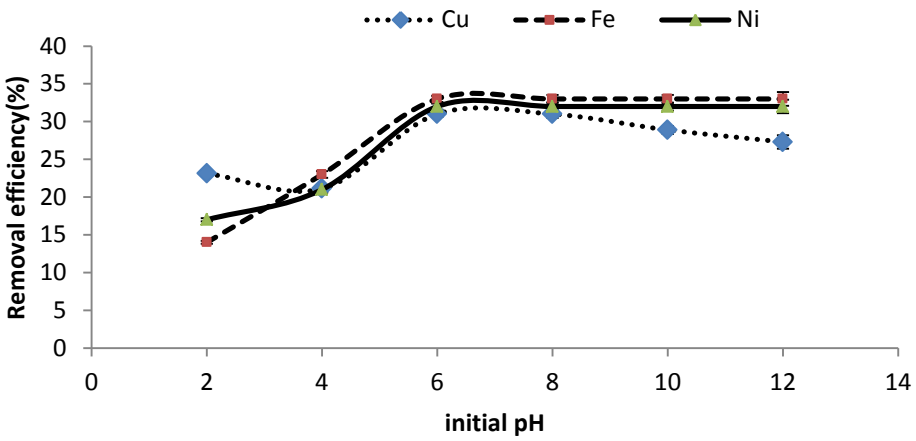

Fig 4.13 Effect of pH on heavy metal ion removal using CSS

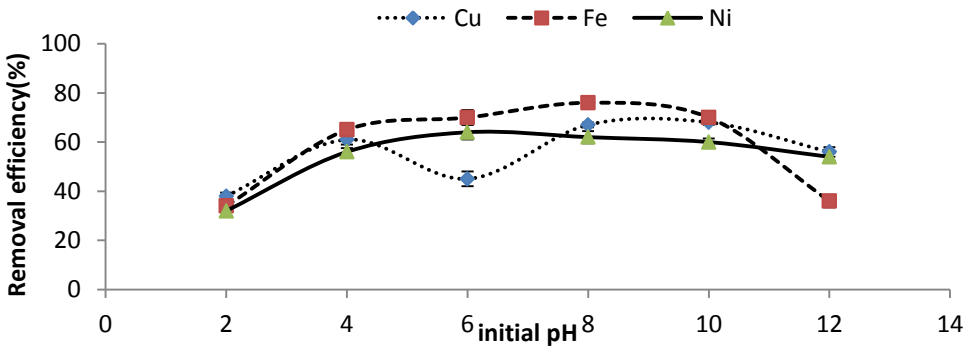

Fig 4.14 Effect of solution pH on heavy metal ion removal using MGBW

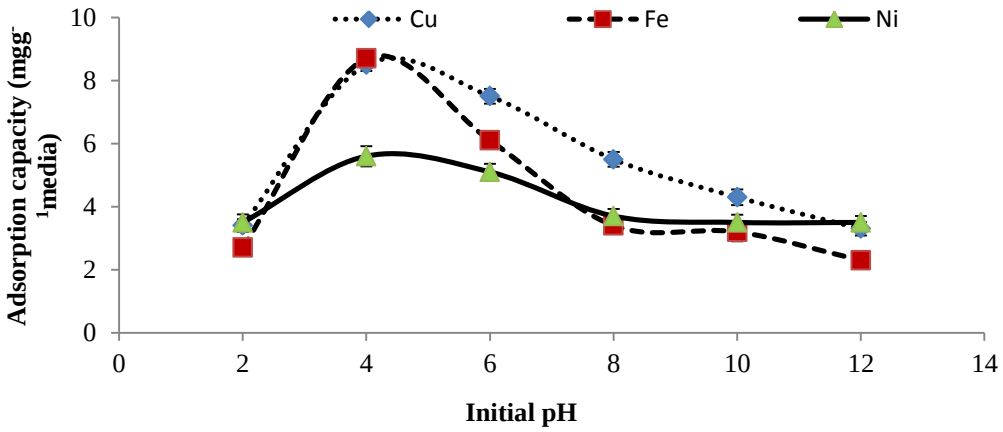

Fig 4.15 The effect of initial pH on Cu (II), Fe (II) and Ni (II) removal using CBW

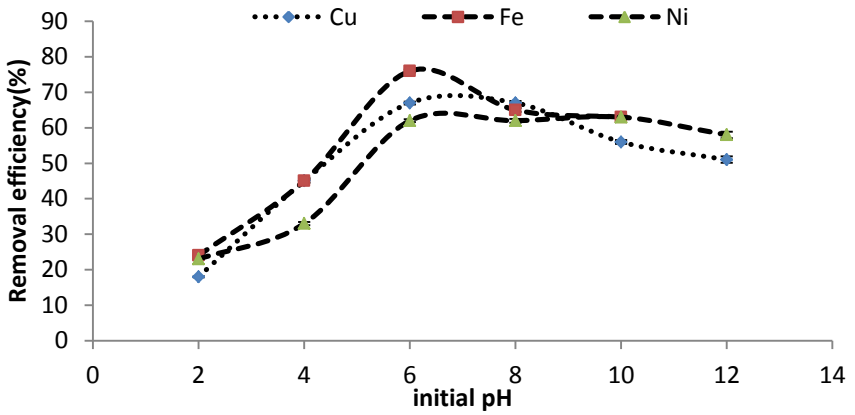

Fig 4.16 Effect of solution pH on heavy metal removal using MGS

4.2.3 The effect of contact time on heavy metal removal

The adsorption capacities of the media with respect to time for the uptake of Cu^{2+}, Fe^{2+} and Ni^{2+} from the solution onto the adsorbents are shown in **Figures 4.17, 4.18, 4.19 and 4.20**. The rate of adsorption process initially depends on the mass transfer stage (Wierzba, 2017). The initial stage is characterized by high intense adsorption due to the availability of active sites on the surface of the adsorbents, therefore large concentration gradient activating the process (Asfaram et al.,2016; Wierzba, 2017). In case of CSS, the optimum time was reached after 15 minutes for the adsorption of both Cu^{2+}, Fe^{2+} and Ni^{2+} (**Fig 4.17**) and equilibrium phase started thereafter. However, in the case of MGBW, the initial stage of mass transfer from the solution to the surface of media lasted approximately 45 minutes for adsorption of both Cu^{2+}, Fe^{2+} and Ni^{2+}. The equilibrium started thereafter and was more pronounced at 60

minutes which was adopted as the optimum time with adsorption capacities of 7.6, 6.7 and 6.2 mgg^{-1} media respectively (**Fig 4.19**). The first stage of metal transfer into surface of MGS lasted 30 minutes for both Cu^{2+}, Fe^{2+} and Ni^{2+} sorption with adsorption capacities of 6.5, 5.9 and 4.2mgg^{-1}media respectively. Equilibrium stage was reached at 45 minutes for Cu^{2+}, Fe^{2+} and Ni^{2+} at adsorption capacities of 6.7, 6.1 and 4.5 mgg^{-1} media respectively (**Fig 4.20**). In case of CBW, the first stage of sorbate transfer lasted for approximately 45 minutes for sorption of $Cu^{2+}$and Fe^{2+} while 30 minutes for Ni^{2+} with adsorption capacity of 4.2 mgg^{-1}media (**Fig 4.18**). The adsorption capacities of CBW at equilibrium is 8.5, 8.7 and 4.2 mgg^{-1}media for sorption of Cu^{2+}, Fe^{2+} and Ni^{2+} respectively. However, different optimum contact times were reported by different authors for sorption of Cu^{2+}, Fe^{2+} and Ni^{2+} (Bouhamed et al., 2016;Osińska, 2017; Ouyang et al., 2019). The main reason for the differences in optimum contact times and adsorption capacities might be the differences in media mineralogy and concentrations of metals.

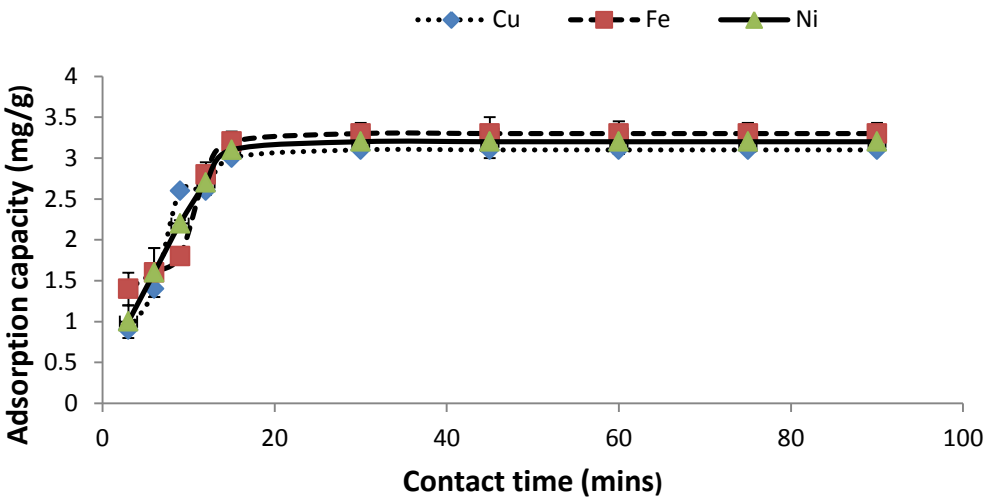

Fig 4.17 Effect of contact time on adsorption of heavy metal ions onto CSS

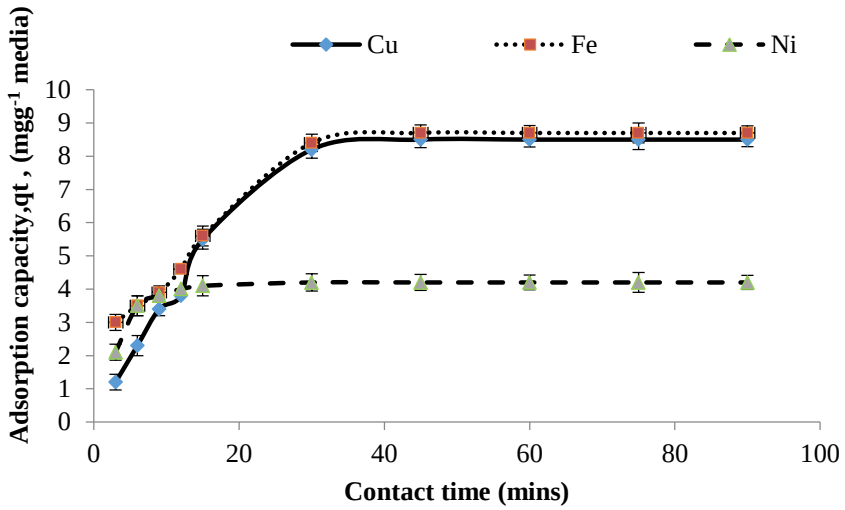

Fig 4.18 Effect of contact time on adsorption of metal ions using CBW

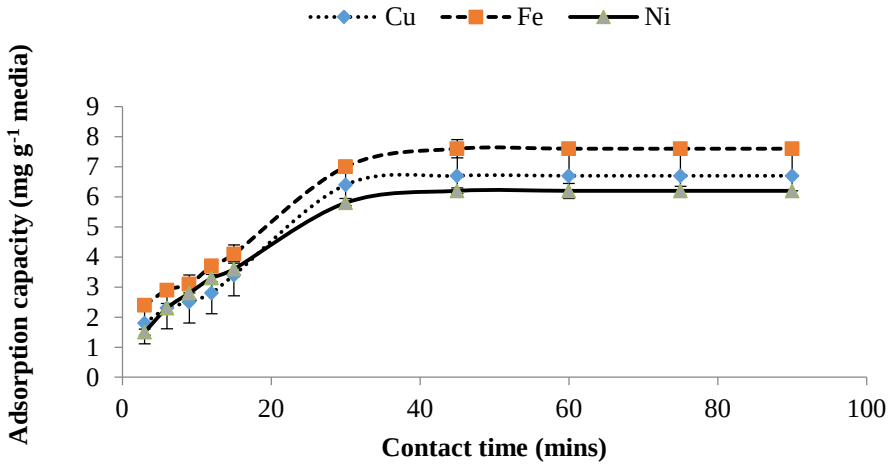

Fig 4.19 Effect of contact time on adsorption using MGBW

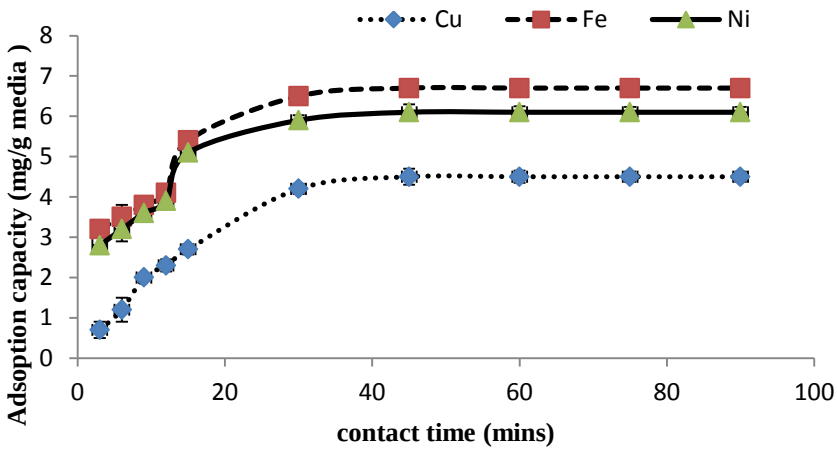

Fig 4.20 Effect of contact time on adsorption capacity using MGS

4.2.4 The influence of particle size on heavy metal ion removal

The relationships between the adsorbent particle size and removal of the heavy metals are shown in **Fig 4.21, 4.22, 4.23 and 4.24.** The aim of this study was to investigate the effect of media size and select the best size for sorption. The results of CSS revealed that the particle size of 0.6 and 1.7 mm had higher Fe^{2+} sorption capacities of 3.84 to 3.78 mgg^{-1} media respectively. Higher sorption capacities observed for smaller particle sizes is attributed to larger external surface area available (Eze et al., 2013). The CSS size of 2.0, 2.36 and 4.75 mm had lower adsorption capacities of 3.3, 1.44 and 1.28 mgg^{-1} media respectively for the adsorption of Fe^{2+} from indicating decrease in adsorption capacity as particle size increased. As for the sorption of Ni^{2+}, CSS revealed adsorption capacities of 1.12, 3.21, 3.3, 2.29 and 1.60 mgg^{-1} media using adsorbent particle sizes of 0.6, 1.18, 1.7, 2.0, 2.36 and 4.75 mm respectively (**Fig 4.22)**. CSS revealed similar adsorption capacity for Cu^{2+} at particle size 0.60 mm. The adsorption capacity increased as particle size was increased from 1.18 mm to 2.0 mm respectively with sorption capacities of 1.17 and 3.1 mgg^{-1} media. A decrease in the sorption capacities can be observed from particle size 2.3 6 mm to 4.75 mm as Cu^{2+} capacities of 1.45 and 0.89 mgg^{-1} media respectively, were observed. The results indicated that MGS had a better sorption of Fe^{2+} at the adsorbent size of 0.6 and 1.18 mm, with adsorption capacities of 6.81 and 6.83 mgg^{-1} media respectively. Media size 1.7-4.75 mm resulted in a slight drop in Fe $^{2+}$ adsorption capacities (**Fig 4.21**). As for sorption of Ni^{2+} from the same system, the sorption capacities raised from media size 0.6 mm to1.7 mm, then dropped from 2 mm to 4.75 mm. Moreover, MGS had Cu^{2+} adsorption capacity 4.34 mgg^{-1}

media at size of 0.6 mm, 4.21 mgg^{-1}media at 1.18 mm, a slight adsorption capacity rise from media size of 1.7 to 4.75 mm, with maximum sorption capacity of 4.5 mgg^{-1} media. Decrease in adsorption capacities of larger particles may be attributed to factors such as resistance of mass transfer and ineffective use of blocked sections of the adsorbent (Ngeontae et al., 2007; Eze et al., 2013). It was not understood why initially adsorption capacity increased with increasing particle sizes. It can be observed from **Fig 4.23** that MGBW revealed almost similar trend for the adsorption of Fe^{2+}, Cu^{2+} and Ni^{2+} from the solution. Maximum adsorption capacities of 7.6, 6.7, and 6.2 mgg^{-1} media were observed for media size of 2.0 mm for Fe^{2+}, Cu^{2+} and Ni^{2+}respectively. Similar trend was observed by Saueprasearsit et al., (2010). The correlation between adsorbent size and adsorption capacities of CBW for Ni^{2+}, Fe^{2+} and $Cu^{2+}$are shown in **Fig 4.24**. The results indicated that CBW of size 0.6, 1.18, 1.7 and 2mm had higher Fe^{2+}adsorption capacities of 8.62, 8.89, 8.84 and 8.70 mgg^{-1}media respectively. Attribution to large surface area of media generated higher adsorption capacities for adsorbent of smaller particle sizes (Eze et al., 2013). A slight drop Fe^{2+}adsorption capacities was observed at size 2.36 mm to 4.75 mm with adsorption capacities of 8.18 to 8.14 mgg^{-1} media respectively. Such a drop in adsorption capacities of particle size 2.36 mm and 4.75 mm may possibly due to some resistance of mass transfer and inability of adsorbates to use blocked sections of media (Ngeontae et al., 2007). The maximum adsorption capacity of 8.89 mgg^{-1} was observed for Fe^{2+} and Cu^{2+} sorption while 4.25 mgg^{-1} for Ni^{2+}sorption both at media size of 1.18 mm. A possibility of intra-particle diffusion from external surface of the media into media pores could result in high sorption capacity for smaller size particles and low adsorption capacity in larger particles (Eze et al., 2013).

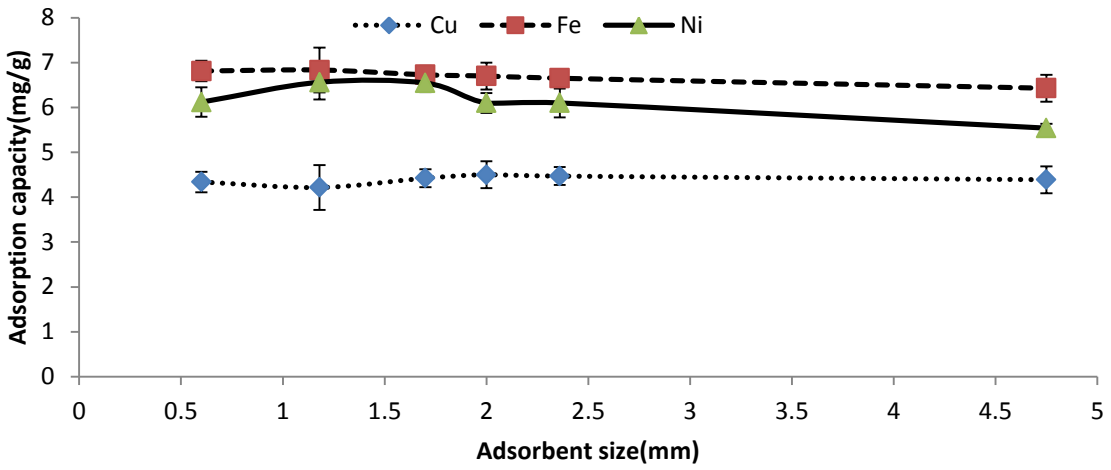

Fig 4.21 Effect of particle size on adsorption of Cu (II), Fe (II) and Ni (II) onto MGS

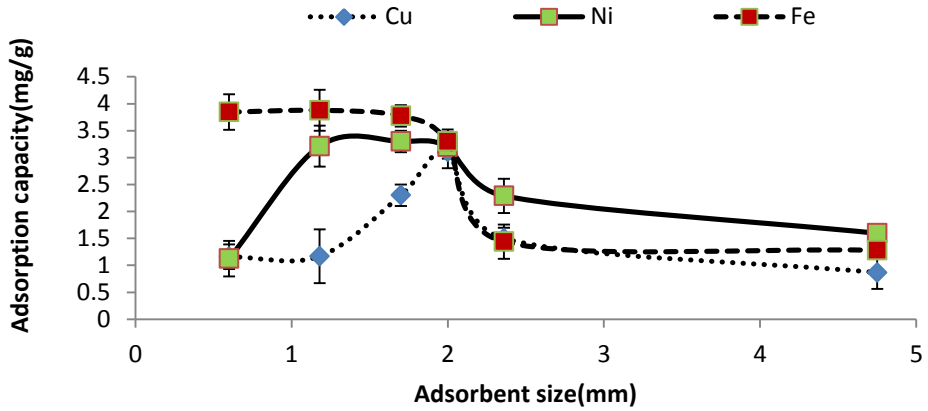

Fig 4.22 Effect of particle size on adsorption of Cu (II), Fe (II) and Ni (II) onto CSS

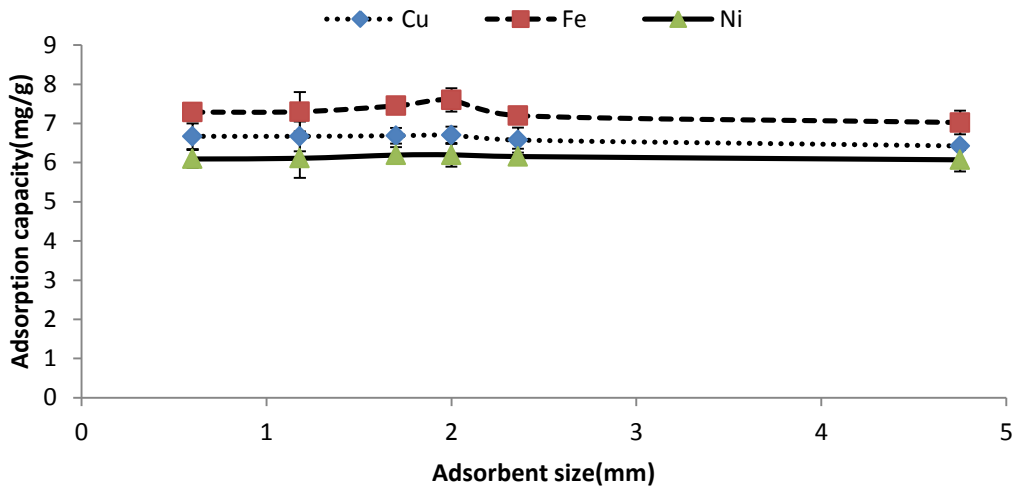

Fig 4.23 Effect of adsorbent size on adsorption of Cu (II), Fe (II) and Ni (II) onto MGBW

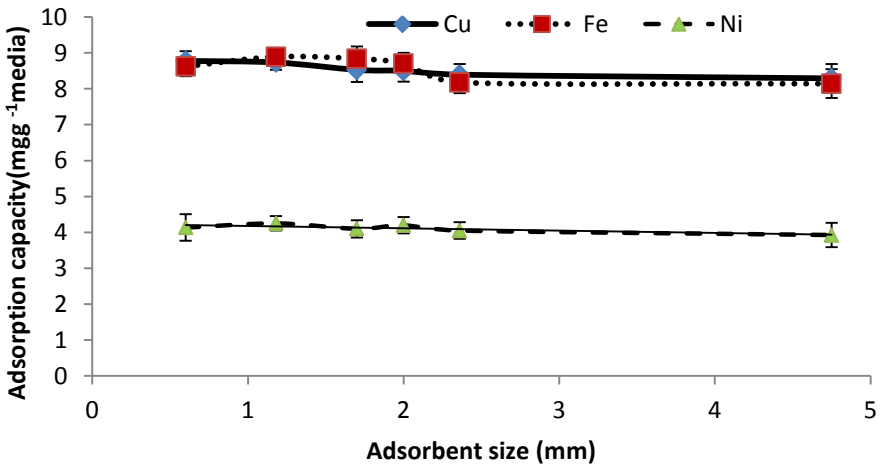

Fig 4.24 Effect of adsorbent size on adsorption of Cu (II), Fe (II) and Ni (II) onto CBW

4.3Adsorption Batch kinetic models

4.3.1Pseudo first and Pseudo second order kinetic models

The coefficients of determination (R^2) from Pseudo second order model for adsorption onto CSS were higher than Pseudo first order (PFO) coefficients of determination (**Table 4.8, Fig 4.25, and Fig 4.26**). This suggests that CSS follow pseudo second order (PSO) kinetic model with R^2 values of 0.995 for sorption of Cu^{2+}, 0.994 for sorption of Fe^{2+} and 0.996 for Ni^{2+}sorption. On the other hand, the coefficients of determination from pseudo first order kinetic model for CSS were observed to be 0.885 for sorption of Cu^{2+}, 0.811 for Fe^{2+} and

0.896 for Ni^{2+} (**Table 4.8**). The experimental adsorption capacities of CSS as shown by pseudo second order kinetic model were almost similar to the calculated values of adsorption capacities. Observations were made (**Table 4.8**) that the model or calculated adsorption capacity for both adsorption of Cu^{2+}, Fe^{2+} and Ni^{2+} using CSS was 3.3 mgg^{-1} in comparison with the experimental adsorption capacities of 3.1,3.3 and 3.2 mgg^{-1} media for sorption of Cu^{2+}, Fe^{2+} and Ni^{2+} respectively. However, in case of pseudo first order kinetic model, the calculated adsorption capacity was 3.3 mgg^{-1} media for adsorption of all metal ions onto CSS. The adsorption capacities values were way off the experimental capacities. In case of CBW, R^2values for PSO for adsorption of Fe (II) and Ni (II) are greater than of PFO suggesting the sorption follow PSO (**Fig 4.27 and Fig 4.28**). However, Cu (II) sorption onto CBW follows PFO with R^2 value of 0.977. On the other hand, sorption of Cu^{2+} and Ni^{2+} using MGBW follow pseudo-first order while sorption of Ni^{2+} follow pseudo second order with R^2 of 0.984 and RMSE of 0.0576 (**Fig 4.29 and Fig 4.30**). As for MGS (**Fig 4.31 and Fig 4.32**), it can be noted that Fe^{2+} and Ni^{2+} sorption follow PFO while Cu^{2+} follow PSO looking at differences in R^2 values. If the adsorption kinetics follow Pseudo first order model, adsorption occurs through diffusion through the interface (Martins *et al.*, 2014). The Lagergren pseudo second order kinetic model implies that chemisorption is the rate controlling mechanism, consequently there was chemical bonding taking place between media surface and metals (Mishra et al., 2017). The adsorption of Cu^{2+}, Ni^{2+} and Fe^{2+}onto both adsorbents indicated that chemisorption process was taking place and intra-particle diffusion was not the only rate controlling mechanism.

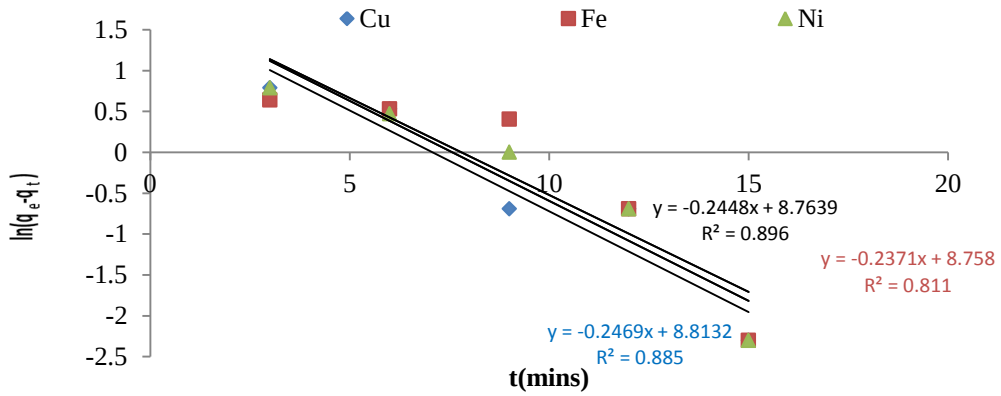

Fig 4.25 Pseudo first order kinetic model for CSS

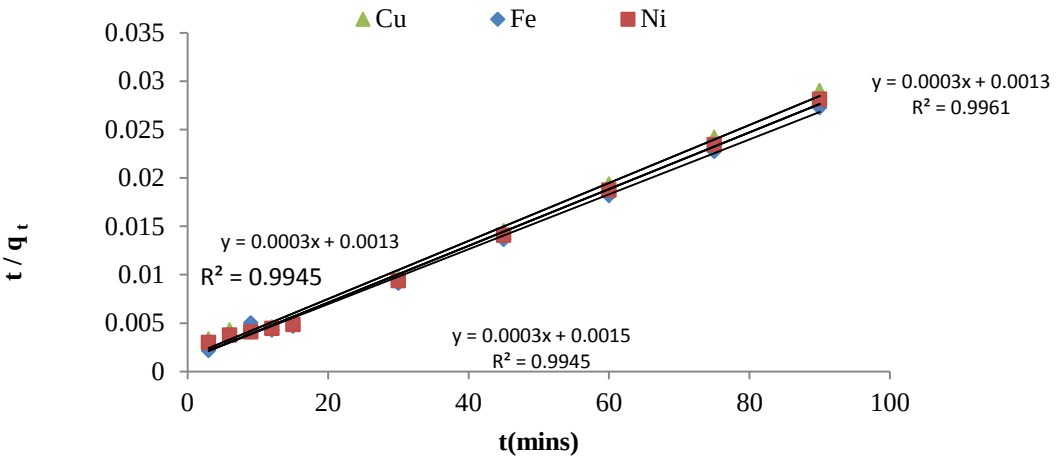

Fig 4.26 Pseudo second kinetic model for CSS

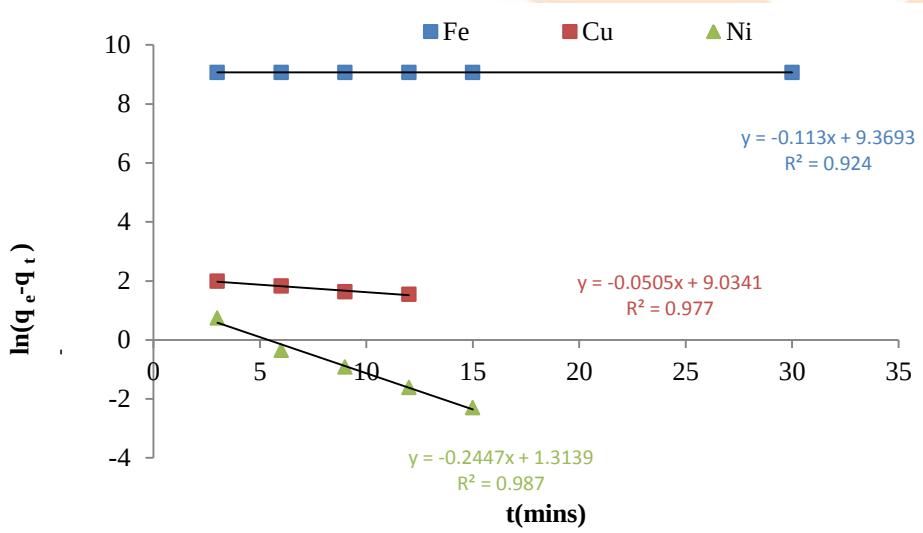

Fig 4.27 Pseudo first order kinetic model for CBW

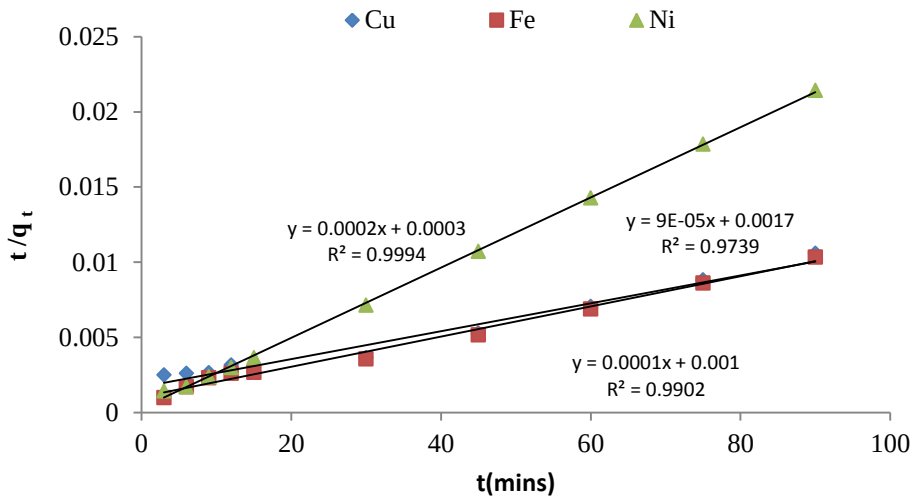

Fig 4.28 Pseudo second order kinetic model for CBW

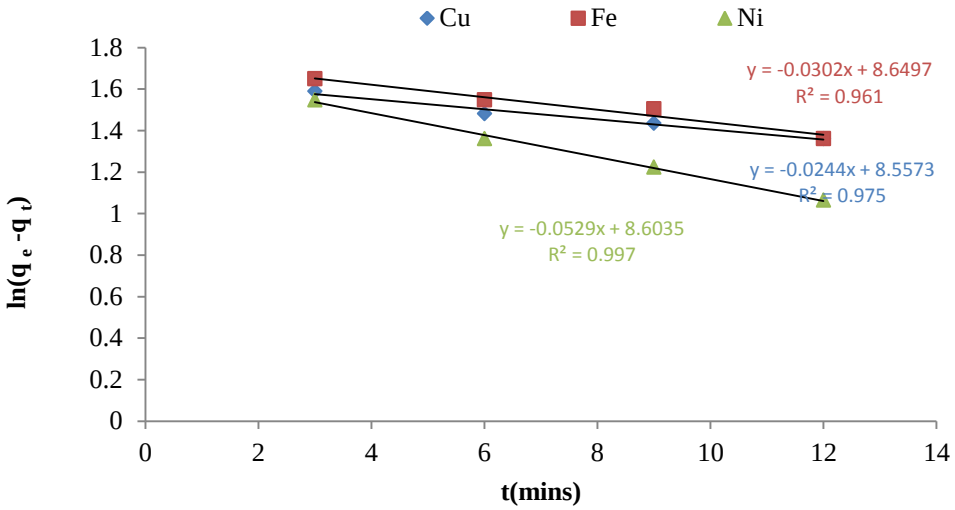

Fig 4.29 Pseudo first order kinetic model for MGBW

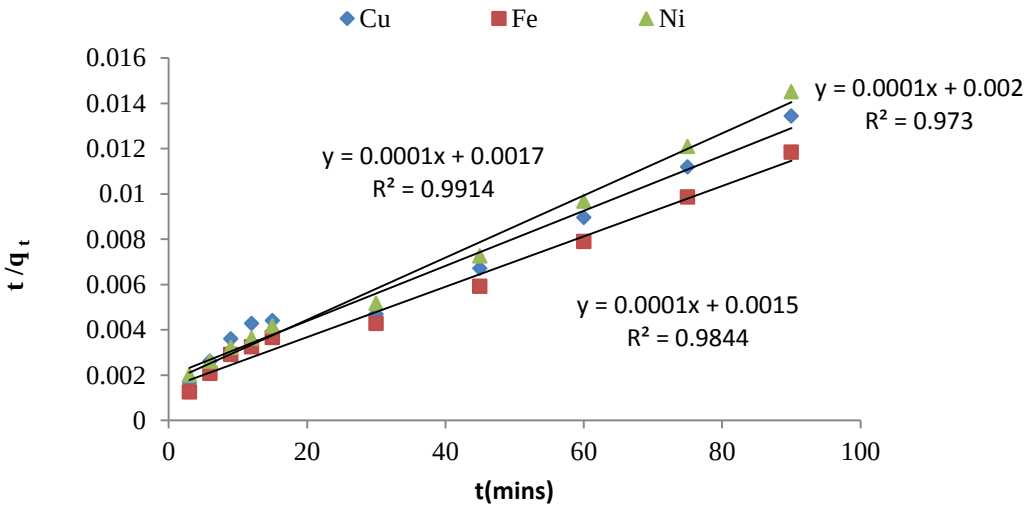

Fig 4.30 Pseudo second kinetic model for MGBW

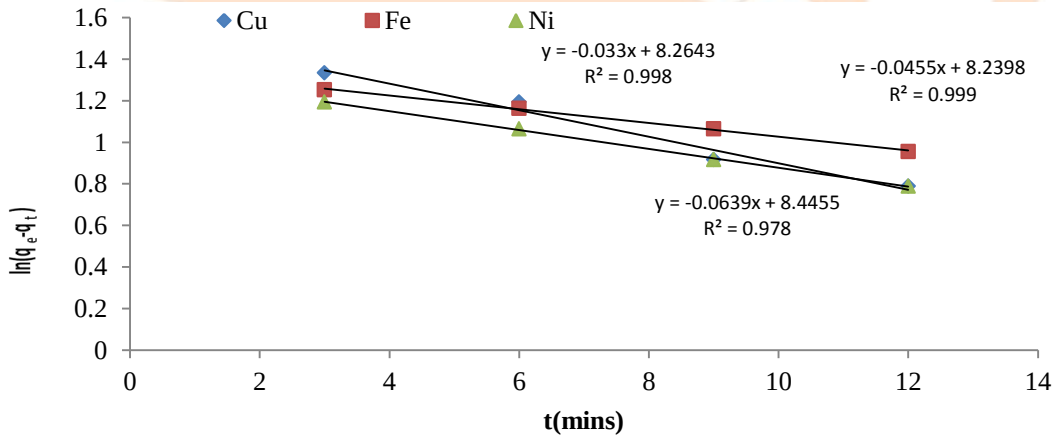

Fig 4.31 Pseudo first order kinetic model for MGS

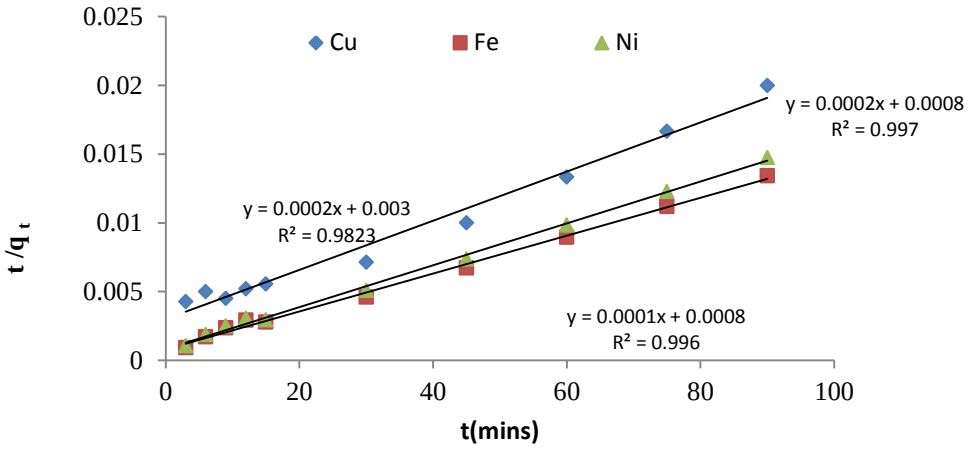

Fig 4.32 Pseudo second order kinetic model for MGS

4.3.2 Intra-particle diffusion model

The plot of intraparticle diffusion model was used to further investigate the adsorption mechanisms involved in the heavy metal removal by the four adsorbents (**Fig 4.33, Fig 4.34, Fig 4.35 and Fig 4.36).** If the plot of qt vs $t^{½}$ is a straight line passing through the origin then the adsorption process is controlled by intraparticle diffusion only (Fierro and Torne, 2008). The graphs for the CSS and CBW show three distinctive steps for Cu^{2+} and Fe $^{2+}$adsorption process and two steps for Ni adsorption (**Fig 4.33 and Fig 4.34**). The graphs were not straight lines and did not pass through the origin suggesting that intraparticle diffusion was not the only rate controlling mechanism but other mechanisms such as film diffusion were also rate controlling. The first step which was the external surface adsorption or instantaneous adsorption was observed during the early stage with intraparticle rate constants of 1.1 mg g^{-1} $min^{-0.5}$ for Cu followed by the second step or gradual adsorption having the rate constant of 0.23 mg g^{-1} $min^{-0.5}$for CSS. Lastly, the equilibrium step was observed where the graphs formed a plateau like curve. Gradual adsorption rate constant was lower that instantaneous rate constant indicating that it was rate controlling on CSS and CBW. The first portion is attributed to the use of readily available sites by the metal ions on the surface of the adsorbents whereas the second step, which was very slow involves the penetration of pollutants from the adsorbent surface into the inner pores of the adsorbent which are limited hence controlling the rate of adsorption (Gupta et al., 2019). For Ni

adsorption onto CSS and CBW there was no distinction between the first and second step suggesting they occurred at the same rate and time.

Unlike CSS and CBW, the adsorption of the three metals onto MGS and MGBW indicated three distinctive steps that were all involved during the process (**Fig 4.35 and Fig 4.36).** The rate constant for the first and second steps during Fe adsorption were 0.73 and 1.2 mg g^{-1} $min^{-0.5}$ for MGBW. In the case of Cu^{2+} adsorption onto MGBW, the corresponding rate constants were 0.8 and 1.82 mg g^{-1} $min^{-0.5}$ respectively. In these two scenarios, the rate constants of the first stages (film diffusion) were lower than the rate constants of the second stages (intra-particle diffusion) indicating that film diffusion was controlling the rate of Fe and Cu ions adsorption onto MGBW. These findings are similar to that observed by Jellali *et al.*, (2011) for phosphate ions adsorption onto phosphates mine wastes. The rate constants for Ni adsorption were 1.02 and 0.9 mg g^{-1} $min^{-0.5}$ respectively, for instantaneous and gradual adsorption. Unlike for the other two ions (Cu and Fe), gradual adsorption was rate controlling the adsorption mechanism. All the graphs have the intercept C indicating that they did not pass through the origin thus intraparticle diffusion was not solely controlling the rate of adsorption. Multi-linearity exhibited by all the graphs is a further indication that there were two or more steps controlling the sorption processes. The intercept gives an indication of the boundary layer thickness (Fierro and Torne, 2008) which should be overcome during mass transfer. It has been reported by (Viegas *et al.*, 2014) that the rate limiting step during adsorption processes help in the determination of practical options that should be introduced to improve the system. For film diffusion being the rate limiting step, turbulent conditions or mixing could be improved through the increase of mixing or stirring speed and in the case of intraparticle being the rate limiting step adsorbent dose could be increased to add more adsorption sites. It was therefore apparent in this study that both stirring speed and media dose could be increased to improve the adsorption process.

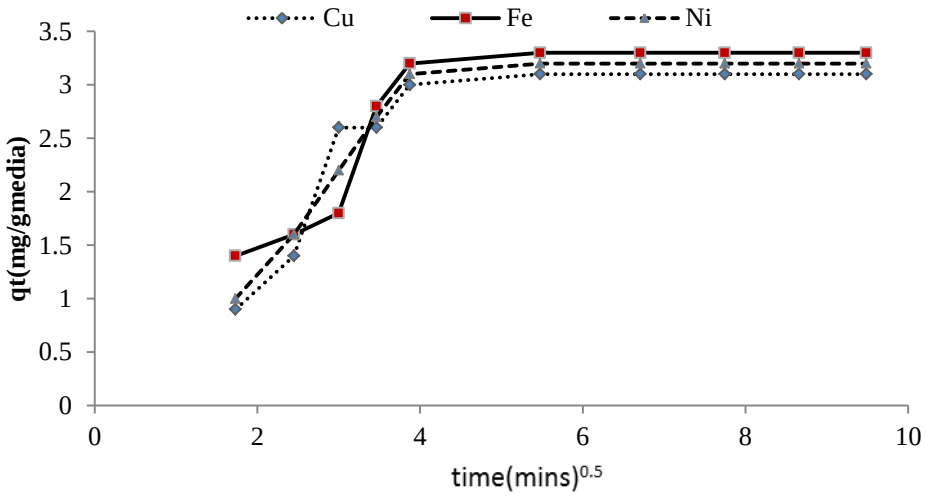

Fig 4.33 Intra-particle diffusion model for CSS

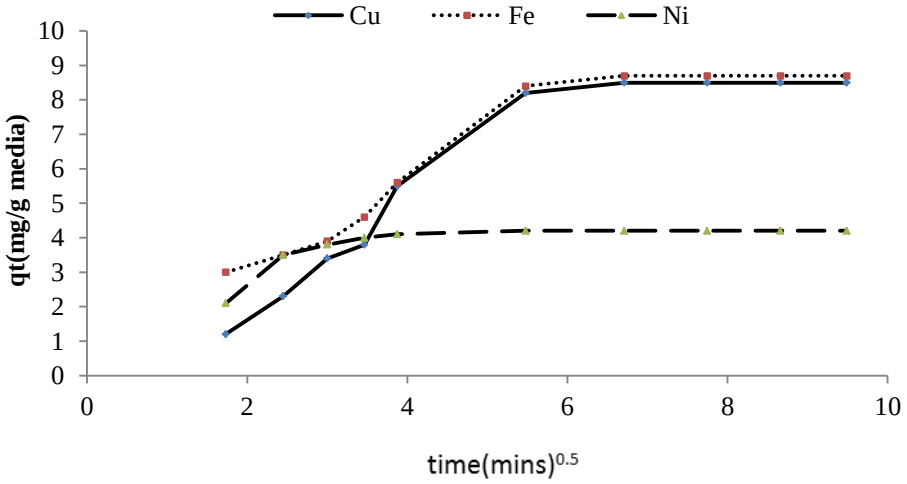

Fig 4.34 Intra-particle diffusion model for CBW

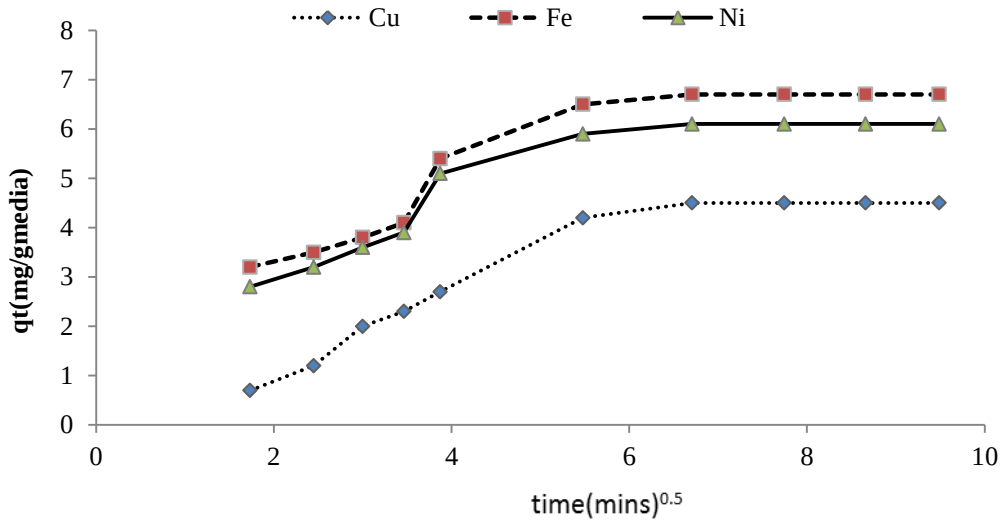

Fig 4.35 Intra-particle diffusion model for MGS

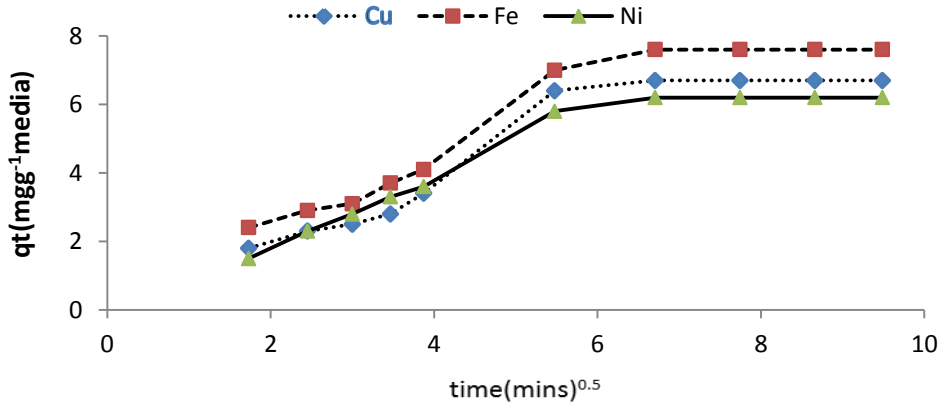

Fig 4.36 Intra-particle diffusion kinetic model for MGBW

Table 4.8 Difference between estimated constants and coefficients of determination associated with batch kinetic models.

		Pseudo-First Order Kinetic Model					Pseudo-Second Order Kinetic Model				
Adsorbents	Metal Ions	q_e model (mgg^{-1})	q_e experimental (mgg^{-1})	k_1 (min^{-1})	R^2	RMSE	q_e model (mgg^{-1})	q_e experimental (mgg^{-1})	k_2((g/mg)min)	R^2	RMSE
CSS	Cu^{2+}	6.504×10^{8}	3.1	0.569	0.885	0.9999	3.3	3.1	61.22	0.995	0.0037
	Fe^{2+}	5.727×10^{8}	3.3	0.546	0.811	0.9999	3.3	3.3	70.64	0.994	0.0000
	Ni^{2+}	5.806×10^{8}	3.2	0.564	0.896	0.9999	3.3	3.2	70.64	0.996	0.0009
MGS	Cu^{2+}	2.789×10^{8}	4.5	0.147	0.978	0.9999	5	4.5	5	0.982	0.0100
	Fe^{2+}	1.837×10^{8}	6.7	0.076	0.998	0.9999	10	6.7	12.50	0.996	0.1089
	Ni^{2+}	1.737×10^{8}	6.1	0.105	0.999	0.9999	5	6.1	50	0.997	0.0484
MGBW	Cu^{2+}	3.608×10^{8}	6.7	0.056	0.975	0.9999	10	6.7	5	0.973	0.1089
	Fe^{2+}	4.464×10^{8}	7.6	0.070	0.961	0.9999	10	7.6	6.67	0.984	0.0576
	Ni^{2+}	4.013×10^{8}	6.2	0.122	0.997	0.9999	10	6.2	5.88	0.991	0.1444
CBW	Cu^{2+}	1.082×10^{8}	8.5	0.116	0.977	0.9999	11.1	8.5	4.77	0.974	0.0548
	Fe^{2+}	2.340×10^{8}	8.7	0.260	0.924	0.9999	10	8.7	10	0.990	0.0169
	Ni^{2+}	20.6	4.2	0.564	0.987	0.6338	5	4.2	50	0.999	0.0256
		Intra-particle Diffusion kinetic Model									
		K_{id}(mg/(gmin$^{-0.5}$)	C		R^2						
CSS	Cu^{2+}	0.2151	1.4685		0.5511						
	Fe^{2+}	0.2327	1.5061		0.6425						
	Ni^{2+}	0.2275	1.4632		0.6161						
MGBW	Cu^{2+}	0.7411	0.7022		0.8710						
	Fe^{2+}	0.7819	1.2474		0.8890						
	Ni^{2+}	0.6430	1.0283		0.8789						
CBW	Cu^{2+}	0.9836	0.6665		0.8461						
	Fe^{2+}	0.8363	1.9814		0.8651						
	Ni^{2+}	0.1577	3.0207		0.4374						
MGS	Cu^{2+}	0.5078	0.4392		0.8627						
	Fe^{2+}	0.5021	2.6891		0.8357						
	Ni^{2+}	0.4496	2.5251		0.8231						

4.4 Adsorption isotherm models

With comparison of the two isotherm models for Cu^{2+} adsorption onto CSS at temperature of 293 K, it can be observed that Langmuir had R^2 = 0.7264, Qmax = 1.515 mgg^{-1} media and K_L = 0.1305 Lmg^{-1} (**Table 4.9**). The Langmuir model did not describe data better than Freundlich model (R^2 = 0.8152, 1/n = 0.5818 and K_f = 0.217mgg^{-1}). Moreover, it can be observed that Freundlich model also described data better for Cu^{2+} adsorption onto CSS at both temperatures of 303 K and 313 K than Langmuir model (**Fig 4.37 and Fig 4.38**). As for Fe^{2+} and Ni^{2+} adsorption onto CSS, it can be observed that Freundlich isotherm model described data better than Langmuir isotherm model at both temperatures of 293 K, 303 K and 313 K (**Fig 4.39, Fig 4.40, Fig 4.41 and Fig 4.42**). The results suggest that CSS surfaces were heterogeneous and the active sites on the adsorbent had different energies (Balouch *et al.*, 2015). It has been reported that values of 1/n < 1 indicate favourable adsorption process, and in addition values of n ranging from 1 to 10 indicate good adsorption and a favourable

physical process (Al-Senani and Al-fawzan, 2018). Values of 1/n were all < 1 therefore suggesting favourable adsorption of metal ions onto CSS. The calculated adsorption intensity values n, at all temperatures were between 1.58 and 2 indicating good adsorption process. Adsorption of Cu^{2+} onto MGBW was better described by Langmuir isotherm than Freundlich isotherm at temperatures of 293 K and 303 K (**Fig 4.43 and Fig 4.44**). The K_L at 293 K was higher than at 303 K indicating that Cu^{2+} had a stronger affinity with adsorbent surface at 293K than at 303 K. The adsorption of Cu^{2+} at 313 K was better described by the Freundlich isotherm than Langmuir isotherm with R^2 values of 0.9056 and 0.8830 respectively for Freundlich and Langmuir models. The Freundlich model better described Fe^{2+} and Ni^{2+} adsorption than Langmuir model at both temperatures (**Table 4.9, Fig 4.45, Fig 4.46, Fig 4.47 and Fig 4.48**). It can also be concluded that MGBW surfaces were heterogeneous with different or exponentially distributed energy levels on the active sites as well. The adsorption intensity values, n, were between 1.15 and 2.16 indicating good adsorption process. Similarly all 1/n values were less than 1 indicating favourable adsorption process. An observation can also be made that CBW had a better fitness on Freundlich isotherm model than Langmuir for sorption of Cu^{2+} at both temperatures of 293 K, 303 K and 313 K. Freundlich model produced R^2 values 0.7519, 0.7704 and 0.7589 respectively at 293 K, 303 K and 313 K for Cu^{2+}sorption, while 0.2955, 0.4321, 0.4039 at 293 K, 303 K and 313 K for Langmuir isotherm model (**Fig 4.51 and Fig 4.52**). A yield of better fitness on Freundlich than Langmuir isotherm model can also be seen on sorption of Fe^{2+} and Ni^{2+} using CBW at both temperatures of 293 K, 303 K and 313 K suggesting heterogeneous sorption (**Fig 4.57-Fig 4.60**). Negative values of q_{max} can be observed on Langmuir isotherm model of CBW. This implies that desorption of metal ions was taking place instead of adsorption at such temperatures. These results contrasts the findings by Abdel et al., (2011) whose data was better fitted by the Langmuir model than Freundlich model for the removal of heavy metals from wastewater using low cost adsorbents. However, the study is comparable to the study conducted by Wang *et al.*, (2020) on the adsorption of cadmium and copper from aqueous solution using sodium ion modified Pisha Sandstone. The adsorbent, MGS had a better fit on Freundlich isotherm model than Langmuir isotherm model for Cu^{2+}sorption (**Fig 4.49 and Fig 4.50**). The indices of performance of model were R^2 =0.6663, 0.7523 and 0.7516 respectively at 293 K, 303 K and 313 K respectively for Freundlich isotherm model. By comparing the R^2 values for Fe^{2+} sorption onto MGS, it can be observed that Freundlich isotherm model fit adsorption data better with R^2 values as 0.2471, 0.4931 and 0.5318 respectively for temperatures 293 K, 303 K and 313 K (**Fig 4.51 and Fig 4.52**). Such results

indicate that the sorption for $Fe^{2+}$was taking place on heterogeneous surfaces of MGS. However, Ni^{2+} sorption onto MGS yielded a better fit on Langmuir isotherm model with the indices model performance, R^2 value of 9×10^{-6} at 293 K (**Fig 4.53 and Fig 4.54**). The results indicated that the adsorption of Ni^{2+} was monolayer sorption with distribution of homogeneous active sites on the surface of MGS. It is however, observed with two models that Ni^{2+} sorption at 303 K and 313 K fit well on Freundlich isotherm model than Langmuir suggesting heterogeneous adsorption on active sites. Moreover, the results are comparable to findings reported by (Hemalatha and Rao, 2014) where data satisfactorily fitted both Langmuir and Freundlich model for sorption of hexavalent chromium and nickel onto calcined brick powder. The study is also comparable to the work reported by (Ouyang *et al.*, 2019) on the adsorptive removal of $Pb^{2+,}$ Cd^{2+}, and Cu^{2+} onto silicate tailings.

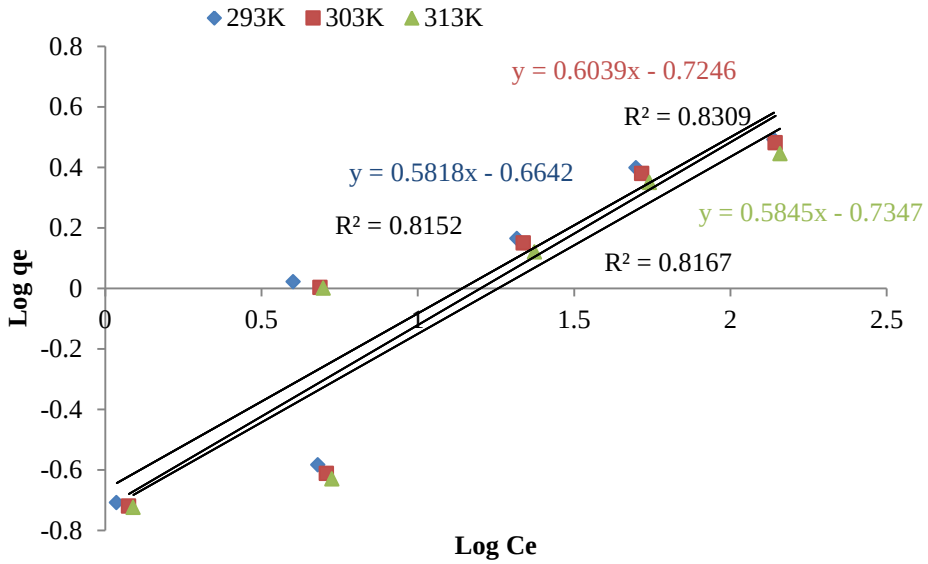

Fig 4.37 Freundlich isotherm Cu (II) for sorption onto CSS at various temperatures

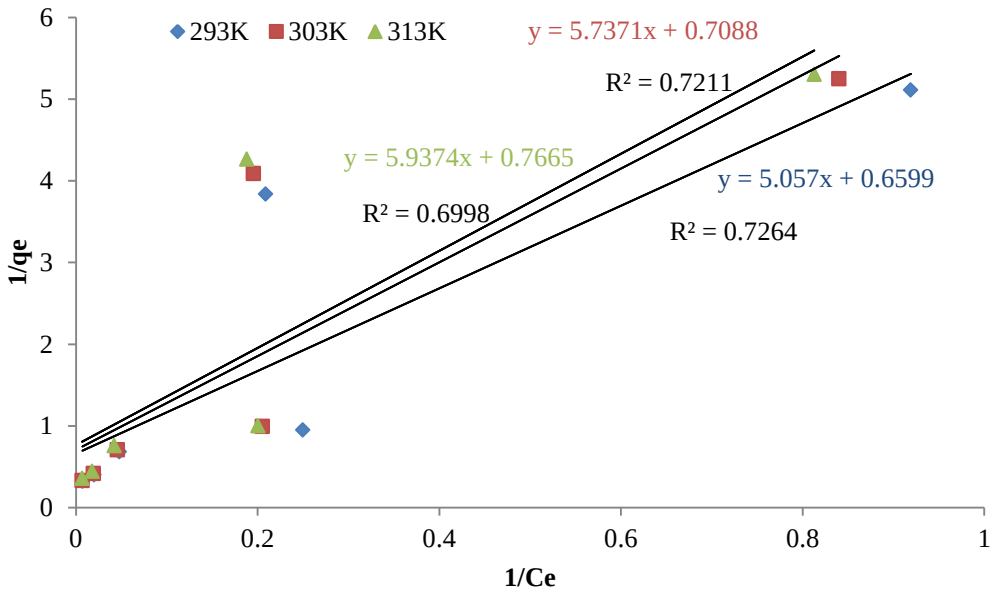

Fig 4.38 Langmuir isotherm for sorption of Cu (II) onto CSS at different temperatures

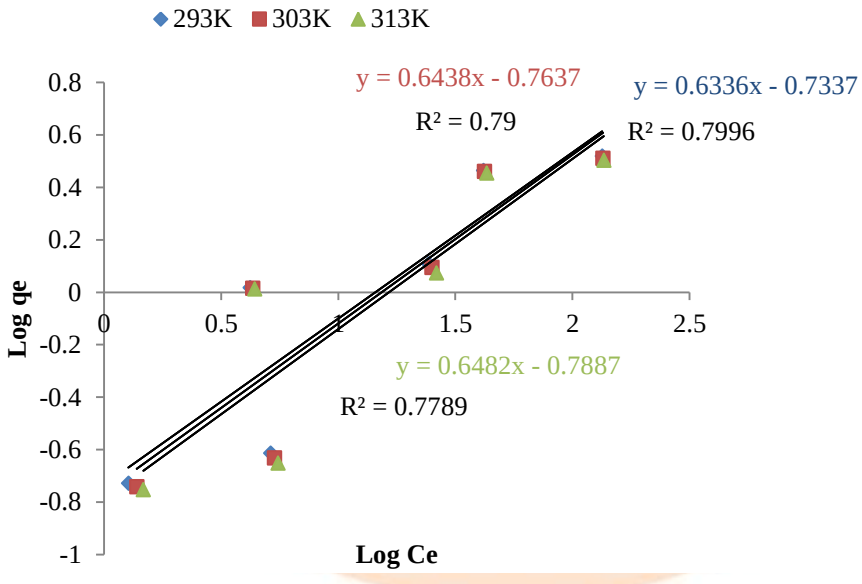

Fig 4.39 Freundlich model for Fe (II) sorption onto CSS at various temperatures

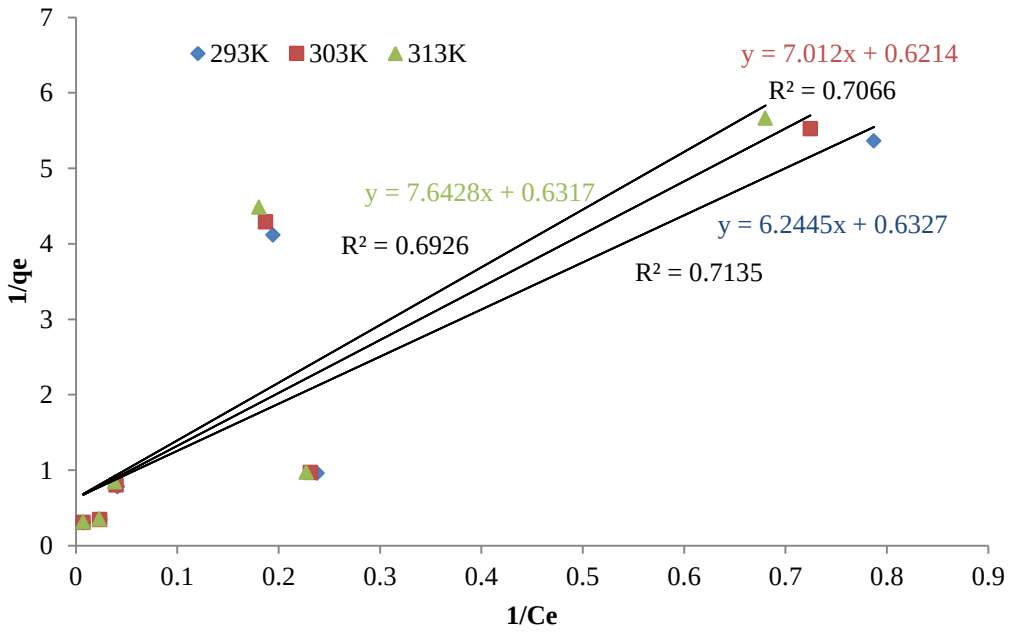

Fig 4.40 Langmuir isotherm for Fe (II) onto CSS at different temperatures

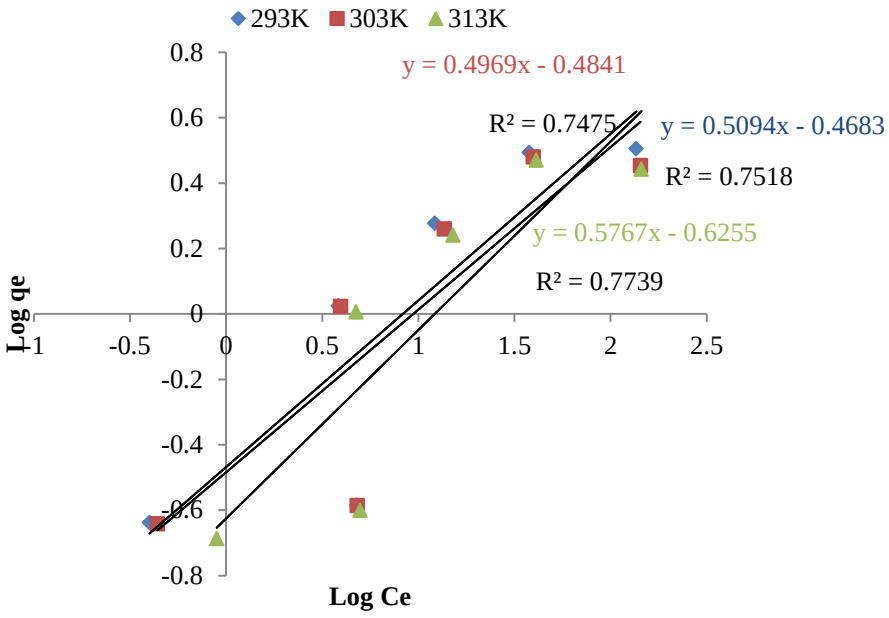

Fig 4.41 Freundlich isotherm for Ni (II) onto CSS at various temperatures

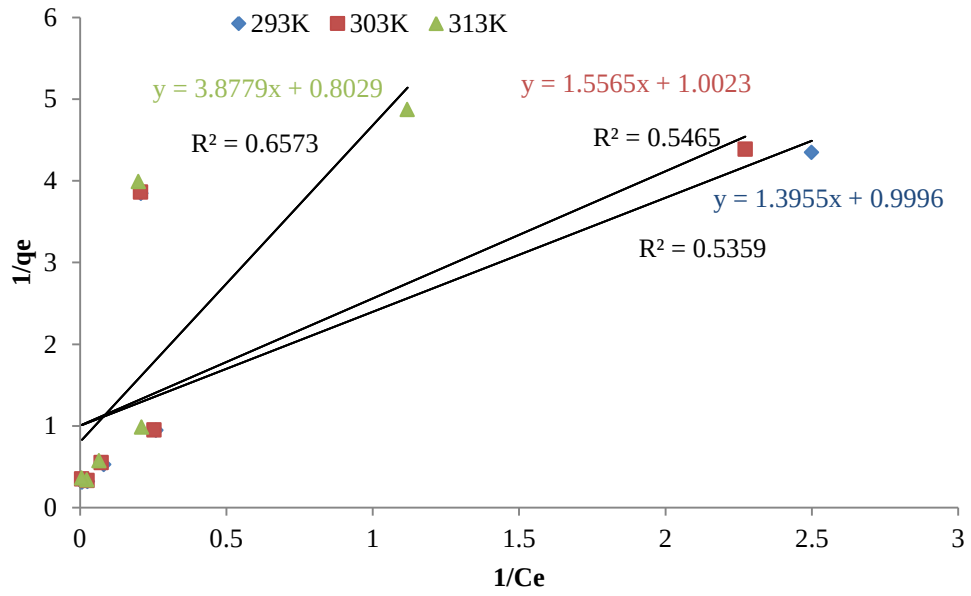

Fig 4.42 Langmuir isotherm for Ni (II) onto CSS at various temperatures

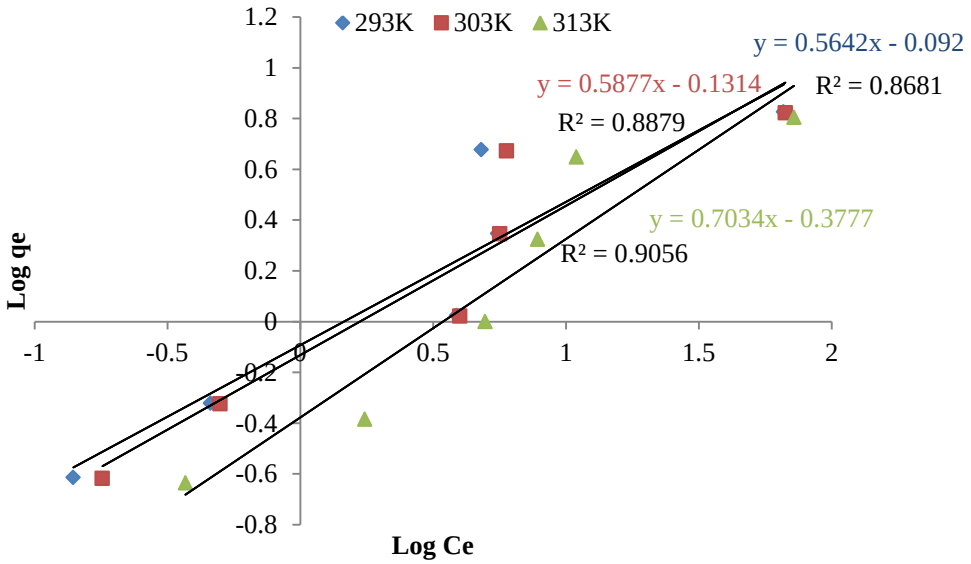

Fig 4.43 Freundlich isotherm for sorption of Cu (II) onto MGBW at different temperatures

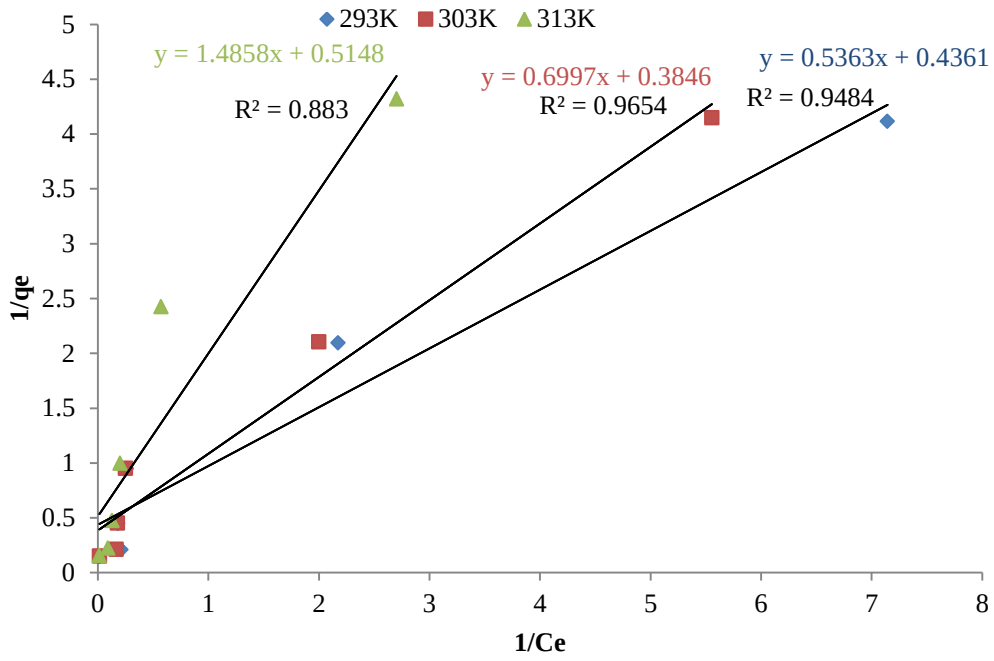

Fig 4.44 Langmuir isotherm for sorption of Cu (II) onto MGBW at different temperatures

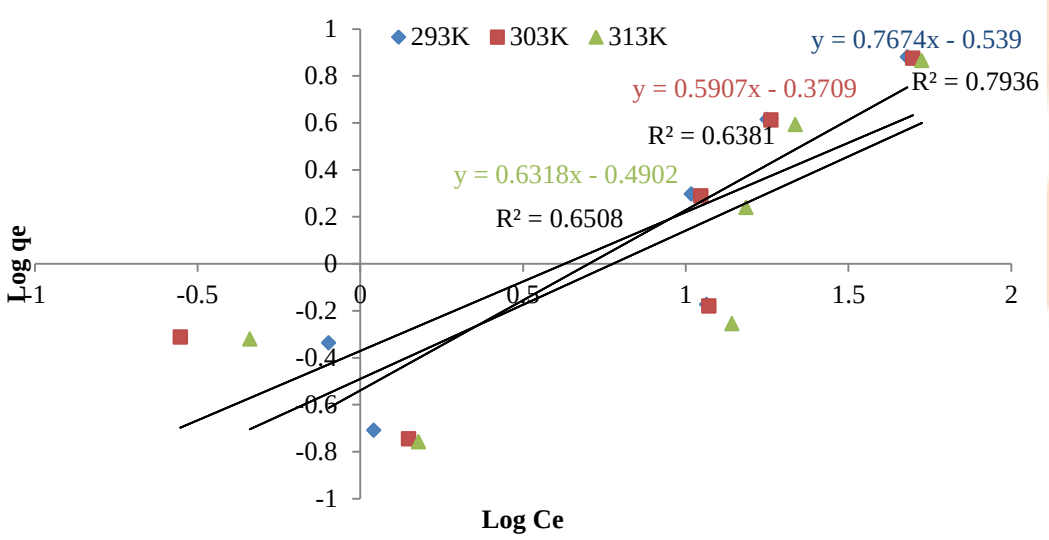

Fig 4.45 Freundlich isotherm for sorption of Fe (II) onto MGBW at different temperatures

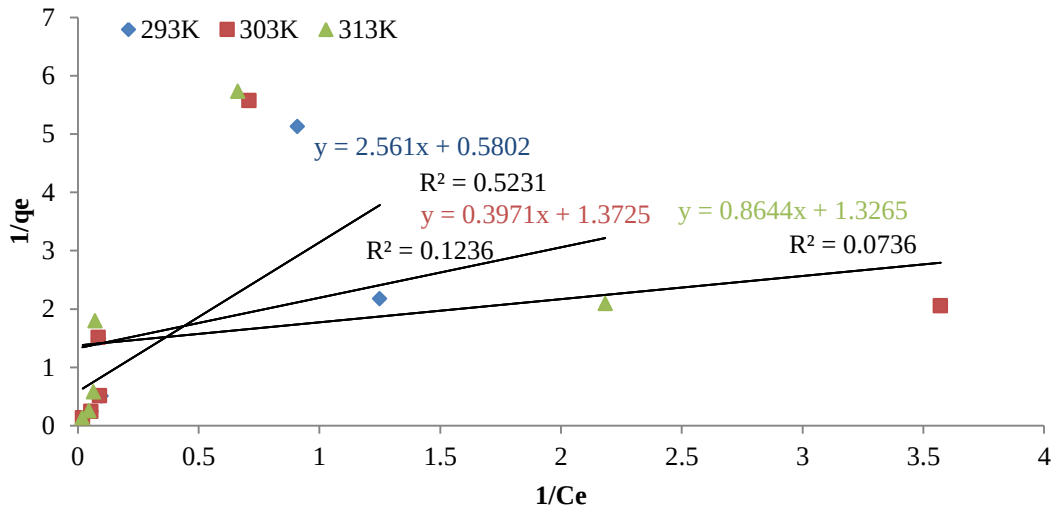

Fig 4.46 Langmuir isotherm for sorption of Fe (II) onto MGBW at different temperatures

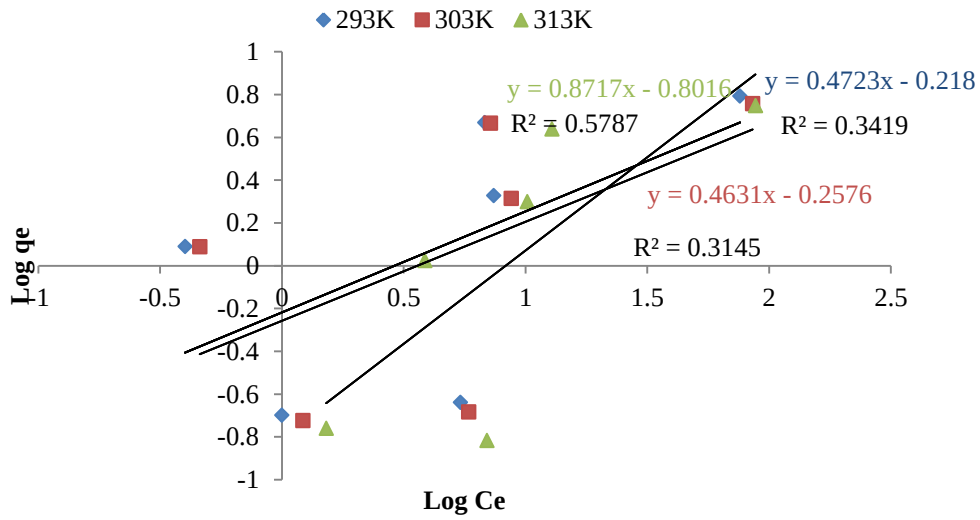

Fig 4.47 Freundlich isotherm for sorption of Ni (II) onto MGBW at different temperatures

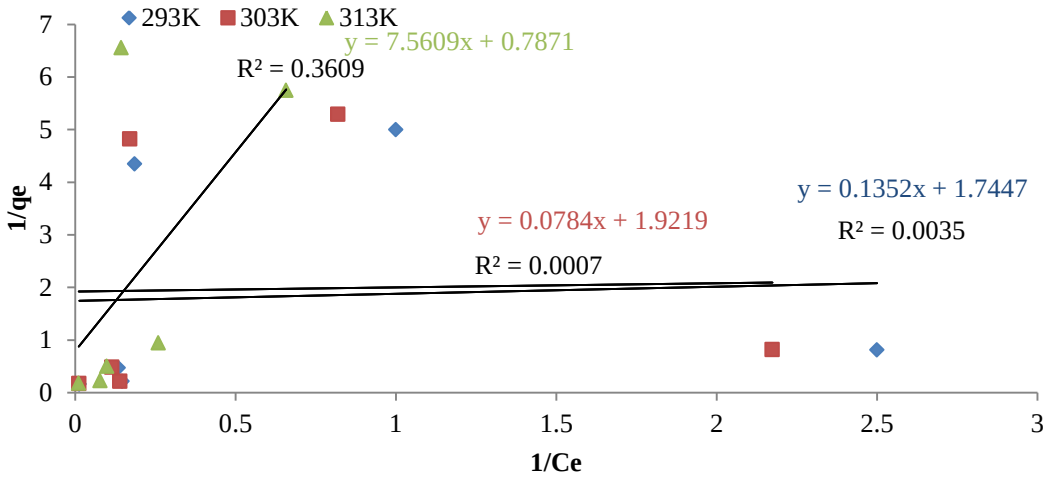

Fig 4.48 Langmuir isotherm for sorption of Ni (II) onto MGBW at different temperatures

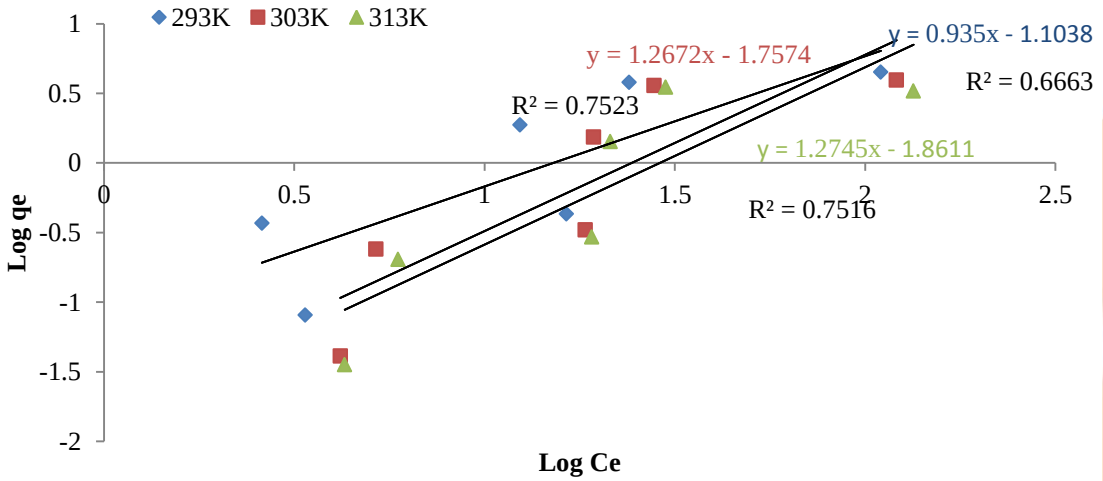

Fig 4.49 Freundlich isotherm for sorption of Cu (II) onto MGS at different temperatures

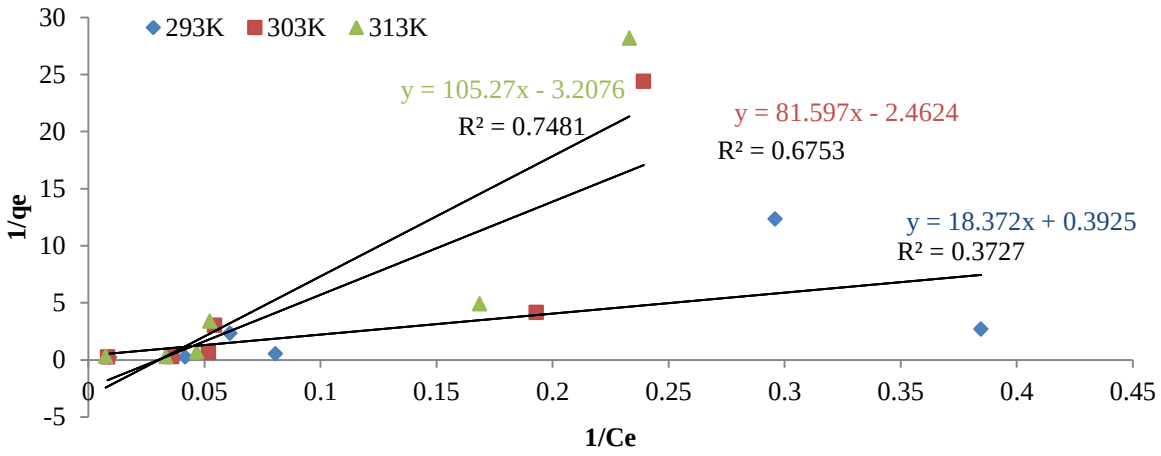

Fig 4.50 Langmuir isotherm for sorption of Cu (II) onto MGS at different temperatures

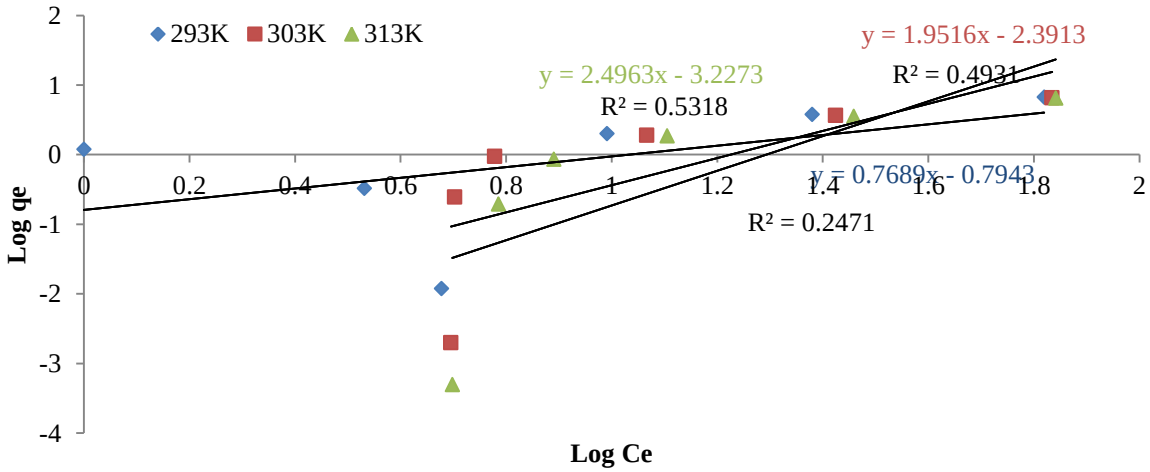

Fig 4.51 Freundlich isotherm for sorption of Fe (II) onto MGS at different temperatures

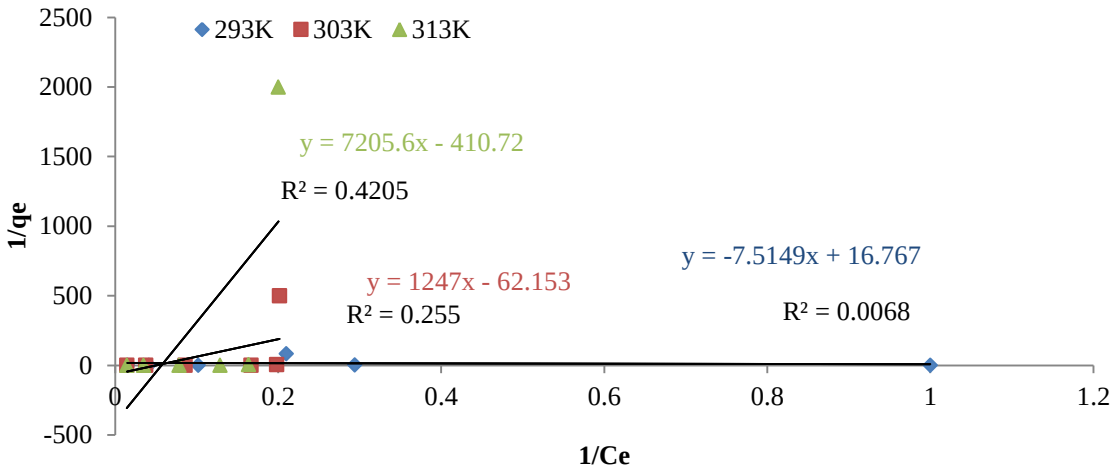

Fig 4.52 Langmuir isotherm for sorption of Fe (II) onto MGS at different temperatures

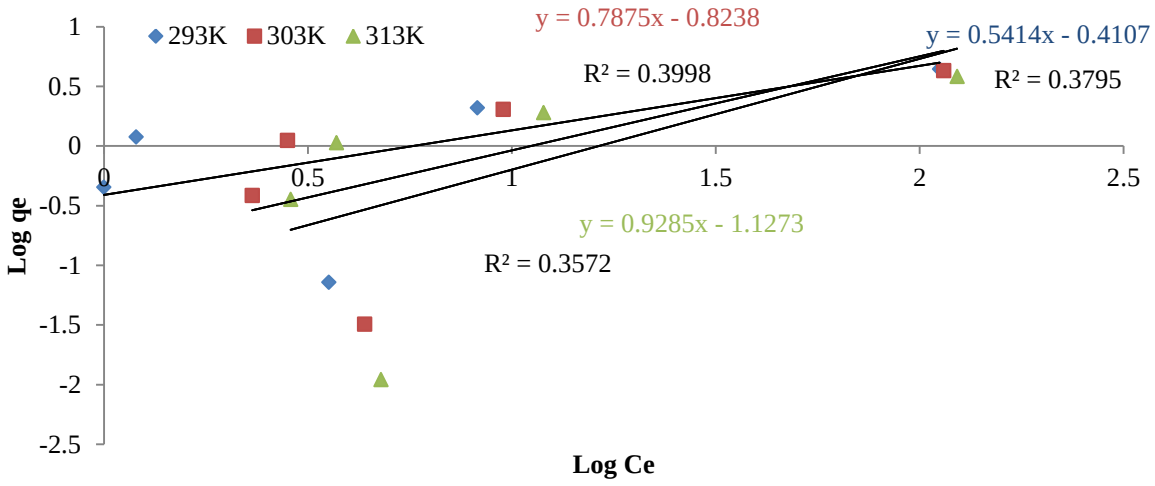

Fig 4.53 Freundlich isotherm for sorption of Ni (II) onto MGS at different temperatures

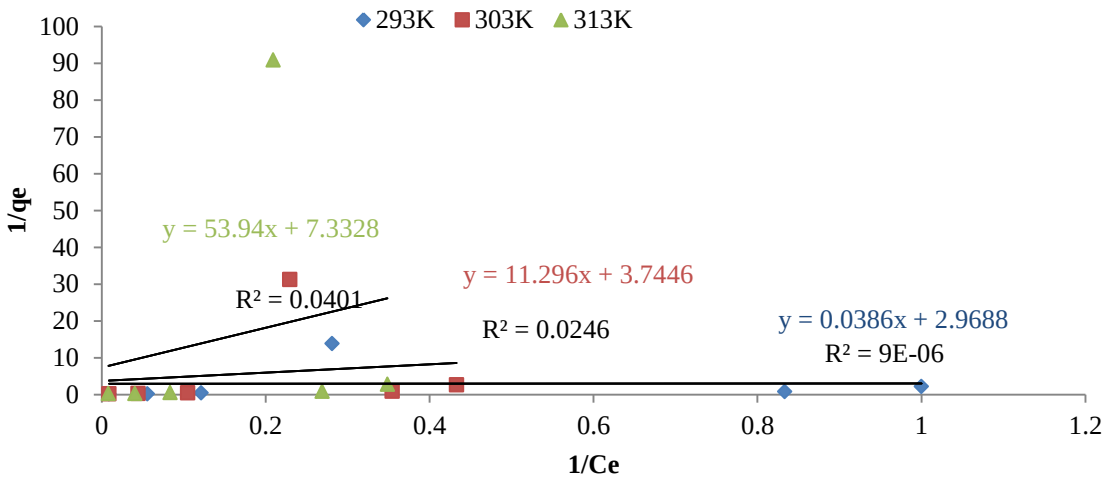

Fig 4.54 Langmuir isotherm for sorption of Ni (II) onto MGS at different temperatures

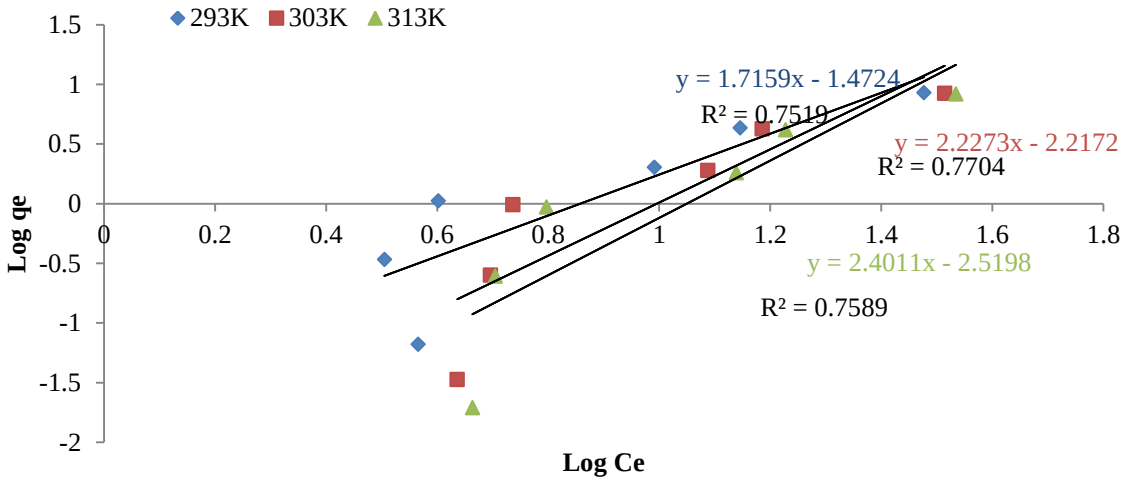

Fig 4.55 Freundlich isotherm for sorption of Cu (II) onto CBW at different temperatures

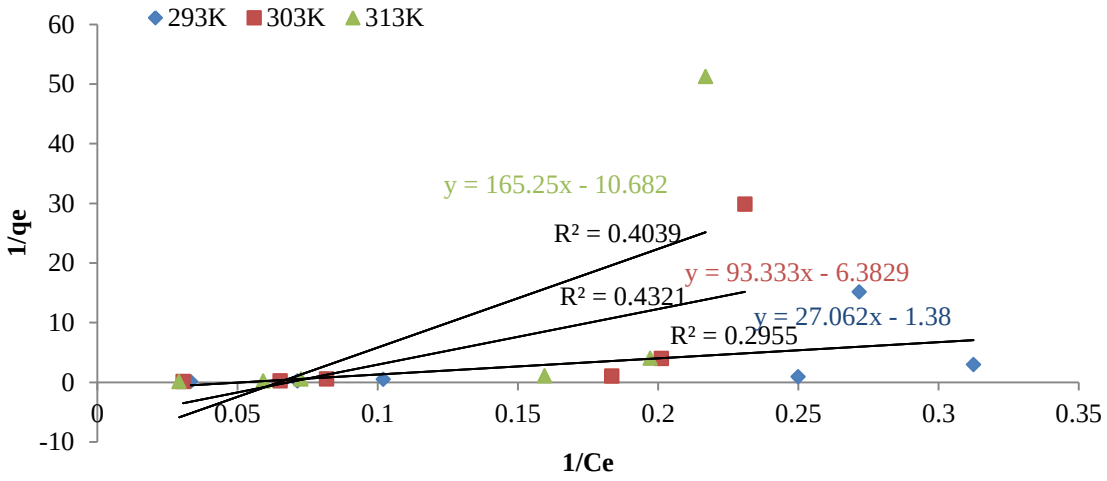

Fig 4.56 Langmuir isotherm for sorption of Cu (II) onto CBW at different temperatures

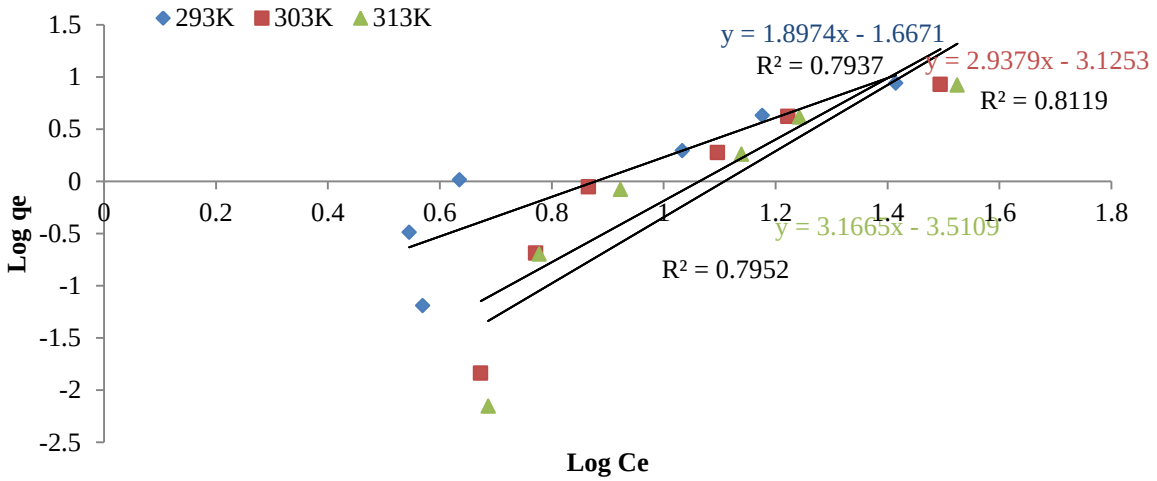

Fig 4.57 Freundlich isotherm for sorption of Fe (II) onto CBW at different temperatures

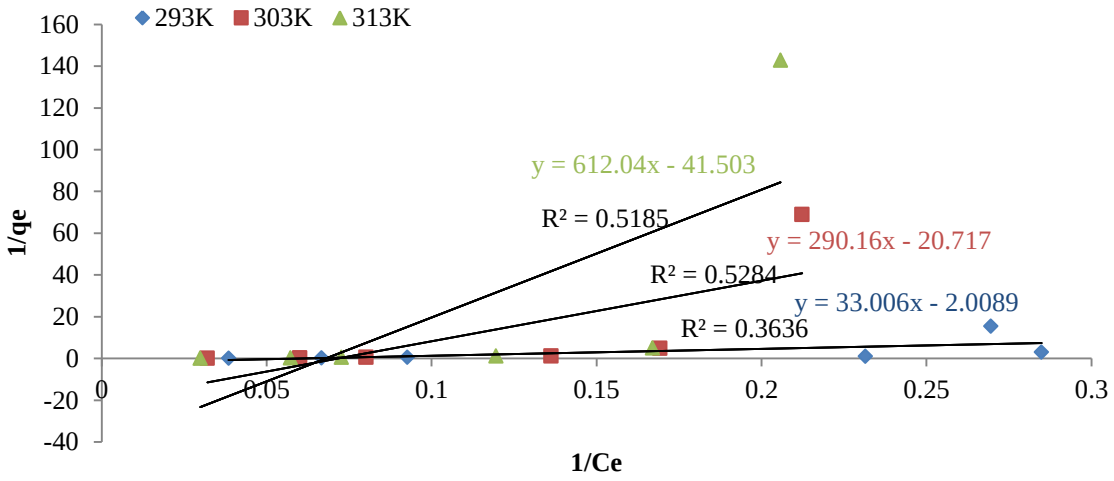

Fig 4.58 Langmuir isotherm for sorption of Fe (II) onto CBW at different temperatures

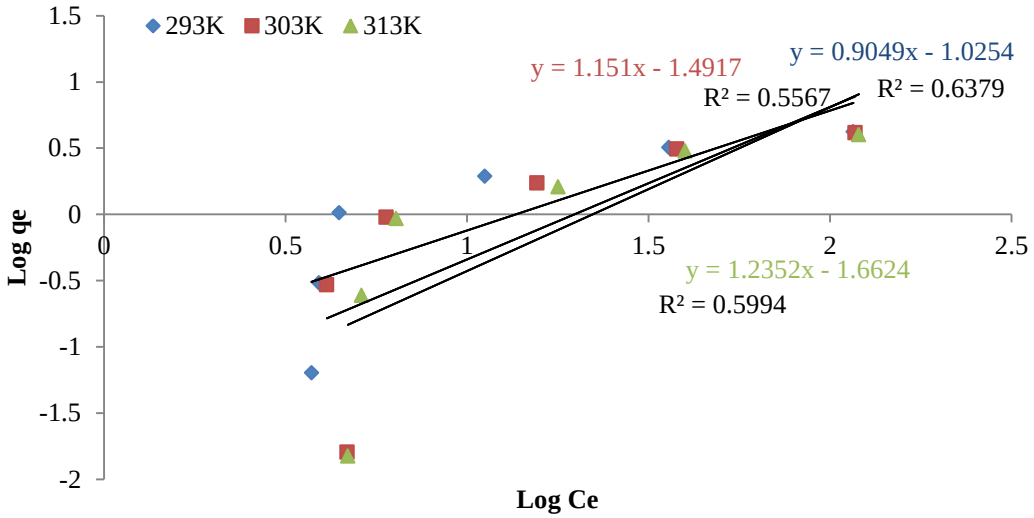

Fig 4.59 Freundlich isotherm for sorption of Ni (II) onto CBW at different temperatures

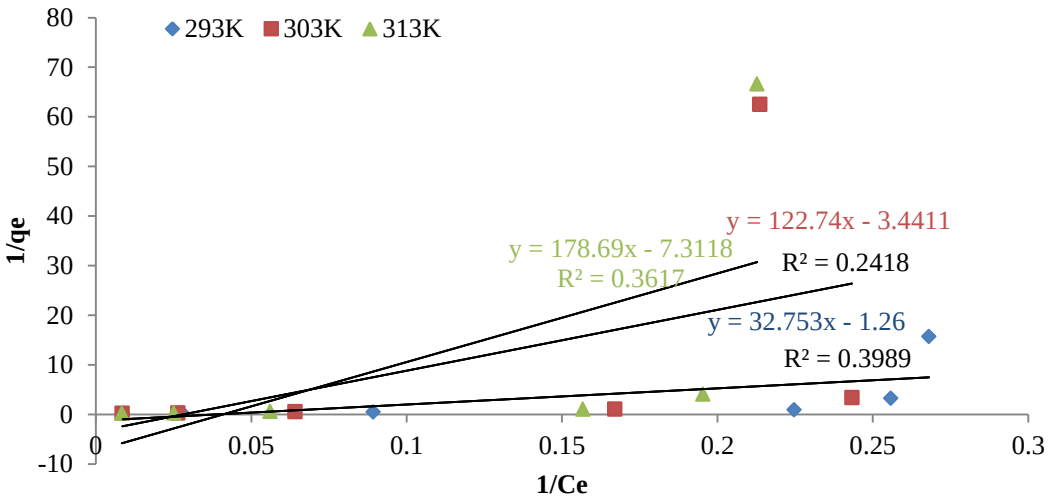

Fig 4.60 Langmuir isotherm for sorption of Ni (II) onto CBW at various temperatures

Table 4.9 Isotherm model parameters of Freundlich and Langmuir for sorption of Cu (II), Fe (II) and Ni (II) onto adsorbents at various temperatures

Adsorbent	Heavy metal ions	Temp (K)	Langmuir constants				Freundlich constants		
			q_{max} (mgg^{-1})	K_L (Lmg^{-1})	R^2	R_L	K_f (mgg^{-1})	1/n	R^2
CSS	Cu (II)	293	1.515	0.1305	0.7264	0.0369	0.217	0.5818	0.8152
		303	1.4108	0.1235	0.7211	0.0389	0.1885	0.6039	0.8309
		313	1.3046	0.1291	0.6998	0.0373	0.1842	0.5845	0.8167
	Fe (II)	293	1.5805	0.1013	0.7135	0.0470	0.1846	0.6336	0.7996
		303	1.6093	0.0886	0.7066	0.0534	0.1723	0.6438	0.7900
		313	1.5830	0.0827	0.6926	0.0570	0.1627	0.6482	0.7789
	Ni (II)	293	1.0004	0.7163	0.5359	0.0069	0.3402	0.5094	0.7518
		303	0.9977	0.6439	0.5465	0.0077	0.3280	0.4969	0.7475
		313	1.2455	0.2070	0.6573	0.0236	0.2369	0.5767	0.7739
MGBW	Cu (II)	293	2.2931	0.8131	0.9484	0.0061	0.8091	0.5642	0.8681
		303	2.6001	0.5497	0.9654	0.0090	0.7389	0.5877	0.8879
		313	1.9425	0.3465	0.8830	0.0142	0.4191	0.7034	0.9056
	Fe (II)	293	1.7235	0.2266	0.5231	0.0216	0.2891	0.7674	0.7936
		303	0.7286	3.4563	0.1236	0.0014	0.4257	0.5907	0.6381
		313	0.7539	1.5345	0.0736	0.0032	0.3234	0.6318	0.6508
	Ni (II)	293	0.5732	12.9038	0.0035	0.0004	0.6053	0.4723	0.3419
		303	0.5203	24.5149	0.0007	0.0002	0.5526	0.4631	0.3145
		313	1.2705	0.1041	0.3609	0.0458	0.1579	0.8717	0.5787
MGS	Cu (II)	293	2.5478	0.0214	0.3727	0.1894	0.0787	0.9350	0.6663
		303	-0.4061	-0.0302	0.6753	-0.1984	0.0175	1.2672	0.7523
		313	-0.3118	-0.0305	0.7481	-0.1961	0.0138	1.2745	0.7516
	Fe(II)	293	0.0596	-2.2327	0.0068	-0.0022	0.1606	0.7689	0.2471
		303	-0.0161	-0.0498	0.255	-0.1116	0.0041	1.9516	0.4931
		313	-0.0024	-0.0578	0.4205	-0.0947	0.0006	2.4963	0.5318
	Ni (II)	293	0.3368	76.9202	9E-06	6.499E-5	0.3884	0.5414	0.3795
		303	0.2671	0.3314	0.0246	0.0149	0.1500	0.7875	0.3998
		313	0.1364	0.1364	0.0401	0.0354	0.0746	0.9285	0.3572
CBW	Cu (II)	293	-0.7246	-0.0510	0.2955	-0.1087	0.0337	1.7159	0.7519
		303	-0.1567	-0.0684	0.4321	-0.0789	0.0061	2.2273	0.7704
		313	-0.0941	-0.0643	0.4039	-0.0843	0.0030	2.4011	0.7589
	Fe (II)	293	-0.0241	-0.06086	0.3636	-0.0895	0.0215	1.8974	0.7937
		303	-0.0483	-0.0714	0.5284	-0.0753	0.0007	2.9379	0.8119
		313	-0.0241	-0.0678	0.5184	-0.0796	0.0003	3.1665	0.7952
	Ni (II)	293	-0.9752	-1.1332	0.3989	-0.0044	0.0943	0.9049	0.6379
		303	-0.6703	-1.2962	0.2418	-0.0039	0.0322	1.1510	0.5567
		313	-0.6015	-1.3459	0.3617	-0.0037	0.2018	1.2352	0.5994

4.5 Thermodynamic studies

Thermodynamic parameters of the adsorptive removal of Cu^{2+}, Fe^{2+} and $Ni^{2+}$from wastewater onto CSS, MGS, CBW and MGBW have been shown in **Table 4.10**. **Table 4.10** also summarised Gibbs free energy (ΔG^o), enthalpy (ΔH^o) and entropy (ΔS^o) values at temperatures of 293 K, 303 K and 313 K. ΔG^o values for CSS, MGBW, MGS and CBW were all positive insinuating that adsorption of all heavy metal ions was not a spontaneous process except Fe(II) removal onto MGS indicating spontaneous adsorption process. The negative values of ΔS^o imply that the motion of all metal ions to the surface of the adsorbent did not require energy, thus the process was endothermic **(**Al-anber, 2016). Contrary findings were reported by Lekgoba et al.,(2020) where the entropy values were positive implying that metal ions required energy to migrate from solution to media surface. The coefficients of determination (R^2) values from the plots to ascertain the entropy and enthalpy were 0.9007, 1.0 and 0.8861 respectively for adsorption of Cu^{2+}, Fe^{2+} and Ni^{2+} onto CSS (**Fig 4.64**). The R^2 values from the plots to ascertain the entropy and enthalpy were 0.8559, 0.9019 and 0.9735 respectively for adsorption of Cu^{2+}, Fe^{2+} and Ni^{2+} onto MGBW (**Fig 4.61**). However, the coefficients of determination (R^2) values from the plots to ascertain the entropy and enthalpy were 0.9931, 0.9658 and 0.8968 respectively for adsorption of Cu^{2+}, Fe^{2+} and Ni^{2+} onto MGS (**Fig 4.62**). In this case, the coefficients of determination (R^2) values from the plots to ascertain the entropy and enthalpy were 0.9791, 0.9475 and 0.953 respectively for adsorption of Cu^{2+}, Fe^{2+} and Ni^{2+} onto CBW (**Fig 4.63**). There was low degree of freedom at the interface as the adsorption reactions expedite at 293 K, 303 K and 313 K as compared to the findings reported by Bouhamed et al., (2012). It has been reported that the heat of adsorption for Van deer Waals force, hydrogen bond, ligand exchange, dipole interaction, and chemical bond range as 4–10, 2– 40, ≈40, 2–29, and >60 $kJ{\cdot}mol^{-1}$, respectively. In this study, ΔH° values for Cu, Fe and Ni sorption onto CSS ranged between 2.0 and 8.0 and this was a suggestion of dipole interaction whereas that of adsorption onto MGBW ranged between 5 – 10 indicative of Van deer Waals force. In case of MGS and CBW, ΔH° values were between 2 and 29 suggesting dipole interactions. The negative values of ΔS were indicative of low affinity of both adsorbents to the metal ions while positive values of ΔH indicate endothermic reactions for both adsorbents (Xu *et al.*, 2017). The findings suggest that at high temperatures the adsorption surfaces of some media are activated and enlarged which promotes formation of more active sites for the adsorption of metal ions (Rahman and Sathasivam, 2015).

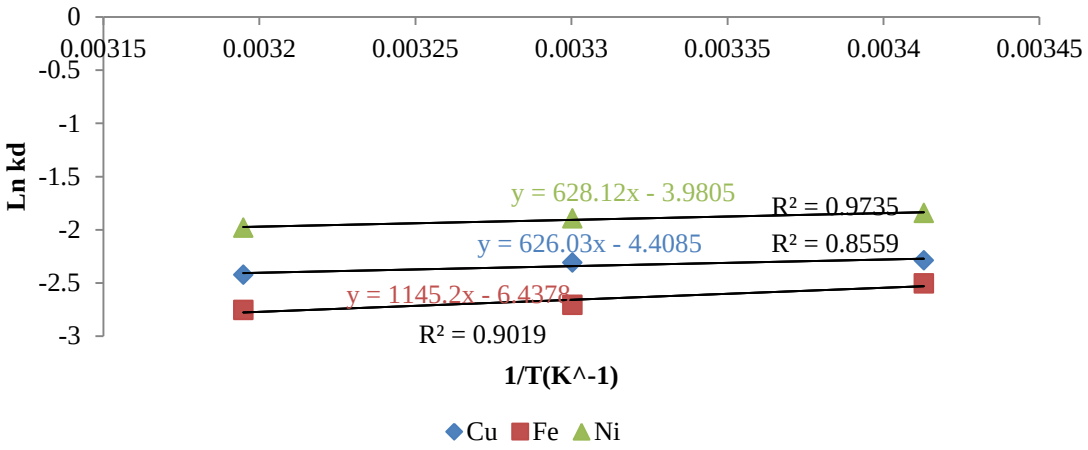

Fig 4.61 Van`t Hoff plots for adsorption of Cu (II), Fe (II) and Ni (II) onto MGBW

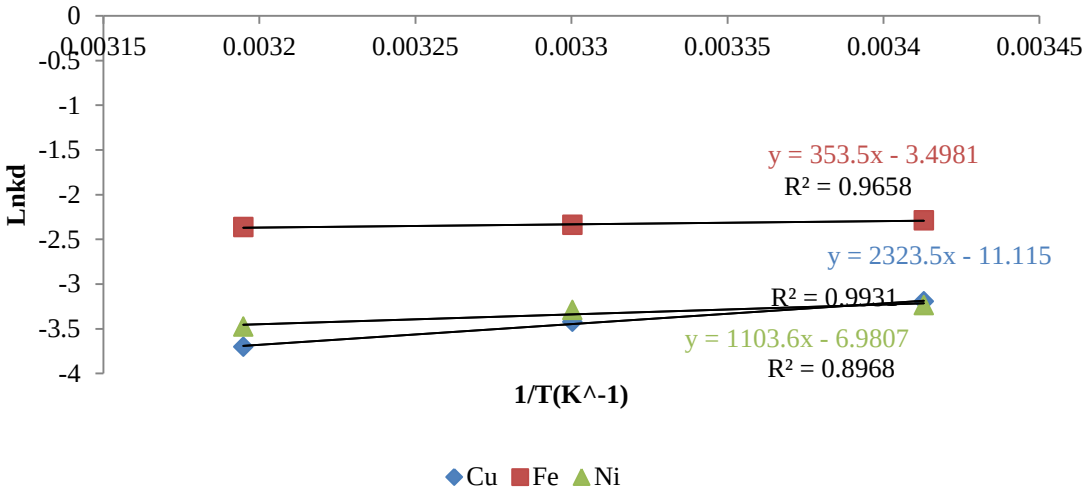

Fig 4.62 Van`t Hoff plots for adsorption of Cu (II), Fe (II) and Ni (II) onto MGS

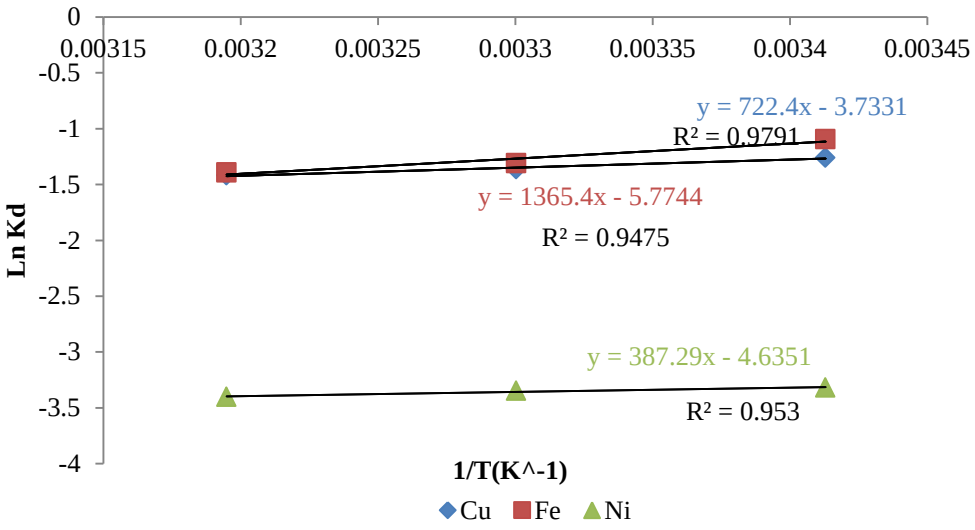

Fig 4.63 Van`t Hoff plots for adsorption of Cu (II), Fe (II) and Ni (II) onto CBW

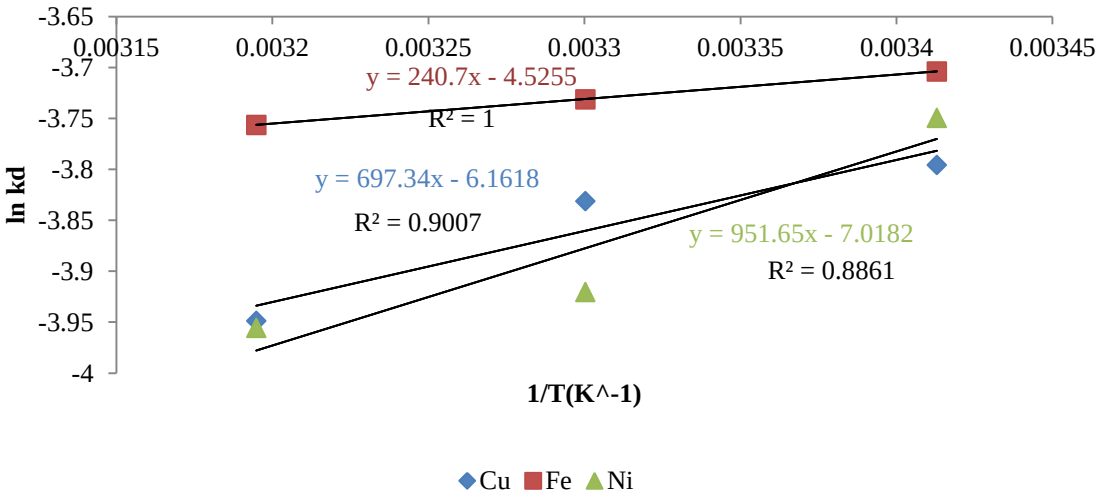

Fig 4.64 Van`t Hoff plots for adsorption of Cu (II), Fe (II) and Ni (II) onto CSS

Table 4.10 Thermodynamic parameters for the adsorption of Cu (II), Fe (II) and Ni (II).

Adsorbents	Metal ion	Temperature (K)	ΔG^o (kJmol^{-1})	ΔH^o (kJmol^{-1})	ΔS^o (kJmol^{-1}K^{-1})
CSS	Cu (II)	293	9.247		
		303	9.651	5.798	-0.051
		313	10.276		
	Fe (II)	293	9.023		
		303	9.399	2.001	-0.038
		313	9.775		
	Ni (II)	293	9.134		
		303	9.876	7.912	-0.058
		313	10.294		
MGBW	Cu (II)	293	5.572		
		303	5.819	5.205	-0.037
		313	6.313		
	Fe (II)	293	6.105		
		303	6.816	9.322	-0.054
		313	7.168		
	Ni (II)	293	4.490		
		303	4.772	5.222	-0.033
MGS	Cu (II)	293	7.786		
		303	8.621	19.318	-0.092
		313	9.639		
	Fe (II)	293	-5.572		
		303	-5.894	2.939	-0.029
		313	-6.153		
	Ni (II)	293	7.885		
		303	8.291	9.175	-0.058
		313	9.054		
CBW	Cu (II)	293	3.072		
		303	3.432	6.006	-0.031
		313	3.691		
	Fe (II)	293	2.667		
		303	3.296	11.352	-0.048
		313	3.620		
	Ni (II)	293	8.084		
		303	8.429	3.220	-0.039
		313	8.856		

4.6 Batch regeneration or reusability studies

Regeneration of media is economically critical for field applications as it decrease process costs (Zhang and Wang, 2015). It can be observed that fresh MGBW had an initial removal efficiency of 67±0.63, 76±0.72 and 62±0.63 % for Cu^{2+}, Fe^{2+} and Ni^{2+}respectively (**Fig 4.65 (a)).** The Cu^{2+}removal efficiency of MGBW dropped to 63, 61 and 57 % respectively in the first, second and third reusability cycles. Moreover, the Fe^{2+}removal efficiency of MGBW also dropped to 66, 54 and 43 % in the first, second and third regeneration trials. A drop in Ni^{2+}removal efficiency was also observed to be 51, 42 and 39 % for the first, second and third reusability trials. In case of CBW, virgin CBW had an initial removal efficiency of 85±0.77, 87±0.76 and 42±0.88 % respectively for divalent copper, iron and nickel (**Fig 4.65 (b)**). It can be noted that CBW attained a drop in removal of 78, 56 and 44 % for Cu^{2+} ,72, 61 and 31 % for Fe^{2+} and 35, 28 and 12 % for Ni^{2+} respectively for the first, second and third regeneration trials. Reusability potential of MGS was also evaluated and it can be noted that fresh MGS had adsorptive removal efficiency of 45±0.57, 65±0.5 and 61±0.68 % respectively for Cu^{2+}, Fe^{2+} and Ni^{2+} (**Fig 4.65 (c)**). The media had corresponding contaminant removal of 36, 55 and 51 % in the first regeneration cycle. However, MGS gave removal

efficiencies of 31, 41 and 37 % in the second reusability cycle for Cu^{2+}, Fe^{2+} and Ni^{2+}respectively while 27, 15 and 10% in the third regeneration cycle trials. In case of CSS, virgin CSS yielded removal efficiencies of 31±0.75, 33±0.46 and 32±0.79 % for Cu^{2+}, Fe^{2+} and Ni^{2+}respectively. A drop in Cu^{2+},Fe^{2+} and Ni^{2+} adsorptive removal efficiencies can also be observed in both first, second and third reusability cycle trials (**Fig 4.65(d)).** A decrease in Ni(II) removal efficiency of Nano-composite of lignocellulose/ montmorillonite was also observed by (Zhang and Wang, 2015). The drop was attributed to increase in temperature which raised desorption of metal ion (Gill et al., 2013;Zhang and Wang, 2015). Cu^{2+} desorption increased in other cycles when 0.1 M HCL, 0.01 M NaOH, 0.1 M EDTA were used(Ahmad et al., 2012) on eggshells coated with iron oxide. According to (Ahmad et al., 2012), the reason for increase in desorption of copper was due to slight destruction of the binding sites of Fe_2O_3(ferric oxide) by acid as well as ion exchange. Overall, CSS, CBW, MGS and MGBW have proven a potential to be regenerated and recycled. In future, other regeneration eluents of low and neutral pH should be investigated in such media.

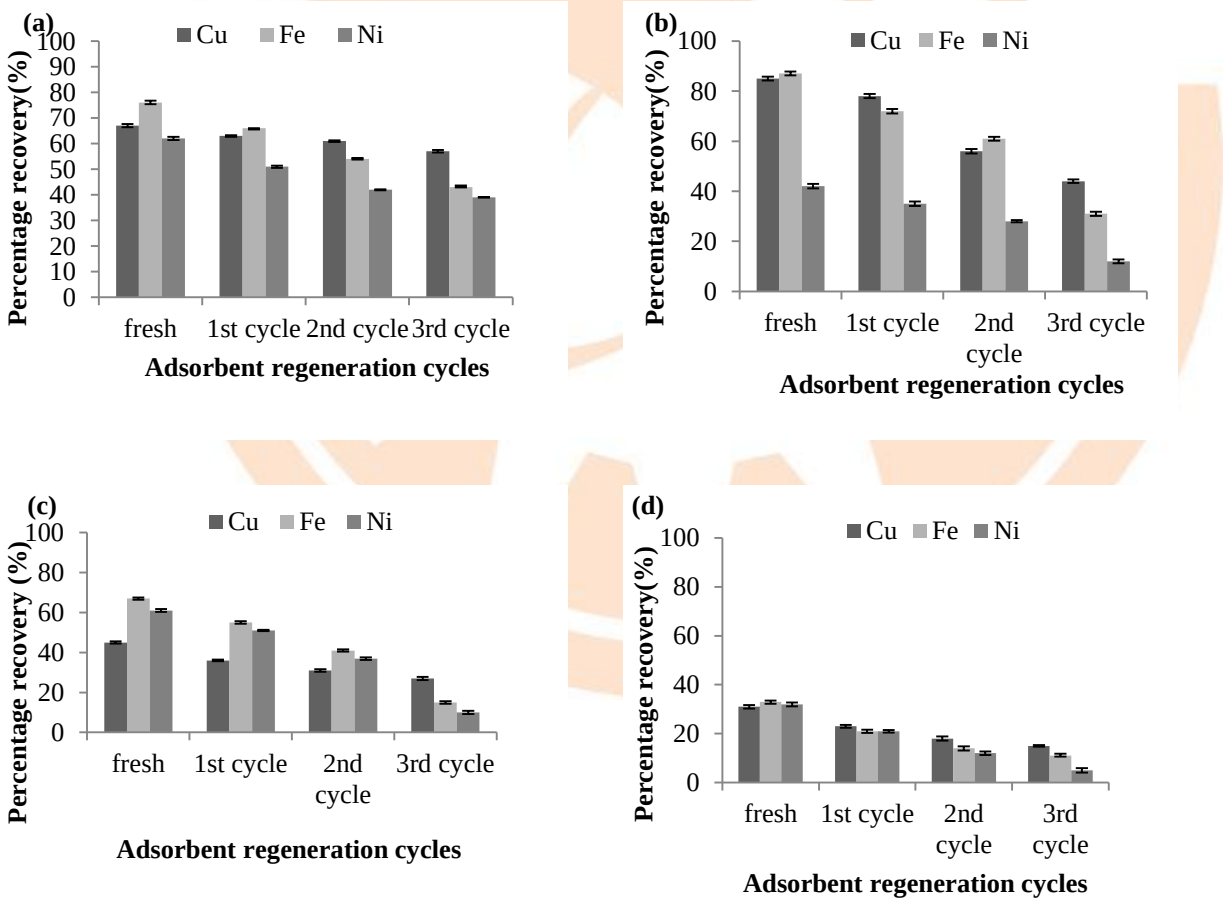

Fig 4.65 Reusability trials for (a) MGBW, (b) CBW, (c) MGS and (d) CSS

4.7 Column studies

In order to have a successful design of a column adsorption system, column breakthrough experimental curves are essential (Öztürk and Kavak, 2005; Lekgoba et al.,2020). In this study, the best two candidates for adsorption of Cu^{2+}, Fe^{2+} and Ni^{2+} being MGBW and CBW were selected for column studies. The column experiments were run at a flow rate of $20mLmin^{-1}$, bed height of 290mm yielding bed volume (BV) of $0.01053m^3$. **Fig 4.66 and Fig 4.67** show a breakthrough curves for adsorption of Cu^{2+}, Fe^{2+} and Ni^{2+} onto MGBW and CBW respectively. The results indicate that Ni^{2+} in treated effluent was high in concentration than Fe^{2+} and Cu^{2+} in the first 1620 minutes for MGBW suggesting less removal. The concentration of Ni^{2+} kept up-surging again from 1530 minutes, dropped after 1710 minutes and increased again after 1800 minutes then dropped afterwards (**Fig 4.66**). As for CBW, Ni^{2+}concentrations were also high between 45 and 2700 minutes compared to Cu^{2+} and Fe^{2+} concentrations (**Fig 4.67**). Ni^{2+} removal started to increase between 2835 and 3015 minutes probably due formation of new active adsorption sites and more contact time. Less removal of Ni^{2+} might be attributed to large ionic radius and low electronegativity of Ni^{2+} compared to Cu^{2+} making it to diffuse slowly in pores of media (Osińska, 2017). At times where ct/co is greater than 1.0, it indicates that there was leaching of Ni^{2+} from surface of MGBW and also there were less or no available active sites. However, it can be noted that Cu^{2+} was adsorbed in large quantities until 5040 minutes, therefore after 90 minutes from 5040 minutes, high concentrations of copper ion of 2.4345 and 12.364 mgL^{-1}were noted after 5130 and 5220 minutes respectively. The concentrations of Cu^{2+} then dropped yielding high Cu^{2+} removal. Such a high adsorptive Cu^{2+}removal may be attributed to small ionic radius and higher electronegativity yielding high diffusion rate into adsorbent pores (Osińska, 2017; Lekgoba et al., 2020). In case of Fe^{2+}, it can be observed that $Fe^{2+}$was also removed in large quantities probably due more available exchangeable sites in the surface of media (Gebretsadik et al.,2020). The breakthrough point is mostly selected randomly at some lower concentrations (Negrea et al., 2011). The breakthrough point is mostly selected randomly at some lower concentrations (Negrea et al., 2011), in this study 1.0 $mgL^{-1}$for nickel and copper, 2.0 mgL^{-1} for iron were selected as consent values based on Botswana Standards (BOS) for discharge in aquatic environments (ephemeral and perennial streams). The first breakthrough times determined by interpolation of analytical data and were found to be 2572.875 minutes = 42.88 hours, 463.15 minutes = 7.72 hours and 2752.79 minutes = 45.88 hours respectively for Cu^{2+}, $Ni^{2+}$and Fe^{2+}sorption onto CBW. The adsorption capacities at such breakthrough points were found to 940.95 mgg^{-1}media, 169.38 mgg^{-1}media and 938.59 mgg^{-1}media respectively

for Cu^{2+}, $Ni^{2+}$and Fe^{2+}. The media is regarded exhausted at ct/co of approximately 90 %. Though the MGBW proved less leaching in batch mode, in this column study, only Ni^{2+}reached breakthrough and went beyond implying more leaching. The total volume of solution treated was 113.40 L which is equivalent to 113400 mL for MGBW while 60300 mL for CBW. Comparing the two media in this study, it can be concluded that CBW outperformed MGBW as most of contaminant concentrations were less than regulatory threshold suggested by BOS for discharge into ephemeral and aquatic streams.

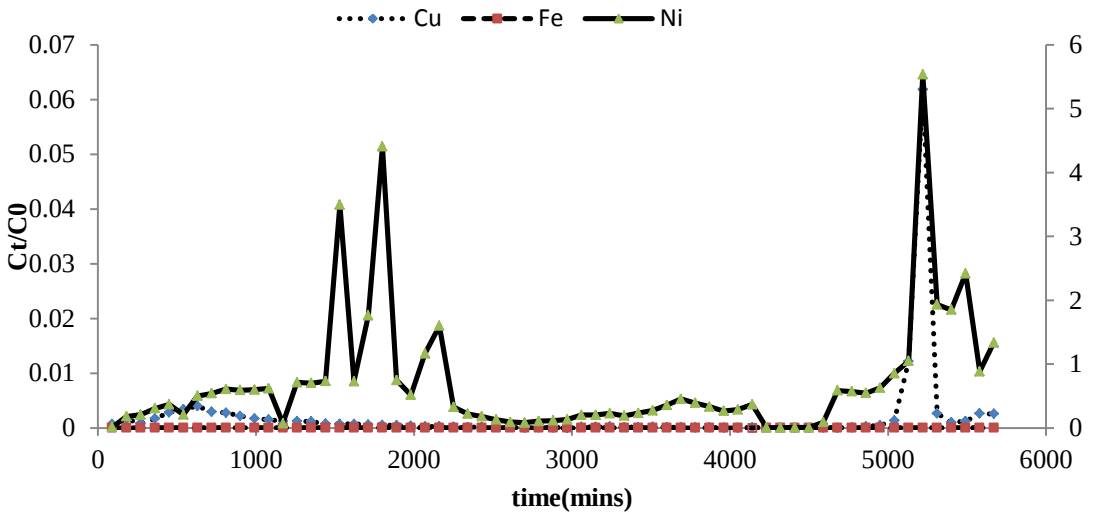

Fig 4.66 Breakthrough curve for Cu^{2+}, Fe^{2+} and Ni^{2+} adsorption onto MGBW

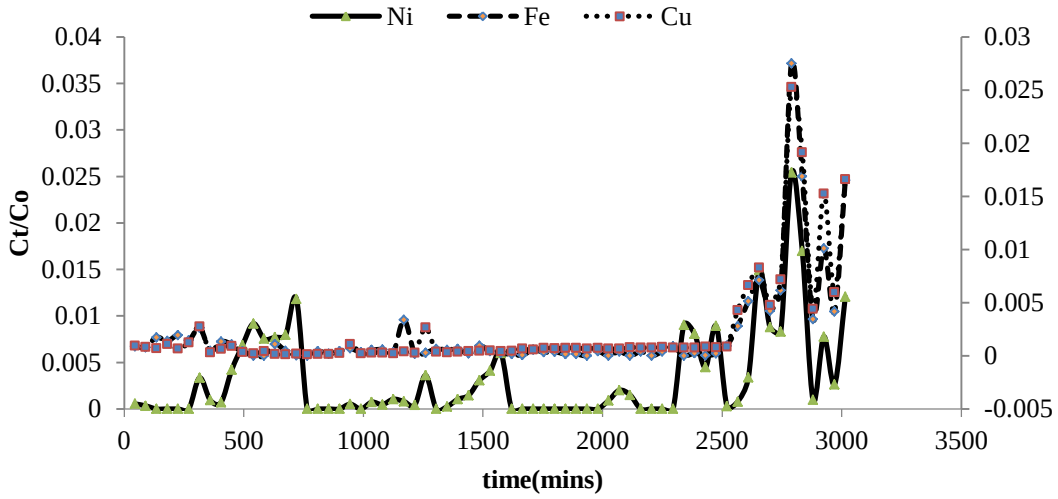

Fig 4.67 Breakthrough curve for Cu^{2+}, Fe^{2+} and Ni^{2+} adsorption onto CBW

4.7.1 Column kinetic models

The common column kinetic models, Yoon-Nelson and Thomas models were employed to depict adsorption of Cu^{2+}, Fe^{2+} and Ni^{2+} in a column. Derivation of Thomas kinetic model is established on second order kinetics presuming the system obey Langmuir isotherm (Trgo et al., 2011) while Yoon Nelson model operates over range of concentration and usually applied to describe saturation and breakthrough time of the system (Sarma et al., 2019). Similar coefficients of determination (R^2) values can be observed in both models for Cu^{2+} and Fe^{2+} adsorption onto MGBW and CBW (**Table 4.11)** and the values were low making results less meaningful. In case of sorption onto MGBW, lower R^2 values of 0.0022 and 0.0039 for Yoon-Nelson and Thomas model respectively (**Table 4.11**) were also found making the performance results of media less meaningful. Ƭ value in Yoon-Nelson model is a measure of how fast 50 % of contaminant breakthrough can be reached (Biswas and Mishra, 2015). In case of MGBW, the model indicated that 23846.33, 18145 and -13952 minutes will be needed to reach 50% Cu^{2+}, Fe^{2+} and Ni^{2+} breakthrough respectively (**Table 4.11**). However, the times required by CBW to reach 50 % breakthrough are 9426.22, 16909 and 11612.63 minutes for Cu^{2+}, Fe^{2+} and Ni^{2+} column sorption (**Table 4.11**). The R^2 values for Thomas and Yoon- Nelson model were too low making the performance results less meaningful. Conclusions cannot be made on models because sometimes they give false information compared to experimental results. In future, column studies should be done under different hydraulic conditions; variation of bed-depths, flow rates to help in optimization of results for the performance of media.

Table 4.11 Yoon-Nelson and Thomas column kinetic model parameters for MGBW and CBW

Adsorbent	Metals ions	Yoon-Nelson model			Thomas model		
		K_{yn} (min^{-1})	Ƭ (min)	R^2	K_{TH} ($L.min^{-1}.mg^{-1}$)	q_o ($mg.g^{-1}$)	R^2
MGBW	Cu^{2+}	-0.0003	23846.33	0.0619	0.0000015	8742.93	0.0619
	Fe^{2+}	0.0004	18145	0.0653	-0.000002	-6652.61	0.0653
	Ni^{2+}	-5E-05	-13952	0.0022	0.00006	0.001833	0.0039
CBW	Cu^{2+}	0.0009	9426.22	0.4032	-0.0000045	-3455.99	0.4032
	Fe^{2+}	0.0005	16909	0.0384	-0.0000025	-6199.45	0.0384
	Ni^{2+}	0.0008	11612.63	0.0473	-0.000004	-4257.61	0.0473

References

Abdel, O. E., Reiad, N. A. and Elshafei, M. M. (2011) 'A study of the removal characteristics of heavy metals from wastewater by low-cost adsorbents', *Journal of Advanced Research*. Cairo University, 2(4), pp. 297–303. doi: 10.1016/j.jare.2011.01.008.

Ahmad, R., Kumar, R. and Haseeb, S. (2012) 'Adsorption of Cu 2+ from aqueous solution onto iron oxide coated eggshell powder: Evaluation of equilibrium, isotherms, kinetics, and regeneration capacity', *Arabian Journal of Chemistry*. King Saud University, 5(3), pp. 353–359. doi: 10.1016/j.arabjc.2010.09.003.

Al-anber, M. A. (2016) 'Thermodynamics Approach in the Adsorption of Heavy Metals', (June). doi: 10.5772/21326.

Al-senani, G. M. and Al-fawzan, F. F. (2018) 'Study on Adsorption of Cu and Ba from Aqueous Solutions Using Nanoparticles of Origanum (OR) and Lavandula (LV)', 2018.

Arias, C. A. *et al.* (2003) 'Removal of indicator bacteria from municipal wastewater in an experimental two-stage vertical flow constructed wetland system', *Water Science and Technology*, 48(5), pp. 35–41. doi: 10.2166/wst.2003.0274.

Asfaram, A.,Ghaedi, M. and Ghezelbash, G.R. (2016) 'Biosorption of Zn^{2+}, Ni^{2+} and Co^{2+} from water samples onto Yarowia lipolytica ISF7 using a response Surface mathodology, and analyzed by inductively coupled plasma optical emission spectrometry (ICP-OES)', RSC Adv. 6, 23599–23610. doi: 10.1039/c5ra27170c.

ASTM C136 "Standard Test Method for Sieve Analysis of Fine and Coarse Aggregates." (www.astm.org)

Bagali, S. S., Gowrishankar, B. S. and Roy, A. S. (2017) 'Optimization , Kinetics , and Equilibrium Studies on the Removal of Lead (II) from an Aqueous Solution Using Banana Pseudostem as an Adsorbent', *Engineering*. Elsevier LTD on behalf of Chinese Academy of Engineering and Higher Education Press Limited Company, 3(3), pp. 409–415. doi: 10.1016/J.ENG.2017.03.024.

Bakhtiari, N., Azizian, S. (2015) 'Adsorption of copper ion from aqueous solution by nanoporous MOF-5 : A kinetic and equilibrium study', J. Mol. Liq. 206, 114–118. https://doi.org/10.1016/j.molliq.2015.02.009

Balouch, A., Kolachi, M, Talpur, F.N, Khan, H. and Bhanger, M.I.(2015) 'Sorption Kinetics ,

Isotherm and Thermodynamic Modeling of Defluoridation of Ground Water Using Natural Adsorbents', *American Journal of Analytical Chemistry* , 4(5).dio: 10.4236/ajac.2013.45028

Biswas, S. and Mishra, U. (2015) 'Continuous Fixed-Bed Column Study and Adsorption Modeling: Removal of Lead Ion from Aqueous Solution by Charcoal Originated from Chemical Carbonization of Rubber Wood Sawdust', *Journal of Chemistry*, 2015. doi: 10.1155/2015/907379.

Biswas, S. and Mishra, U. (2015) 'Continuous Fixed-Bed Column Study and Adsorption Modeling: Removal of Lead Ion from Aqueous Solution by Charcoal Originated from Chemical Carbonization of Rubber Wood Sawdust', *Journal of Chemistry*, 2015. doi: 10.1155/2015/907379.

Bouhamed, F., Elouear, Z,Bouzid, J. and Ouddane B. (2016) 'Multi-component adsorption of copper, nickel and zinc from aqueous solutions onto activated carbon prepared from date stones', *Environmental Science and Pollution Research*, 23(16), pp. 15801–15806. doi: 10.1007/s11356-015-4400-3.

Bouhamed, F., Elouear, Z. and Bouzid, J. (2012) 'Adsorptive removal of copper(II) from aqueous solutions on activated carbon prepared from Tunisian date stones: Equilibrium, kinetics and thermodynamics', *Journal of the Taiwan Institute of Chemical Engineers*. Taiwan Institute of Chemical Engineers, 43(5), pp. 741–749. doi: 10.1016/j.jtice.2012.02.011.

Bowden, L.I., Jarvis,A.P, Younger,P.L.and Johnson,K.L. (2009) 'Phosphorus removal from waste waters using basic oxygen steel slag', *Environmental Science and Technology*, 43(7), pp. 2476–2481. doi: 10.1021/es801626d.

Chancey, R. T. *et al.* (2010) 'Comprehensive phase characterization of crystalline and amorphous phases of a Class F fly ash', *Cement and Concrete Research*. Elsevier Ltd, 40(1), pp. 146–156. doi: 10.1016/j.cemconres.2009.08.029.

Drizo, A., Frost, C. A, Grace, M, J.and Smith,K. A.(1999) 'Physico-chemical screening of phosphate-removing substrates for use in constructed wetland systems', *Water Research*, 33(17), pp. 3595–3602. doi: 10.1016/S0043-1354(99)00082-2.

El-Shahat, M. F. and Shehata, A. M. A. (2013) 'Adsorption of lead, cadmium and zinc ions from industrial wastewater by using raw clay and broken clay-brick waste', *Asian Journal of*

Chemistry, 25(8), pp. 4284–4288.

Eze, S., Igwe, J. and Dipo, D. (2013) 'Effect of particle size on adsorption of heavy metals using chemically modified and unmodified fluted pumpkin and broad-leafed pumpkin pods', *International Journal of Biological and Chemical Sciences*, 7(2). doi: 10.4314/ijbcs.v7i2.40.

Farhan, S. N. and Khadom, A. A. (2015) 'Biosorption of heavy metals from aqueous solutions by Saccharomyces Cerevisiae', *International Journal of Industrial Chemistry*. Springer Berlin Heidelberg, pp. 119–130. doi: 10.1007/s40090-015-0038-8.

Favero, J. da S. *et al.* (2016) 'Physical and chemical characterization and method for the decontamination of clays for application in cosmetics', *Applied Clay Science*. Elsevier B.V., 124–125, pp. 252–259. doi: 10.1016/j.clay.2016.02.022.

Fierro, V. and Torne, V. (2008) 'Adsorption of phenol onto activated carbons having different textural and surface properties', 111, pp. 276–284. doi: 10.1016/j.micromeso.2007.08.002.

Flouty, R. and Estephane, G. (2012) 'Bioaccumulation and biosorption of copper and lead by a unicellular algae Chlamydomonas reinhardtii in single and binary metal systems: A comparative study', *Journal of Environmental Management*. Elsevier Ltd, 111, pp. 106–114. doi: 10.1016/j.jenvman.2012.06.042.

Garg, V.K., Gupta, R., Yadav, A.B. and Kumar, R. (2003) 'Dye removal from aqueous solution by adsorption on treated sawdust'. *Bioresour. Technol.* 89, 121–124. https://doi.org/10.1016/S0960-8524(03)00058-0

Gebretsadik, H., Gebrekidan, A. and Demlie, L. (2020) 'Removal of heavy metals from aqueous solutions using Eucalyptus Camaldulensis : An alternate low cost adsorbent Removal of heavy metals from aqueous solutions using Eucalyptus Camaldulensis : An alternate low cost adsorbent'. doi: 10.1080/23312009.2020.1720892.

Gill, R., Mahmood, A. and Nazir, R. (2013) 'Biosorption potential and kinetic studies of vegetable waste mixture for the removal of Nickel(II)', *Journal of Material Cycles and Waste Management*, 15(2), pp. 115–121. doi: 10.1007/s10163-012-0079-4.

Guo, J. and Lua, A. C. (2003) 'Textural and chemical properties of adsorbent prepared from palm shell by phosphoric acid activation', *Materials Chemistry and Physics*, 80(1), pp. 114–119. doi: 10.1016/S0254-0584(02)00383-8.

Gupta, S., Sharma, S. K. and Kumar, A. (2019) 'Biosorption of Ni (II) ions from aqueous solution using modified Aloe barbadensis Miller leaf powder', *Water Science and Engineering*. Elsevier Ltd, 12(1), pp. 27–36. doi: 10.1016/j.wse.2019.04.003.

Han, C.,Wang,Z, Yang,W, Wu,Q,Yang,H.and Xue,X. (2016) 'Effects of pH on phosphorus removal capacities of basic oxygen furnace slag', *Ecological Engineering*. Elsevier B.V., 89, pp. 1–6. doi: 10.1016/j.ecoleng.2016.01.004.

Healy, M. G., Rodgers, M. and Mulqueen, J. (2007) 'Treatment of dairy wastewater using constructed wetlands and intermittent sand filters', *Bioresource Technology*, 98(12), pp. 2268–2281. doi: 10.1016/j.biortech.2006.07.036.

Hemalatha, P. V and Rao, V. V. P. (2014) 'Adsorption Batch Studies on Calcined Brick Powder in Removing Chromium and Nickel Ions', *International Journal of Advanced Research in Chemical Science (IJARCS)*, 1(6), pp. 14–21.

Janbuala, S. and Wasanapiarnpong, T. (2015) 'Effect of rice husk and rice husk ash on properties of lightweight clay bricks', *Key Engineering Materials*, 659(July 2017), pp. 74–79. doi: 10.4028/www.scientific.net/KEM.659.74.

Jellali, S., Wahab, M.A, Hassine, R.B, Hamzaoui, A.H. and Bousselmi, L. (2011) 'Adsorption characteristics of phosphorus from aqueous solutions onto phosphate mine wastes', *Chemical Engineering Journal*. Elsevier B.V., 169(1–3), pp. 157–165. doi: 10.1016/j.cej.2011.02.076.

Jozanikohan, G. and Abarghooei, M. N. (2022) 'The Fourier transform infrared spectroscopy (FTIR) analysis for the clay mineralogy studies in a clastic reservoir', *Journal of Petroleum Exploration and Production Technology*. Springer International Publishing, (Stanienda 2016). doi: 10.1007/s13202-021-01449-y.

Kapur, M. and Mondal, M. K. (2014) 'Competitive sorption of Cu(II) and Ni(II) ions from aqueous solutions: Kinetics, thermodynamics and desorption studies', *Journal of the Taiwan Institute of Chemical Engineers*. Taiwan Institute of Chemical Engineers, 45(4), pp. 1803–1813. doi: 10.1016/j.jtice.2014.02.022.

Kargi, F. and Cikla, S. (2006) 'Biosorption of zinc(II) ions onto powdered waste sludge (PWS): Kinetics and isotherms', *Enzyme and Microbial Technology*, 38(5), pp. 705–710. doi: 10.1016/j.enzmictec.2005.11.005.

Khan, M. N. and Sarwar, A. (2007) 'Determination of points of zero charge of natural and treated adsorbents', *Surface Review and Letters*, 14(3), pp. 461–469. doi: 10.1142/S0218625X07009517.

Lai, Y., Thirumavalavan, M. and Lee, J. (2010) 'Effective adsorption of heavy metal ions (Cu , Pb , Zn) from aqueous solution by immobilization of adsorbents on Ca-alginate beads', 2248. doi: 10.1080/02772240903057382.

Lekgoba, T., Ntuli, F. and Falayi, T. (2020) 'Application of coal fly ash for treatment of wastewater containing a binary mixture of copper and nickel', *Journal of Water Process Engineering*. Elsevier Ltd, (July), p. 101822. doi: 10.1016/j.jwpe.2020.101822.

Letina, D. and Letshwenyo, W. M. (2018) 'Investigating waste rock, tailings, slag and coal ash clinker as adsorbents for heavy metals: Batch and column studies', *Physics and Chemistry of the Earth*. Elsevier, 105(March), pp. 184–190. doi: 10.1016/j.pce.2018.02.013.

Letshwenyo, M. W. and Sima, T. V. (2020) 'Phosphorus removal from secondary wastewater effluent using copper smelter slag', *Heliyon*. Elsevier Ltd, 6(6), p. e04134. doi: 10.1016/j.heliyon.2020.e04134.

Mihailova, I. and Mehandjiev, D. (2010) 'Characterization of fayalite from copper slags', *Journal of the University of Chemical Technology and Metallurgy*, 45(3), pp. 317–326. Available at: https://www.researchgate.net/publication/256503470.

Mishra, S. R., Chandraa,R , Jipsi K.A .and Savariya, DB. (2017) 'Kinetics and isotherm studies for the adsorption of metal ions onto two soil types', *Environmental Technology and Innovation*. Elsevier B.V., 7, pp. 87–101. doi: 10.1016/j.eti.2016.12.006.

Ngeontae, W., Aeungmaitrepirom, W. and Tuntulani, T. (2007) 'Chemically modified silica gel with aminothioamidoanthraquinone for solid phase extraction and preconcentration of Pb(II), Cu(II), Ni(II), Co(II) and Cd(II)', *Talanta*, 71(3), pp. 1075–1082. doi: 10.1016/j.talanta.2006.05.094.

Nithya, K., Sathish, A., Kumar, P.S. and Ramachandran, T. (2018) 'Fast kinetics and high adsorption capacity of green extract capped superparamagnetic iron oxide nanoparticles for the adsorption of Ni (II) ions', J. Ind. Eng. Chem. 59, 230–241. https://doi.org/10.1016/j.jiec.2017.10.028

Nosrati, A., Addai-mensah, J. and Skinner, W. (2009) ‘pH-mediated interfacial chemistry and particle interactions in aqueous muscovite dispersions’, Chemical Engineering Journal. 152, 406–414. https://doi.org/10.1016/j.cej.2009.05.001

Osińska, M. (2017) ‘Removal of lead(II), copper(II), cobalt(II) and nickel(II) ions from aqueous solutions using carbon gels’, *Journal of Sol-Gel Science and Technology*, 81(3), pp. 678–692. doi: 10.1007/s10971-016-4256-0.

Ouyang, D., Zhuo,Y, Hu ,L, Zeng ,Q, Hu,Y.and He,Z. (2019) ‘Research on the adsorption behavior of heavy metal ions by porous material prepared with silicate tailings’, *Minerals*, 9(5), pp. 1–16. doi: 10.3390/min9050291.

Öztürk, N. and Kavak, D. (2005) ‘Adsorption of boron from aqueous solutions using fly ash: Batch and column studies’, *Journal of Hazardous Materials*, 127(1–3), pp. 81–88. doi: 10.1016/j.jhazmat.2005.06.026.

Rahman, S. and Sathasivam, K. V (2015) ‘Heavy Metal Adsorption onto Kappaphycus sp . from Aqueous Solutions : The Use of Error Functions for Validation of Isotherm and Kinetics Models’. Hindawi Publishing Corporation, 2015. doi: 10.1155/2015/126298.

Rüscher, C. H., Lohaus, L. and Jirasit, F. (2022) ‘Alkali-Activated Slags and CEMI / CEMIII Pastes : Implications for Next Generation Concretes’.

Sabela, M. I.,Kunene,K,Kanchi,S, Xhakaza,N.M, Bathinapatla,A, Mdluli,P, Sharma,D.and Bisetty,K. (2019) ‘Removal of copper (II) from wastewater using green vegetable waste derived activated carbon: An approach to equilibrium and kinetic study’, *Arabian Journal of Chemistry*. The Authors, 12(8), pp. 4331–4339. doi: 10.1016/j.arabjc.2016.06.001.

Sanad, S. A., Moniem,S.M.A, Abdel-Latif,M.L,Hossein,H.A.and El-Mahllawy,M.S.(2021) ‘Sustainable management of basalt in clay brick industry after its application in heavy metals removal’, *Journal of Materials Research and Technology*. Elsevier Ltd, 10, pp. 1493–1502. doi: 10.1016/j.jmrt.2020.12.070.

Sarma, G. K., Sen Gupta, S. and Bhattacharyya, K. G. (2019) ‘Nanomaterials as versatile adsorbents for heavy metal ions in water: a review’, *Environmental Science and Pollution Research*. Environmental Science and Pollution Research, 26(7), pp. 6245–6278. doi: 10.1007/s11356-018-04093-y.

Saueprasearsit, P., Nuanjaraen, M. and Chinlapa, M. (2010) 'Biosorption of lead(Pb2+) by Luffa cylindrica Fiber...Saueprasearsit et al., 2010.pdf'.

Sharma, A. and Bhattacharyya, K. G. (2005) 'Adsorption of chromium (VI) on azadirachta indica (Neem) Leaf Powder', *Adsorption*, 10(4), pp. 327–338. doi: 10.1007/s10450-005-4818-x.

Sima, T. V., Letshwenyo, M. W. and Lebogang, L. (2018) 'Efficiency of waste clinker ash and iron oxide tailings for phosphorus removal from tertiary wastewater: Batch studies', *Environmental Technology and Innovation*. Elsevier B.V., 11, pp. 49–63. doi: 10.1016/j.eti.2018.04.008.

Sohail, A. *et al.* (2015) 'Biosorption of Heavy Metals onto the Bark of Prosopis Spicigira : A Kinetic Study for the Removal of Water Toxicity Division of Analytical Chemistry , Institute of Chemical Sciences ', 7(4), pp. 300–310. doi: 10.5829/idosi.aejts.2015.7.4.96236.

Tang, S. C. N. and Lo, I. M. C. (2013) 'Magnetic nanoparticles: Essential factors for sustainable environmental applications', *Water Research*. Elsevier Ltd, 47(8), pp. 2613–2632. doi: 10.1016/j.watres.2013.02.039.

Tejada-Tovar, C., Gonzalez-Delgado, A. D. and Villabona-Ortiz, A. (2019) 'Characterization of residual biomasses and its application for the removal of lead ions from aqueous solution', *Applied Sciences (Switzerland)*, 9(21). doi: 10.3390/app9214486.

Trgo, M., Medvidović, N. V. and Perić, J. (2011) 'Application of mathematical empirical models to dynamic removal of lead on natural zeolite clinoptilolite in a fixed bed column', *Indian Journal of Chemical Technology*, 18(2), pp. 123–131.

Wang, X. Cui, Y, Peng, Q, Fan, C, Zhang, Z. and Zhang, X. (2020) 'Removal of Cd (II) and Cu (II) from Aqueous Solution by Na + - Modified Pisha Sandstone', 2020.

Wierzba, S. (2017) 'Biosorption of nickel (II) and zinc (II) from aqueous solutions by the biomass of yeast Yarrowia lipolytica', *Polish Journal of Chemical Technology*, 19(1), pp. 1–10. doi: 10.1515/pjct-2017-0001.

Viegas, R. M. C., Campinas, M , Costa, H .and Rosa, M.J. (2014) 'How do the HSDM and Boyd's model compare for estimating intraparticle diffusion coefficients in adsorption processes', *Adsorption*, 20(5–6), pp. 737–746. doi: 10.1007/s10450-014-9617-9.

Xu, L., Zheng, X, Cui, H, Zhu, Z, Liang, J. and Zhou, J. (2017) 'Equilibrium, Kinetic, and Thermodynamic Studies on the Adsorption of Cadmium from Aqueous Solution by Modified Biomass Ash', *Bioinorganic Chemistry and Applications*, 2017. doi: 10.1155/2017/3695604.

Xue, C. *et al.* (2021) 'Analysis on the Strength of Cement Mortar Mixed with Construction Waste Brick Powder', *Advances in Civil Engineering*, 2021. doi: 10.1155/2021/8871280.

Zhang, X. and Wang, X. (2015) 'Adsorption and desorption of Nickel(II) ions from aqueous solution by a lignocellulose/montmorillonite nanocomposite', *PLoS ONE*, 10(2), pp. 1–21. doi: 10.1371/journal.pone.0117077.

CHAPTER 5: CONCLUSIONS AND RECOMMENDATIONS FOR FUTURE WORKS

5.1 CONCLUSIONS

1. The investigation on effects of process parameters such as contact time, pH, dosage, particle size on heavy metal adsorption was done. The upsurge in contact time, pH and temperature increased the adsorptive removal of Cu^{2+}, Ni^{2+} and Fe^{2+} and adsorption capacities of both adsorbents. The increase in adsorbent size resulted in decrease in adsorption capacities of both media. The increase in adsorbent dosage decreased the adsorptive removal of adsorbates. The adsorption capacities of CSS, MGBW, CBW and MGS were 3.3, 7.6, 8.7 and 5.9 mgg^{-1}media respectively for Fe^{2+} removal at 303 K, dosage = 2.0 g/100 mL solution, initial concentration = 200 mgL^{-1}after 45 minutes agitation of solution with pH varying from 2-12. However, adsorptive capacities of CSS, MGBW, CBW and MGS were 3.2, 6.2, 4.2 and 4.2 mgg^{-1}media with respect to Ni^{2+} removal while adsorption capacities of 3.1, 6.7, 8.5 and 6.5 mgg^{-1}media were attained for Cu^{2+} using CSS, MGBW, CBW and MGS respectively at the same conditions.
2. The adsorption mechanisms involved during adsorption were also determined. The adsorption of both ions onto CSS was sufficiently described by Freundlich than Langmuir isotherm model at both temperatures of 293 K, 303 K and 313 K. Cu^{2+} adsorptive removal onto MGBW at 293 K and 303 K follow Langmuir while Freundlich isotherm model at 313 K. In case of CBW, Freundlich isotherm model best described removal mechanism and indicated that sorption of both metals occurred in heterogeneous active sites. The adsorption of Cu^{2+}, Ni^{2+} and Fe^{2+}onto both adsorbents indicated that chemisorption process was taking place and intraparticle diffusion was not the only rate controlling mechanism. As for CBW, the adsorption process was best described by Pseudo Second Order kinetic model and Freundlich isotherm model insinuating that chemisorption occurred in heterogeneous active sites. Thermodynamic studies of Cu^{2+}, Ni^{2+} and Fe^{2+} onto CSS, MGS, CBW and MGBW indicated that the adsorption was non spontaneous process and was exothermic except Fe (II) removal onto MGS which indicated spontaneous adsorption process.

3. The regeneration or reusability potential of used media was investigated using an alkaline eluent, sodium hydroxide. Overall, CSS, CBW, MGS and MGBW have proven a successful potential to be regenerated and recycled in three regeneration cycles.
4. The environmental effects of using copper smelter slag and brick waste as adsorbents was investigated through leaching test. It can be concluded that the environmental application of MGBW and CBW is quite promising than of CSS and MGS as they do not leach heavy metals hence non-hazardous.
5. In column studies, CBW and MGBW were selected as best candidates for column studies. It can be concluded that the R^2 values for Thomas and Yoon- Nelson model were too low making the performance results less meaningful. Conclusions cannot be made on models which sometimes give false information compared to experimental results. In future, column studies should be done under different hydraulic conditions; variation of bed-depths, flow rates to help in optimization of results for the performance of media.

5.2 RECOMMENDATIONS FOR FUTURE WORKS

This research work shows promising results on beneficiation of brick wastes and copper smelter slag but there are still some further studies to be conducted in the future. Such future works are as follows;

1. Through a study on leachability of adsorbents was conducted, only leaching of three heavy metals was investigated. Such investigation should be done incorporating other heavy metals, anions to reveal proper environmental friendliness of such media.
2. Despite the promising adsorptive characteristics and performance of adsorbents, investigations on the effect of abrasion on adsorbents performance should be conducted. Such information could be used during design and construction of adsorption systems. Moreover, such information could be utilised in backwashing or regeneration processes of media.
3. Cation Exchange Capacity (CEC) of both media should be determined to have a proper understanding on the ion exchangeability during adsorption.
4. In future, column studies should be done under different hydraulic conditions; variation of bed-depths, flow rates.

5. In future, other regeneration eluents of low and neutral pH should be used investigated on such media.
6. Column regeneration studies should also be done to determine the restoration capacity of media in a column setup.
7. Investigations on both column and batch studies should further be conducted in future using real wastewater before field trials.